The Geology of North America
Decade Map Volume 1
1991

Chapter 11

Seismicity of the Intermountain Seismic Belt

Robert B. Smith and Walter J. Arabasz
Department of Geology and Geophysics, University of Utah, Salt Lake City, Utah 84112

INTRODUCTION

In this chapter we present an overview of the Intermountain seismic belt (ISB), a first-order feature of the Seismicity Map of North America (Engdahl and Rinehart, 1988). The ISB is a prominent northerly-trending zone of mostly shallow (<20 km) earthquakes, about 100 to 200 km wide, that extends in a curvilinear, branching pattern at least 1500 km from southern Nevada and northern Arizona to northwestern Montana (Fig. 1). Our study area, defined by the bounds of Figure 1, covers a sizable part of the western United States encompassing the ISB and is informally referred to herein as the Intermountain region.

Contemporary deformation in the ISB is dominated by intraplate extension. Forty-nine moderate to large earthquakes ($5.5 \leqslant M_S \leqslant 7.5$) since 1900 and spectacular late Quaternary faulting with a predominance of normal to oblique-normal slip make the Intermountain region a classic study area for intraplate extensional tectonics. Information from the Intermountain region, relating for example to paleoseismology (Schwartz, 1987), seismotectonic framework (Smith and others, 1989), contemporary deformation from geodetic measurements and seismic moments of earthquakes (Savage and others, 1985; Eddington and others, 1987), and strong ground motion in normal-faulting earthquakes (Westaway and Smith, 1989a) has added significantly to understanding extensional seismotectonics worldwide. Particularly valuable contributions have come from field and seismological observations of two large normal-faulting earthquakes in the Intermountain region—the 1959 Hebgen Lake, Montana, earthquake (M_S = 7.5) and the 1983 Borah Peak, Idaho, earthquake (M_S = 7.3)—both described herein. Our basic intent in this chapter is to provide an interpretive guide to the seismicity of the ISB. We also summarize and discuss observations from the Intermountain region that are relevant to general aspects of extensional intraplate tectonics.

The coherence of the ISB as a regional earthquake belt became apparent with evolving compilations of seismicity (Heck, 1938; Woolard, 1958; Ryall and others, 1966). The earthquake belt was well defined in Barazangi and Dorman's (1969) global seismicity map of shallow earthquakes and was first called the "Intermountain Seismic Belt" in joint abstracts by Sbar and Barazangi (1970) and Smith and Sbar (1970). Follow-up papers by Sbar and others (1972), and especially one by Smith and Sbar (1974), gave modern seismotectonic overviews (see also Smith, 1978; Arabasz and Smith, 1981; and Stickney and Bartholomew, 1987).

The ISB roughly follows the eastern margin of a broad region of late Cenozoic crustal extension in western North America. This seismically active boundary with more stable continental interior to the east has been interpreted as a subplate boundary (Smith and Sbar, 1974; Smith, 1978). It is well known that, on a regional scale, the ISB coincides with a persistent deformational belt in western North America that has been recurrently active since late Precambrian time (Levy and Christie-Blick, 1989; Anderson, 1989) and which is now characterized by pronounced lateral heterogeneities in crust-mantle structure across the ISB (e.g., Smith and others, 1989). Contemporary deformation in the region marks a continuation of late Cenozoic extension and volcanism (in the Yellowstone–Snake River Plain volcanic system and in southern Utah), whose various modern stages began roughly 10 to 15 m.y. ago (Anderson, 1989).

Regional-scale earthquake pattern

There is a general north-south regional continuity to the ISB (see the Seismicity Map of North America, Engdahl and Rinehart, 1988), but we can distinguish at least three parts—referred to herein as the southern, central, and northern ISB (Fig. 1)—for convenient reference. These subdivisions of the ISB may be arguable, but we believe distinctive features of the central ISB, as described in this paper, differentiate it from the ISB to the north and south. Referring to Figures 1 and 2 (see also Fig. 3 for additional features and place names), the southern ISB (36° to 42¼°N) coincides with a tectonic transition zone between the Basin and Range province on the west and the Colorado Plateau–Middle Rocky Mountain provinces on the east. In southwestern Utah at about 38°N there is a southward bifurcation of the ISB. A

Smith, R. B., and Arabasz, W. J., 1991, Seismicity of the Intermountain Seismic Belt, *in* Slemmons, D. B., Engdahl, E. R., Zoback, M. D., and Blackwell, D. D., eds., Neotectonics of North America: Boulder, Colorado, Geological Society of America, Decade Map Volume 1.

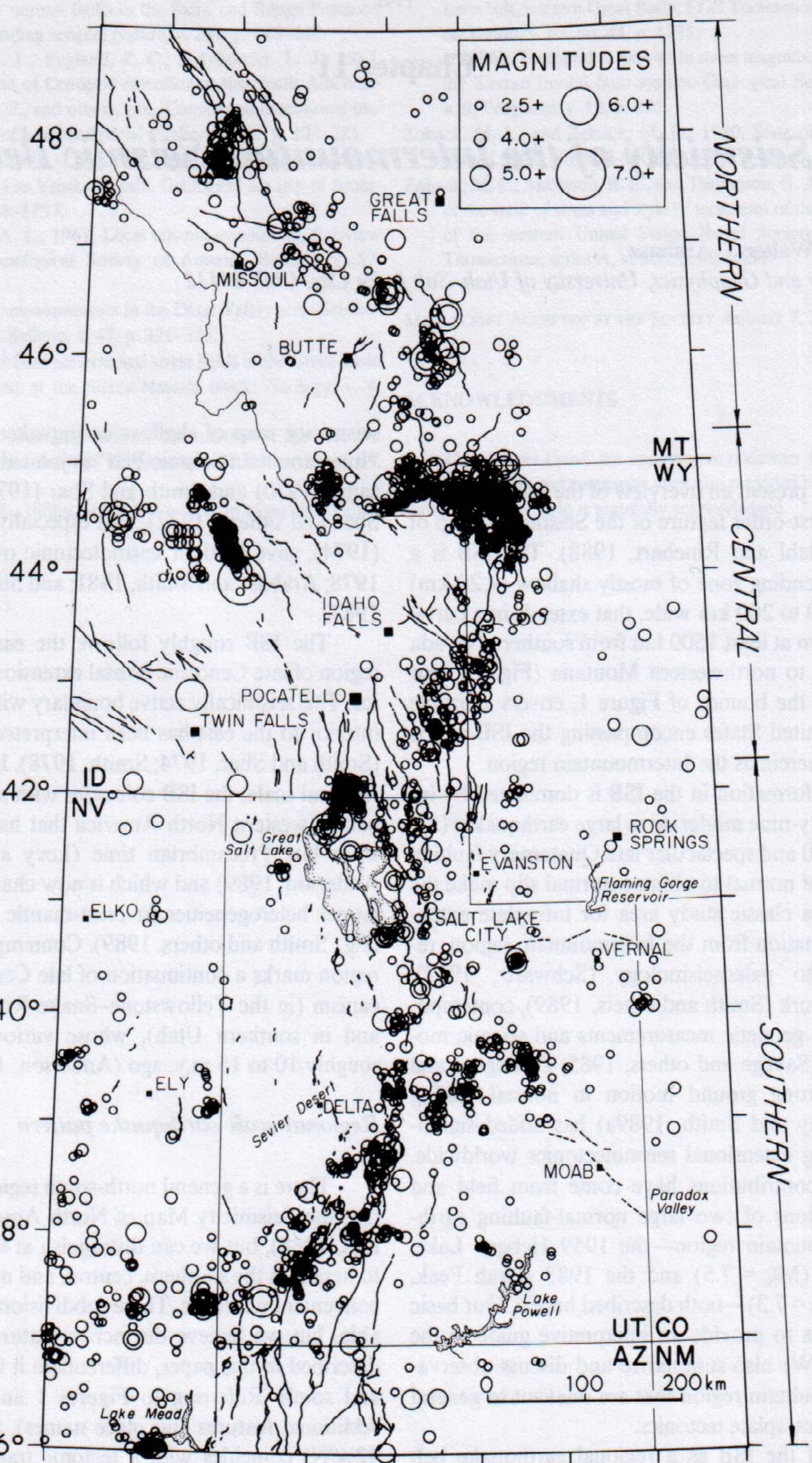

Figure 1. Earthquakes in the Intermountain region, 1900–1985, outlining the Intermountain seismic belt (ISB), together with selected Cenozoic faults identified in Figure 3. Earthquake data are from the compilation of Engdahl and Rinehart (1988; this volume). Northern, central, and southern parts of the ISB are delimited for reference.

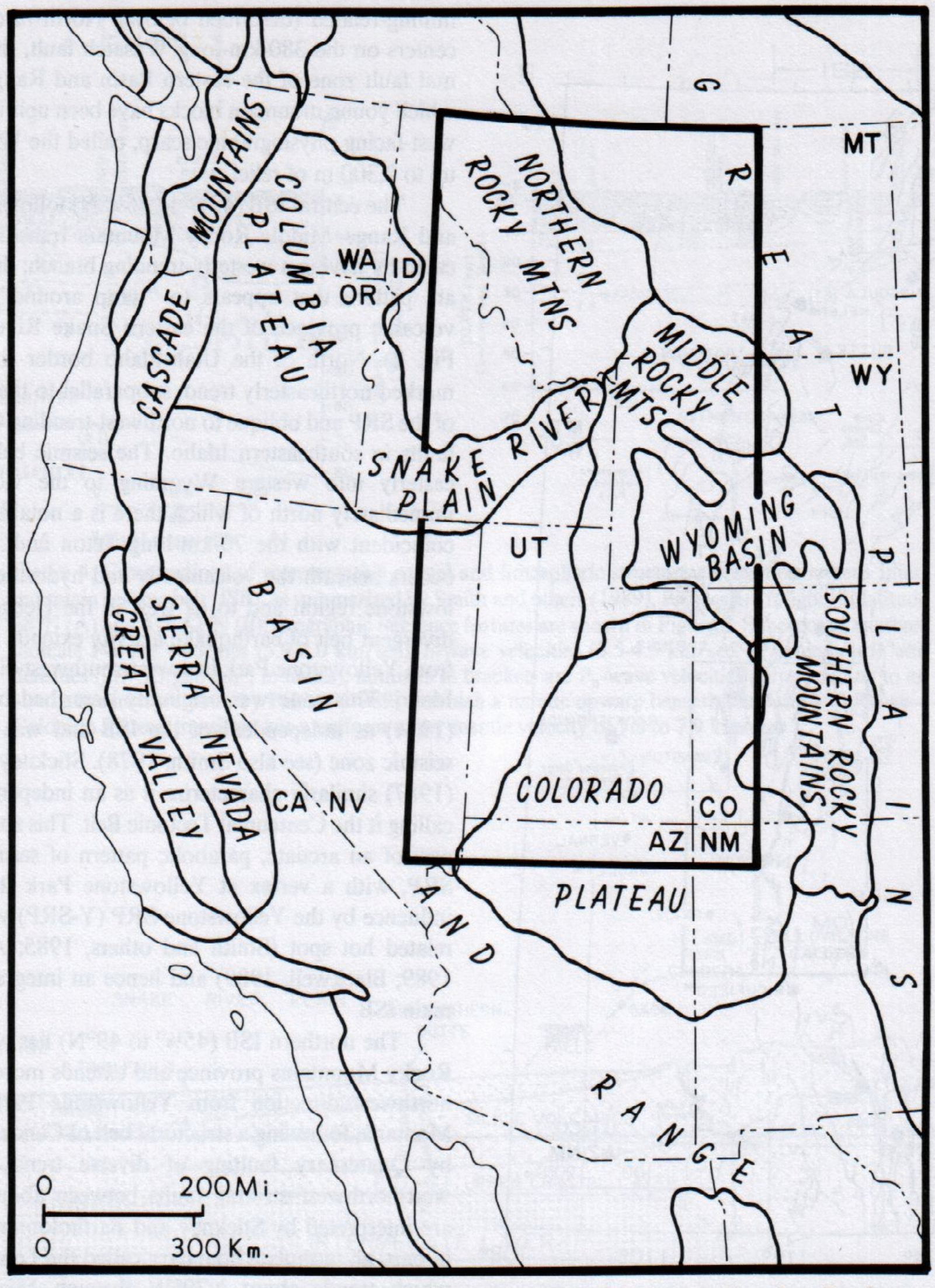

Figure 2. Map of the western United States showing physiographic provinces and location of study area (bold outline) shown in Figures 1, 3, 6, 8, 9, and 20.

distinct belt of seismicity continues southwestward some 200 km across southern Nevada, partly including induced earthquakes related to underground nuclear explosions at the Nevada Test Site in southern Nevada (Rogers and others, this volume); this belt transects the local north-south tectonic grain and coincides with the midpoint of a steep regional gravity gradient (Eaton and others, 1978) between the northern and southern sections of the Basin and Range province. The other part of the bifurcation is a weaker zone of scattered earthquakes that extends southward into central Arizona through a broad belt of Quaternary faulting (see Kruger-Kneupfer and others, 1985, Fig. 3).

In southwestern Utah (Fig. 1), earthquakes of the southern ISB follow a northeasterly structural trend to about 39°N, where both structure and the earthquake belt change to a northerly trend. Clustered earthquakes defining an inverted U-shaped pattern of epicenters in east-central Utah between 39° and 40°N are

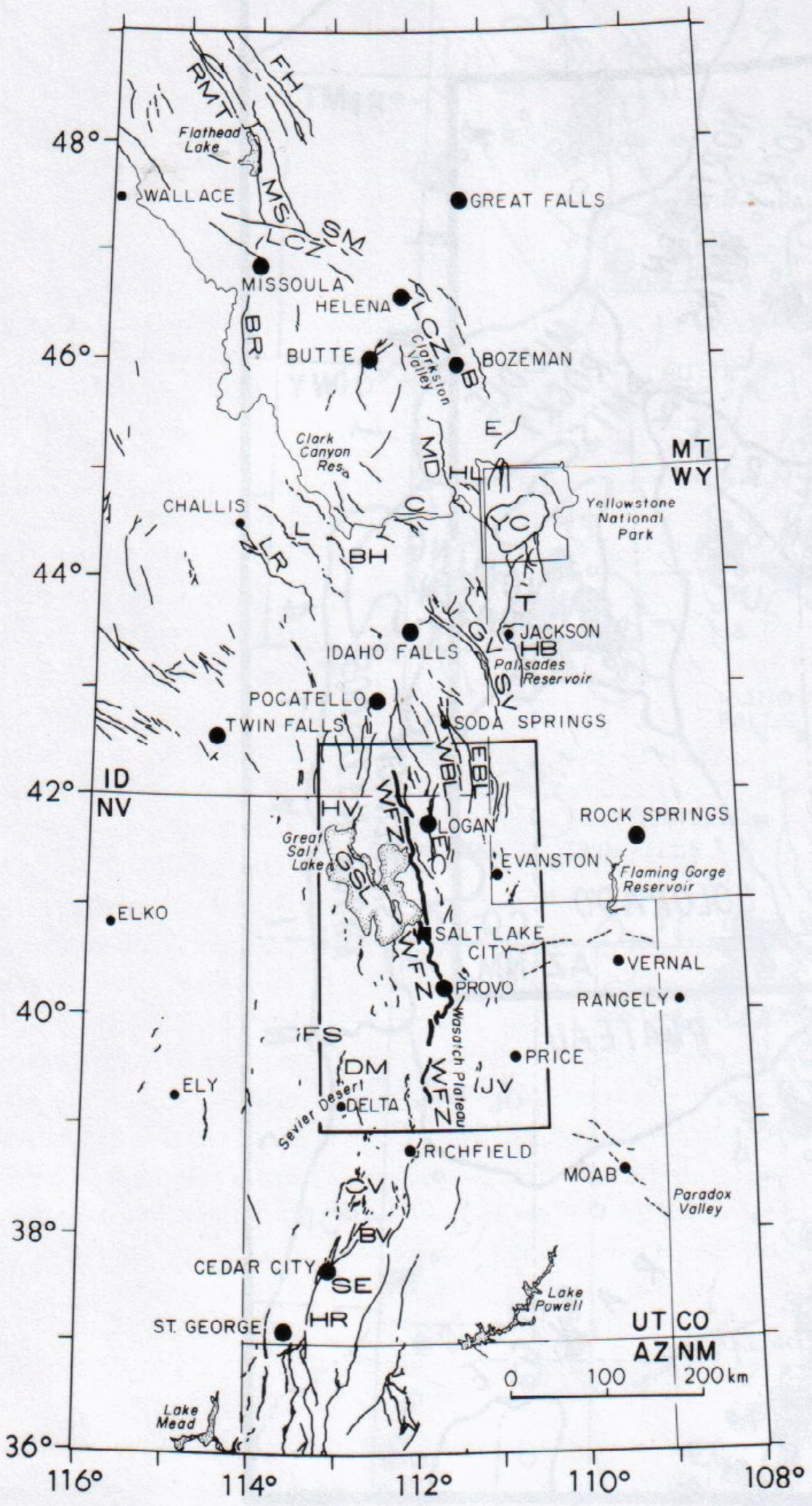

Figure 3. Location map of place names and selected late Cenozoic normal faults of the Intermountain region. Rectangle outlines Wasatch Front area shown in Figure 12, wherein other faults are identified. Abbreviations of faults are as follows: B = Bridger; BH = Beaverhead; BR = Bitterroot; BV = Beaver; C = Centennial; CV = Cove Fort; DM = Drum Mountains; E = Emigrant; EBL = East Bear Lake; EC = East Cache; FH = Flathead; FS = Fish Springs; GSL = Great Salt Lake; GV = Grand Valley; HB = Hoback; HL = Hebgen Lake; HR = Hurricane; JV = Joes Valley; L = Lemhi; LR = Lost River; MD = Madison; MS = Mission; SM = St. Mary's; SE = Sevier; SV = Star Valley; T = Teton; WBL = West Bear Lake. Other labeled tectonic features are: LCZ = Lewis and Clark Zone (see Fig. 18); RMT = Rocky Mountain trench; YC = Yellowstone Caldera.

mining-related (described below). Northward in Utah the ISB centers on the 380-km-long Wasatch fault, the preeminent normal fault zone of the eastern Basin and Range province, along which young mountain blocks have been uplifted to form a major west-facing physiographic scarp, called the Wasatch Front, with up to 2,300 m of relief.

The central ISB (42¼° to 45¼°N) follows, in part, the Basin and Range–Middle Rocky Mountain transition, but is complicated by having a westerly-trending branch; the result is an arcuate pattern that appears to "wrap around" the late Tertiary volcanic province of the eastern Snake River Plain (SRP; see Fig. 2). North of the Utah-Idaho border the ISB takes on a marked northeasterly trend, subparallel to the southeastern edge of the SRP and oblique to northwest-trending Quaternary normal faults in southeastern Idaho. The seismic belt continues northeasterly into western Wyoming to the vicinity of Jackson, immediately north of which there is a notable gap in seismicity coincident with the 70-km-long Teton fault. Intense seismicity occurs beneath the volcanically and hydrothermally active Yellowstone region and to its west in the Hebgen Lake region. A divergent belt of earthquake activity extends more than 400 km from Yellowstone Park in a west-southwest direction into central Idaho. This zone was originally described by Smith and Sbar (1974) as independent of the ISB and was termed the Idaho seismic zone (see also Smith, 1978). Stickney and Bartholomew (1987) similarly characterize it as an independent seismic zone, calling it the Centennial Tectonic Belt. This zone, however, forms part of an arcuate, parabolic pattern of seismicity flanking the SRP, with a vertex at Yellowstone Park that suggests causal influence by the Yellowstone-SRP (Y-SRP) volcanic system and related hot spot (Smith and others, 1985; Anders and others, 1989; Blackwell, 1989) and hence an integral relation with the main ISB.

The northern ISB (45¼° to 49°N) lies within the Northern Rocky Mountains province and extends more than 400 km in a northwest direction from Yellowstone Park to northwestern Montana, following a structural belt of Cenozoic basins bounded by Quaternary faulting of diverse trend. Earthquakes and west-northwest–striking faults between about 46½° and 48°N are interpreted by Stickney and Bartholomew (1987) to reflect, in part, an intraplate boundary called the Lewis and Clark Zone, which trends about N70°W through Missoula and Helena (Fig. 3).

SEISMOTECTONIC FRAMEWORK

Crustal structure and structural style

The geophysical framework of the Intermountain region has recently been summarized by Smith and others (1989). The crustal and upper-mantle velocity structure in the region is typified by the cross sections shown in Figures 4 and 5. The southern ISB coincides with a transition from thinner, extended crust and lithosphere on the west to thicker, more stable crust and

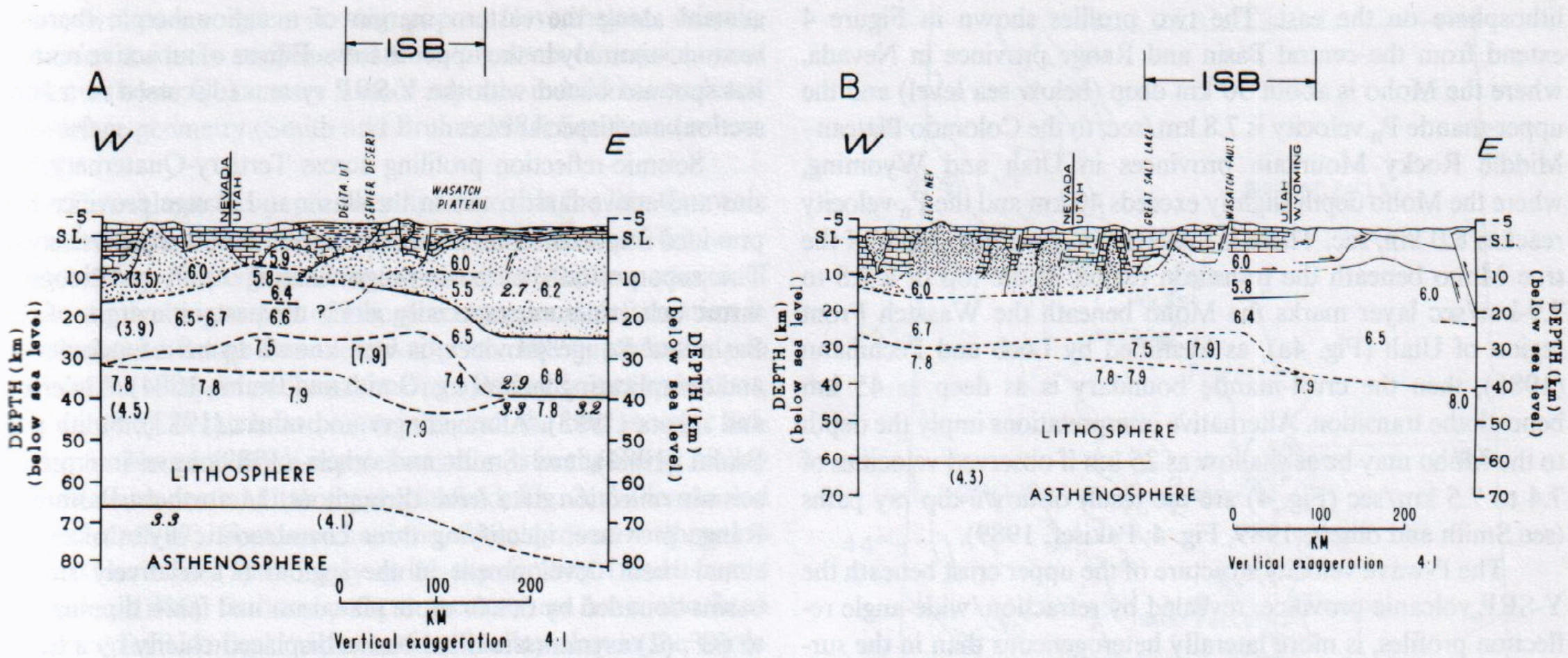

Figure 4. Cross sections of representative crustal and lithospheric structure across the southern Intermountain seismic belt (ISB), as summarized by Smith and others (1989). Profiles are roughly at latitude 38°N (A) and 41°-42°N (B); geographic reference features are shown in Figure 3. Superposed numbers indicate P-wave velocities (5.9-8.0 km/sec), S-wave velocities (3.5-4.5 km/sec, in parentheses), and densities (2.7-3.3 gm/cm^3, in italics); numbers in brackets are P_n-wave velocities corresponding to an alternative interpretation by Pakiser (1989) in which a mantle upwarp beneath the Basin and Range–Colorado Plateau transition has a uniform upper mantle velocity of 7.8 to 7.9 km/sec.

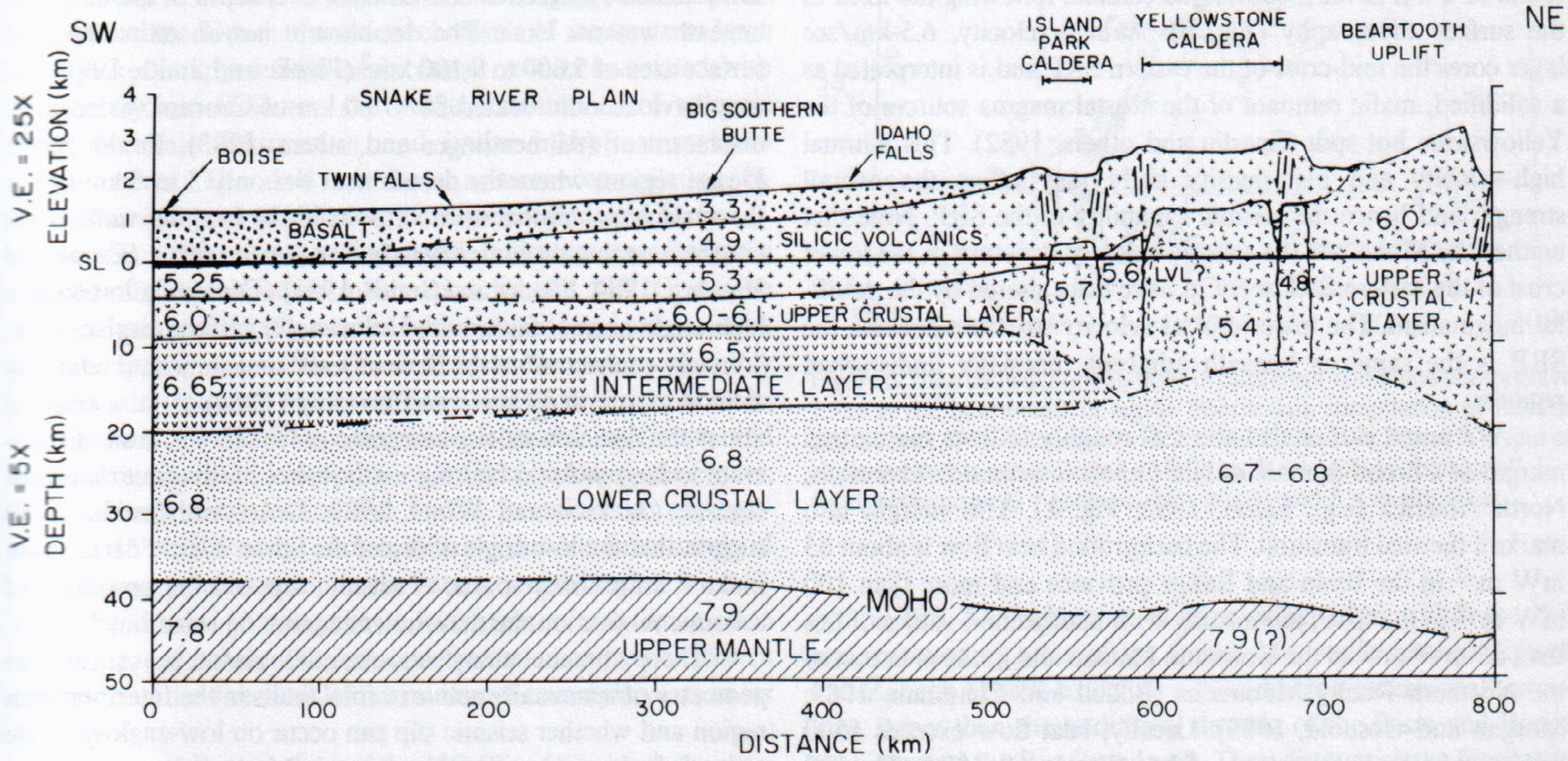

Figure 5. Cross section of crustal structure along the Snake River Plain in Idaho (representative of part of the central ISB) into the Beartooth uplift of Montana (representative of the northern ISB). Superposed numbers indicate P-wave velocities (km/sec). Data from 1978 and 1980 Yellowstone–Snake River Plain seismic-refraction experiment (Braile and others, 1982; Smith and others, 1982).

lithosphere on the east. The two profiles shown in Figure 4 extend from the central Basin and Range province in Nevada, where the Moho is about 30 km deep (below sea level) and the upper-mantle P_n velocity is 7.8 km/sec, to the Colorado Plateau–Middle Rocky Mountain provinces in Utah and Wyoming, where the Moho depth slightly exceeds 40 km and the P_n velocity reaches 8.0 km/sec. There is uncertainty about the depth of the true Moho beneath the transition region. If the top of a 7.8 to 7.9-km/sec layer marks the Moho beneath the Wasatch Front region of Utah (Fig. 4a), as identified by Loeb and Pechmann (1986), then the crust-mantle boundary is as deep as 45 km beneath the transition. Alternative interpretations imply the depth to the Moho may be as shallow as 25 km if observed velocities of 7.4 to 7.5 km/sec (Fig. 4) are the result of down-dip ray paths (see Smith and others, 1989, Fig. 4; Pakiser, 1989).

The P-wave velocity structure of the upper crust beneath the Y-SRP volcanic province, revealed by refraction/wide-angle reflection profiles, is more laterally heterogeneous than in the surrounding thermally undisturbed areas of the ISB. At Yellowstone a caldera-wide low-velocity body extends to depths of about 15 km and is thought to reflect a remnant magma reservoir with materials ranging from melts to hot, cooling granitic rocks (Smith and others, 1982). Along the SRP, the systematic decrease in elevation southwestward away from the caldera also reflects a systematic change in crustal structure. The near-surface basaltic layer thins northeastward from 2 km in southwestern Idaho, the suggested beginning of the trace of the Yellowstone hot spot, to zero thickness at Yellowstone; correspondingly, the deeper silicic layer thickens northeastward from zero thickness in southwestern Idaho to 2 km at the Yellowstone caldera, following the form of the surface topography (Fig. 5). A high-velocity, 6.5-km/sec layer cores the mid-crust of the eastern SRP and is interpreted as a solidified, mafic remnant of the crustal magma sources of the Yellowstone hot spot (Sparlin and others, 1982). This unusual high-velocity and high-density body may affect the overall strength and hence the seismic capability of the SRP. Note that neither the Moho nor the seismic velocity structure of the lower crust of the eastern SRP seem to have been altered by the youthful magmatism. The lower-crustal velocity structure beneath the SRP is the same as beneath adjacent thermally undisturbed regions.

We noted earlier that the ISB roughly follows the eastern margin of a broad domain of late Cenozoic extension in western North America (e.g., Eaton, 1982, Fig. 1). This margin also marks a thermal transition. The background heat flow is about 85 mW m^{-2} in the Basin and Range province and more than 100 mW m^{-2} in the SRP, contrasting with background values of less than 65 mW m^{-2} in the Colorado Plateau and in the area east of the Northern Rocky Mountains (Bodell and Chapman, 1982; Morgan and Gosnold, 1989). Locally, heat flow exceeds 1500 mW m^{-2} in the Yellowstone caldera (Blackwell, 1989). The ISB thus follows a structural and thermal transition to more stable continental interior with lower heat flow. The transition may be a locus of active lithospheric thinning (see Fig. 4A), occurring in general along the eastern margin of a regional-scale thermotectonic anomaly in the upper mantle. Effects of an active mantle hot spot associated with the Y-SRP system (discussed in a later section) are a special case.

Seismic-reflection profiling across Tertiary-Quaternary basins and active fault zones in the Basin and Range province has provided important information on upper-crustal structural style. The superposition of basin-range faulting upon pre-Neogene thrust belt structure, especially along the eastern margin of the Basin and Range province, is well known to be a fundamental and complicating factor (e.g., Smith and Bruhn, 1984). Anderson and others (1983), Allmendinger and others (1983), Smith and Bruhn (1984), and Smith and others (1989) have interpreted seismic-reflection data from throughout the northern Basin and Range province, identifying three characteristic styles of extensional basin development in the region: (1) relatively simple basins bounded by one or more planar normal faults dipping 45° to 60°; (2) asymmetric tilted basins displaced chiefly by a listric or planar low-angle normal fault; and (3) complex basins, typically with subbasins, associated with both planar and listric normal faults that sole into low-angle detachments.

Low-angle detachment faulting may have contributed substantially to Cenozoic crustal extension in at least part of the Intermountain region. The best example is the case of the Sevier Desert detachment (see sawteeth pattern beneath the Sevier Desert in Fig. 4A). High-quality seismic-reflection data (Allmendinger and others, 1983; Smith and Bruhn, 1984; Planke and Smith, 1991) show that the Sevier Desert detachment extends laterally with an average 10° to 15° westward dip at least 70 km from near the surface in central Utah to a depth of about 15 km beneath western Utah. The detachment has an estimated total surface area of 5,600 to 9,100 km^2 (Planke and Smith, 1991) and may have accommodated 30 to 60 km of Cenozoic extensional displacement (Allmendinger and others, 1983). In the Sevier Desert region, where the detachment lies only 3 to 5 km below the surface, prominent normal faults in the hanging wall do not cut the detachment but either abut or merge with it (Crone and Harding, 1984; Planke and Smith, 1991). The configuration of a high-angle normal fault, with Holocene(?) surface displacement, "directly connected" to the Sevier Desert detachment at relatively shallow depth, led Crone and Harding (1984) to raise concern about the detachment's seismogenic potential. Reviews of moderate to large normal-faulting earthquakes in diverse extensional regimes (Jackson and White, 1989; Doser and Smith, 1989) suggest that the low angle of dip of the Sevier Desert detachment make it an unlikely source of seismic slip, but the possibility of aseismic motion on the detachment cannot be ruled out.

There remain many uncertainties about the subsurface geometry of seismically active normal faults in the Intermountain region and whether seismic slip can occur on low-angle or listric normal faults known to be present. Moderately- to steeply-dipping planar geometries for the seismically active faults are typically inferred from aftershock locations and from the focal mechanisms of large earthquakes (e.g., Smith and others, 1985), a

point we pursue later in this paper. Nevertheless, seismic-reflection evidence suggests that some segments of major normal faults with late Quaternary surface ruptures indeed have a listric subsurface geometry (Smith and Bruhn, 1984; Smith and others, 1989).

Throughout this paper we emphasize that the late Cenozoic structural style of the Intermountain region is dominated by normal faulting. There is growing awareness of the importance of strike-slip faulting as part of Neogene extensional deformation in the Basin and Range Province (Anderson, 1989), particularly in parts of the southern and western Great Basin (Rogers and others, this volume). In the Intermountain region, the best geologic evidence for Neogene strike-slip deformation is in the Sevier Valley area of south-central Utah (near Richfield, Fig. 3; Anderson and Barnhard, 1987). Focal mechanisms of background earthquakes in that same area also imply strike-slip faulting (Arabasz and Julander, 1986). Strike-slip focal mechanisms have also been observed for historical moderate-sized earthquakes in the northern ISB of Montana (Doser, 1989a), in the Hansel Valley area of northwestern Utah (near HV, Fig. 3; Doser, 1989b), and in southeastern Nevada (Smith and Sbar, 1974). Our present understanding of extension in the Intermountain region may underestimate the importance of strike-slip deformation.

Contemporary deformation

Regional stress field. Stress observations give important information about the pattern and mechanics of intraplate extension in the Intermountain region. Figure 6 shows the orientations of minimum horizontal compressive stress, S_{hmin}, variously deduced from the T-axes of focal mechanisms of moderate to large earthquakes, mapped fault-displacement vectors associated with Quaternary and Holocene slip events, orientations of volcanic dikes, borehole deformation, and in-situ hydrofracture stress measurements. The data are from a recent compilation by Zoback and Zoback (1989) for the continental United States.

Focal mechanisms and geologic indicators are the main sources of available stress information for the ISB. Given the ambiguity of selecting the correct fault plane in focal mechanisms, the principal stress axis directions were determined by assuming the standard Coulomb failure criterion with a coefficient of internal fraction of zero. This constraint places the maximum and minimum principal stress directions (corresponding to the P-axes, for maximum compression, and T-axes, for minimum compression) at 45° to the nodal planes. Because the dominant mode of contemporary deformation in the Intermountain region is extension, the T-axes give a general indication of relative motion within areas of coherent intraplate deformation and are consistent indicators of the directions of the minimum compressive stress for this region.

The overall stress field of the ISB (Fig. 6) is generally characterized by NE-trending S_{hmin} orientations in the northern ISB and the western part of the central ISB and ENE-to-ESE-trending S_{hmin} orientations in the southern ISB and the eastern part of the central ISB. The coherence of these orientations within the ISB and surrounding areas of the Rocky Mountains has led Zoback and Zoback (1989) to define a "Cordilleran extensional" province, larger than the traditional domain of the Basin and Range province and the Rio Grande rift. They distinguish the interior of the Colorado Plateau, however, as a distinct stress province with a WNW-trending orientation of maximum horizontal compressive stress S_{Hmax}. This is reflected in Figure 6 by the difference in

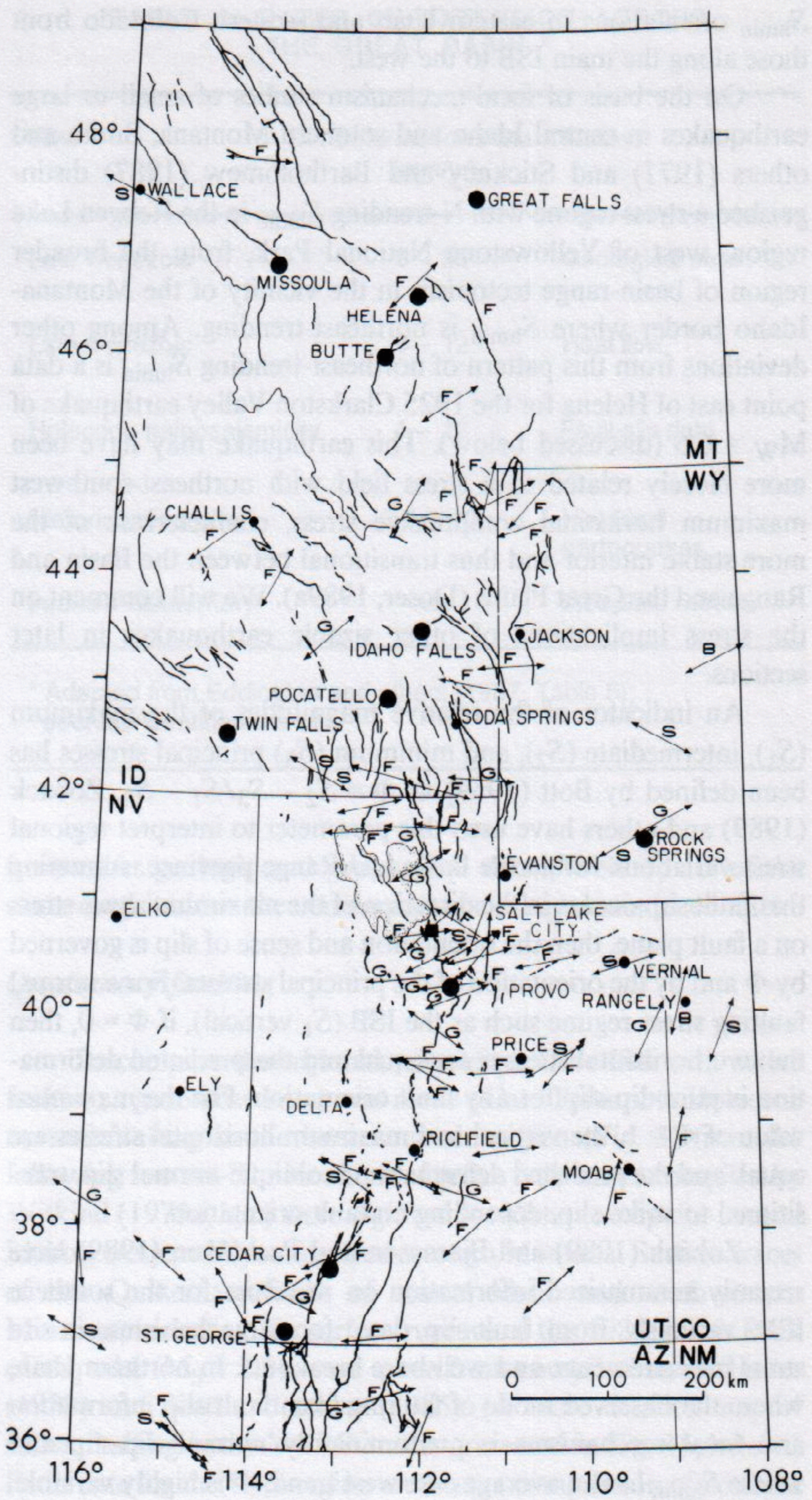

Figure 6. Map showing orientations of minimum horizontal compressive stress in the Intermountain region from a data compilation of Zoback and Zoback (1989), together with selected faults, as in Figure 3. Types of stress indicators are indicated as follows: B = borehole "breakout", F = focal mechanism, G = geologic, M = mixed, and S = in situ stress.

S_{hmin} orientations in eastern Utah and western Colorado from those along the main ISB to the west.

On the basis of focal-mechanism studies of small to large earthquakes in central Idaho and southern Montana, Smith and others (1977) and Stickney and Bartholomew (1987) distinguished a stress regime with N-trending S_{hmin} in the Hebgen Lake region, west of Yellowstone National Park, from the broader region of basin-range tectonism in the vicinity of the Montana-Idaho border where S_{hmin} is northeast-trending. Among other deviations from this pattern of northeast-trending S_{hmin} is a data point east of Helena for the 1925 Clarkston Valley earthquake of M_W = 6.6 (discussed below). This earthquake may have been more closely related to a stress field with northeast-southwest maximum horizontal compressive stress, characteristic of the more stable interior and thus transitional between the Basin and Range and the Great Plains (Doser, 1989a). We will comment on the stress implications of other sizable earthquakes in later sections.

An indicator of the relative magnitudes of the maximum (S_1), intermediate (S_2), and minimum (S_3) principal stresses has been defined by Bott (1959) as $\Phi = S_2 - S_3/S_1 - S_3$. Zoback (1989) and others have used this parameter to interpret regional stress variations within the Basin and Range province. Assuming that fault slip occurs in the direction of the maximum shear stress on a fault plane, then the orientation and sense of slip is governed by Φ and by the orientation of the principal stresses. For a normal faulting stress regime such as the ISB (S_1 vertical), if $\Phi = 0$, then the two horizontal stresses are equal and the predicted deformation is pure dip-slip for any fault orientation. For the maximum value of $\Phi = 1$, the vertical and maximum horizontal stresses are equal, and the predicted deformation is oblique-normal slip, transitional to strike-slip, depending on fault orientation.

Zoback (1989) and Bjarnason and Pechmann (1989) have recently summarized information on Φ-values for the southern ISB, variously from fault-slip data, focal mechanisms, in-situ stress measurements, and well-bore breakouts. In northern Utah, where the observed mode of faulting from fault-slip information and focal mechanisms is predominantly normal dip-slip and where S_{hmin} has an average east-west trend, Φ is highly variable. Averaged values of Φ (Zoback, 1989; Bjarnason and Pechmann, 1989) range from low values (0.0 to 0.3) for in-situ stress measurements and well-bore breakouts through intermediate values (0.3 to 0.7) for late Quaternary fault-slip measurements to slightly higher values (0.5 to 0.9) for focal mechanisms. In south-central Utah along the Basin and Range–Colorado Plateau transition, there is an observed mixture of dip-slip and strike-slip deformation, both in focal mechanisms (Arabasz and Julander, 1986) and in fault slip (Anderson and Barnhard, 1987). The observations can be explained by a high Φ-value and local changes in the relative magnitudes of (near-equal) vertical and maximum horizontal principal stresses under a relatively constant east-trending S_{hmin} (see Zoback, 1989). Bjarnason and Pechmann (1989) and Zoback (1989) have independently calculated an average Φ-value of 0.8 for grouped focal mechanisms in this area. There is little information on Φ-values for the central and northern ISB, except for a study of the main shock and aftershocks of the 1983 Borah Peak, Idaho, earthquake by Smith and others (in preparation), who find a Φ-value of 0.65, consistent with the observed oblique-normal faulting (described below).

Strain rates. Earthquake focal mechanisms and seismic moments have been used by Eddington and others (1987) to calculate regionalized strain rates and corresponding deformation rates produced by historical earthquakes in the western United States, following the method of Kostrov (1974). Available results for the central and southern ISB are shown in Figure 7. The figure shows 14 selected areas of inferred homogeneous stress in which the moment tensors of historical earthquakes have been summed and diagonalized to get the direction and magnitude of horizontal principal strain. Together with the S_{hmin} orientations in Figure 6,

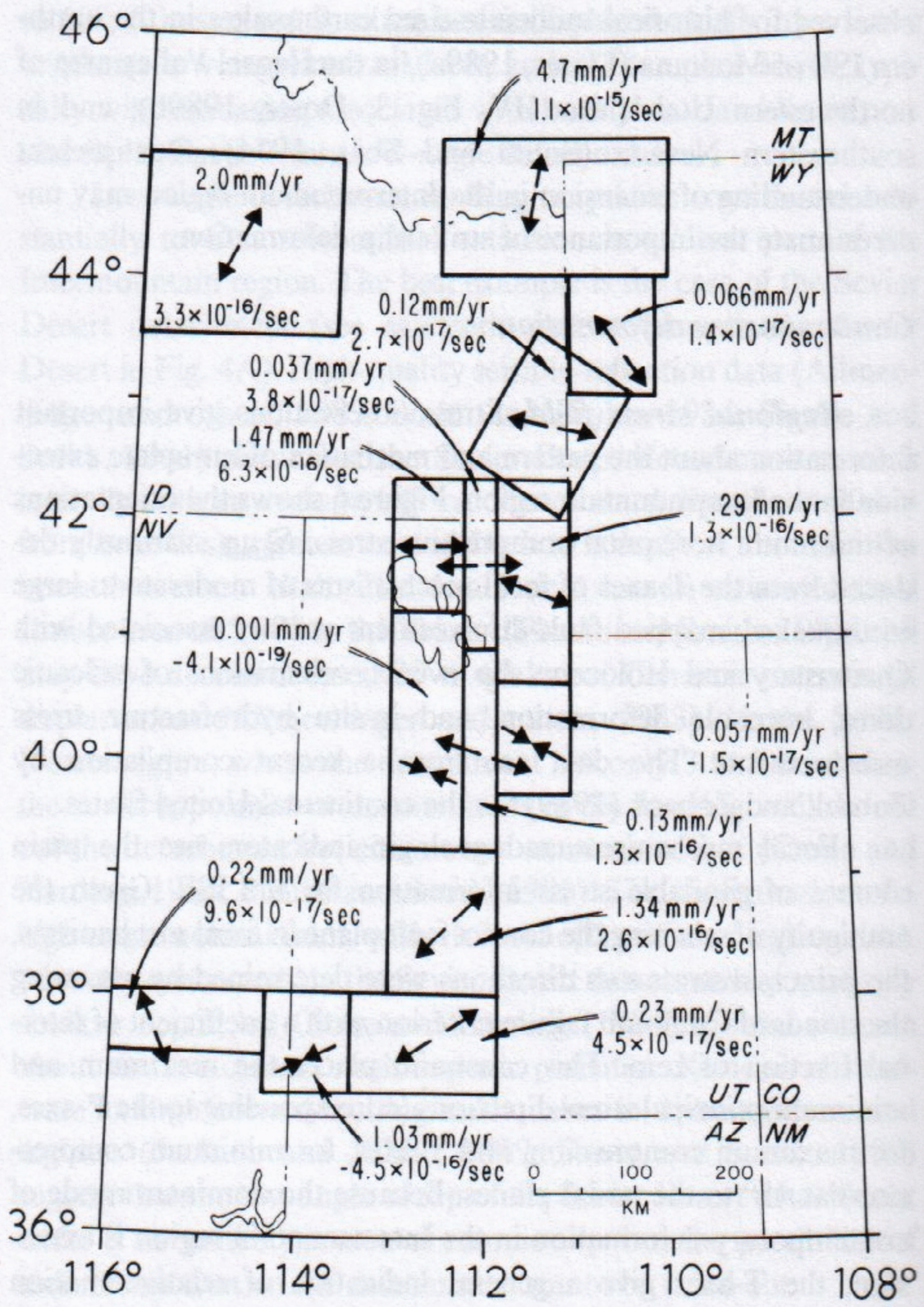

Figure 7. Strain and deformation rates in part of the Intermountain region based upon summations of seismic moments from historical earthquakes, after Eddington and others (1987). Earthquakes within areas of assumed homogeneous strain, shown by boxes, were used to determine the summed seismic moment. Information shown for each box includes: orientation of the horizontal principal strain axis (arrows); the deformation rate, in mm/yr (upper number); and the horizontal strain rate, in sec^{-1} (lower number).

the strain-rate and deformation data in Figure 7 provide an overall perspective of contemporary deformation in the central and southern ISB.

In the central ISB (Figure 7, top), historical seismicity in central Idaho implies NNE–SSW extensional strain and yields a strain rate of the order of 10^{-16}/sec. In the Hebgen Lake–Yellowstone Park region to the east, the most seismically active region of the entire U.S. Cordillera, the extensional strain rate of 1.1×10^{-15}/sec (4.7 mm/yr deformation rate) is more than three times greater, and the horizontal principal strain axis trends more northerly. For parts of the central ISB south of Yellowstone Park, much smaller extensional strain rates of the order of 10^{-17}/sec and deformation rates of 0.07 to 1.2 mm/yr were calculated. The northwest-southeast direction of horizontal principal strain in the Teton region is considered uncertain because of sparse data; in southeastern Idaho, a better-resolved extensional strain direction is nearly east-west.

In the southern ISB, general east-west extensional strain of the order of 10^{-16}/sec or smaller characterizes Utah's Wasatch Front area. Deformation rates range from 0.001 mm/yr in the western part of the Wasatch Front area to 1.5 mm/yr in the northwestern part. Regarding the latter subregion, we note that the depicted strain information would not be significantly affected by a recently revised focal mechanism (Doser, 1989b) implying predominantly strike slip rather than dip slip for the M = 6.6 Hansel Valley earthquake of 1934. Because the direction of the T-axis for the revised solution (Doser, 1989b) is nearly identical to that for the original dip-slip solution (Dewey and others, 1973) used by Eddington and others (1987), the averaged moment rate and direction of deformation given in Figure 7 would not be significantly changed. In southern Utah, extensional strain rates of 10^{-16}/sec to 10^{-17}/sec are comparable to those for most of the Wasatch Front area, but the strain direction is northeast-southwest. A possible change to northeast-southwest compression is suggested for one subregion in southwesternmost Utah. The significance of this local apparent change in mode of deformation is uncertain. The northwest-southeast extensional strain direction shown for a subregion in southeastern Nevada is consistent with that for other parts of southern and central Nevada analyzed by Eddington and others (1987).

Deformation rates intrinsically depend on the dimensions of the subregion being considered, so comparisons must be made with care. Nevertheless, data summarized by Eddington and others (1987) for the western United States make it evident that deformation rates for most of the intraplate ISB are one to two orders of magnitude lower than those along the western North American plate boundary. The ISB deformation rates can be evaluated in another way. Eddington and others (1987) summed earthquake deformation rates along east-west profiles across the northern and southern Great Basin, including the ISB, to obtain integrated extension rates of 8 to 10 and 3 to 4 mm/yr, respectively, with approximately 1 mm/yr taken up across the ISB (Doser and Smith, 1982). Estimates of Late Cenozoic total deformation rates of 1 to 20 mm/yr for the Great Basin determined from other geologic and geophysical data (Table 1) are of the same magnitude as the contemporary earthquake-induced rates.

TABLE 1. RATES OF EXTENSION ACROSS THE GREAT BASIN *

Time	Deformation Rate (mm/yr)	Method
Late Cenozoic	3 - 20	Geological strain
Late Cenozoic	3 - 12	Heat flow
Holocene paleoseismicity	1 - 12	Fault-slip data
Historic seismicity	3.5 - 10	Historical earthquakes
Inferred Quaternary	<9	Intraplate models

* Adapted from Eddington and others (1987, Table 5); sources identified therein.

Quaternary faulting

To compare the regional seismicity of the ISB with active faulting, a generalized map was made of late Tertiary to Holocene normal faulting in the Intermountain region (Fig. 3) from the following sources. The locations of active fault traces compiled by Witkind (1975a, b, c) were digitized for Idaho (except for central Idaho), western Wyoming, and western Montana. Surface traces of late Quaternary faults of central Idaho and southwestern Montana, including the surface rupture of the 1983 Borah Peak earthquake (M_S = 7.3), were taken from compilations by Haller (1988) and Scott and others (1985). (A more detailed map of active faulting in the Y-SRP area is presented in Fig. 15, below.) Fault data for the Utah region are from a compilation of Arabasz and others (1987) for the Wasatch Front area (outlined in Fig. 3), supplemented elsewhere by data from Anderson and Miller's (1979) Quaternary fault map of Utah. Quaternary faults for northern Arizona are from the Arizona Quaternary fault map of Scarborough and others (1986). We did not attempt to make a complete compilation of fault data for eastern Nevada as this area was considered marginal to our discussion. Figure 3 thus serves as a fair representation of known or suspected active faults in late Cenozoic time in the Intermountain region, but we caution that the fault compilation is non-uniformly complete.

Age of normal faulting and correlation with topography. Dating the inception and evolution of normal faulting on individual faults in the Intermountain region is generally handicapped by a lack of suitable exposures and datable materials. There are some exceptions. Geochemical studies of altered fault

rock in the exhumed footwall of the Wasatch fault (Parry and Bruhn, 1986, 1987) indicate an origin at 11 km depth 17.6 ± 0.7 m.y. ago. The Teton fault in Wyoming has a total vertical displacement of as much as 6 to 9 km that began 7 to 9 m.y. ago (Love and Reed, 1971). On a regional basis, there is evidence for two stages of Cenozoic extensional tectonism and normal faulting in many parts of the Basin and Range province. As reviewed by Levy and Christie-Blick (1989) and Anderson (1989), a first early stage of Cenozoic extension began about 37 Ma and was apparently restricted to a relatively narrow region of high strain in eastern Nevada, western Utah, and southern Idaho and was accompanied by calc-alkaline volcanism, detachment faulting, and core-complex formation. The second stage was the classic episode of Basin and Range extension and epeirogeny responsible for the present topography and the steeply dipping normal faults of the ISB. This modern stage generally began 15 to 10 Ma in the northern Basin and Range province, but earlier in the southern part of the province.

The distinctive north–northeast- to northwest-trending basin-range topography of the ISB involves sediment-filled basins and tilted range blocks bounded by large normal faults with significant Quaternary displacement. The observed coseismic deformation associated with normal faulting during large earthquakes and theoretical modeling suggest that both footwall uplift of the mountain blocks and hanging-wall subsidence of the adjacent asymmetric basins have been fundamental in developing basin-range topography (e.g., King and others, 1988; see also Fig. 24, below). For individual ranges, relative crest height along the range seems to correlate with the size and frequency of young fault displacements along the base of the range. For example, along the Teton fault in Wyoming, the maximum heights of Quaternary scarps ranging up to 50 m high correspond with the highest parts of the Teton Range (Smith and others, 1990a, b). The 1983 Borah Peak earthquake (M_S = 7.3) ruptured one of the most active central segments of the Lost River fault zone, which was coincidentally adjacent to the highest part of the Lost River Range (Scott and others, 1985), including Borah Peak, the highest point in Idaho. Crest heights along the Wasatch Range are greater along the active central segments of the Wasatch fault than along distal segments with lower late Pleistocene–Holocene slip rates (Schwartz and Coppersmith, 1984). Relative topographic relief serves as an indicative but insufficient guide to the location of segments of range-front normal faults likely to produce future surface-faulting earthquakes.

Threshold of surface faulting and maximum magnitude

Summaries of information and discussion about the minimum magnitude needed to produce coseismic surface faulting in the Intermountain region are given by Doser (1985a) and Arabasz and others (1987). The threshold magnitude appears to be in the range of $6.0 \leqslant M_L \leqslant 6.5$, based on the historical record of earthquakes in the ISB and in the Basin and Range province. Arabasz and others (1987) adopt $M_L = 6.3 \pm 0.2$ as an estimate of the threshold in the Utah region and argue that earthquakes up to this size can occur anywhere in the southern ISB, even where there is no geologic evidence for Quaternary surface faulting.

The M_S = 7.5 Hebgen Lake earthquake of 1959 (described in detail herein) is considered by some to represent the maximum earthquake size for the ISB (e.g., Doser, 1985a). This earthquake, however, was smaller than at least two other large earthquakes in the Basin and Range province. The 1872 Owens Valley, California, earthquake had an estimated moment magnitude of 7¾ to 8 and was associated with a predominantly strike-slip surface rupture up to 110 km long, with a maximum lateral offset of 7 m and a maximum vertical offset of 4.4 m; the 1915 Pleasant Valley, Nevada, earthquake of surface-wave magnitude 7.6 had a 60-km-long rupture and a maximum vertical displacement of 5.8 m (dePolo and others, 1989). The Hebgen Lake earthquake had a shorter rupture length, but had comparable displacement to these two earthquakes. Because there are adjoining fault segments in the ISB with potential rupture lengths exceeding that of the Hebgen Lake earthquake, and comparable to those of the Pleasant Valley and Owens Valley earthquakes, it is reasonable to consider maximum-magnitude earthquakes slightly greater than M_S = 7.5 for particular faults in the ISB (e.g., Arabasz and others, 1987, adopt a maximum magnitude of Ms = 7.5 to 7.7 for the Wasatch Front area).

Estimates of the maximum magnitude for earthquakes on any particular fault in the ISB have uncertainties relating not only to the prediction of future rupture characteristics but also to the conversion of those rupture characteristics to estimated magnitudes. This problem is particularly important for seismic hazard analysis. For example, in an evaluation of probabilistic ground shaking for the Wasatch Front, Youngs and others (1987) used fault length-magnitude relations of Bonilla and others (1984) to estimate maximum magnitudes of M_S = 7.2 to 7.5 for the longest segments of the Wasatch fault in northern Utah. In a seismotectonic study of the Jackson Lake dam in Wyoming, Gilbert and others (1983) selected a maximum credible earthquake of magnitude (unspecified scale) 7.5 based on comparisons of observed scarp lengths and fault length with rupture length-magnitude relations such as those of Slemmons (1977). Thenhaus and Wentworth (1982) suggested a maximum magnitude of 7½ for eastern Idaho and central and western Utah, and adopted a value of 7¾ specifically for the Wasatch fault. For a site at the Idaho National Engineering Laboratory near Idaho Falls, Idaho, Woodward-Clyde Consultants (1979) relied upon a global compilation of data for surface-faulting earthquakes to assign a peak ground acceleration, using the 1959, M_S = 7.5 Hebgen Lake earthquake as a maximum-magnitude event for that area.

THE EARTHQUAKE RECORD IN THE INTERMOUNTAIN REGION

The traditional earthquake record for the Intermountain region—consisting of historical seismicity (based on non-instrumental reports of felt earthquakes) and instrumental

seismicity—is much less substantial than for other parts of the United States. This is because of the region's relatively late settlement, historically sparse population, and late seismographic coverage. In contrast, comparatively abundant information has been gathered in this part of the United States on the timing and character of prehistoric earthquakes from paleoseismology. In this section, we restrict attention to the traditional earthquake record.

Pre-instrumental information

Reports of historical seismicity in the Intermountain region date only from the mid 1800s when systematic modern settlement began. Diverse Indian cultures were well established in the region after A.D. 100 to 1300 but left no known record of specific felt earthquakes. During the 1820s and 1830s, a few hundred fur trappers made up most of the non-Indian population of the region. Mormon pioneers entered the Salt Lake Valley in 1847 and promptly started a regional colonizing program. Within a few decades, Mormon settlements extended throughout large portions of the Intermountain West (Wahlquist, 1981), with the exception of Montana, where the settlements began chiefly as mining camps after the 1850s. The first documented earthquakes in the Intermountain region date from 1850 in Utah (Arabasz and McKee, 1979), 1869 in Montana (Qamar and Stickney, 1983), 1871 in Wyoming (Hayden, 1872), and 1879 in Idaho (Townley and Allen, 1939). The highly non-uniform distribution of population before 1900 throughout the Intermountain region implies great variability in the threshold of detection and in location errors for pre-instrumental earthquakes.

The pre-instrumental earthquake record for the Intermountain region comes from multiple sources. Coffman and others (1982) cite many early reports, records, and compilations for earthquakes in the "Western Mountain Region" before 1928. For 1928 and later, annual reports published by the U.S. Department of Commerce under the title *United States Earthquakes* are key sources. Williams and Tapper (1953) made an important historical study of Utah earthquakes from 1850, the time of publication of the first newspaper in Utah, through 1949. Cook and Smith (1967) extended this record to 1965, including computer determinations of the first instrumental seismicity for the Utah region from systematic regional recording. Modern compilations of historical seismicity in the study area include those of Arabasz and McKee (1979) and Stover and others (1986), for the Utah region, and Qamar and Stickney (1983) for Montana.

Instrumental recording and seismic networks

Seismographic recording in the Intermountain region began with the installation of two modified Bosch-Omori pendulum seismographs on the University of Utah campus in Salt Lake City in 1907 (Arabasz, 1979). Figure 8 shows stages of subsequent instrumental coverage of the Intermountain region in 1948, 1968, and 1988. By 1948, electromagnetic seismographs were operating in at least eight locations in the region (dated circles, Fig. 8A). Systematic reporting of seismological data to the U.S. Coast and Geodetic Survey (USCGS) from Salt Lake City began in 1938, one year before the Bosch-Omoris were replaced by more modern instruments (Arabasz, 1979). For each of the other dated stations shown in Figure 8A, reporting to the USCGS began immediately after installation (see *United States Earthquakes*).

In 1968, there were at least 25 seismographic stations in the study area (triangles, Fig. 8A), virtually all with on-site recording. The changes from 1948 to 1968 almost exclusively reflect additions in the 1960s (see Poppe, 1980). These relate to stations in the western part of the area shown in Figure 8A installed with the motivation, in part, to record underground nuclear explosions from the Nevada Test Site, the development in Utah of a skeletal statewide network (Arabasz and others, 1979), local monitoring of mining-related seismicity in east-central Utah and in northern Idaho, dam-site monitoring at Flaming Gorge and Glen Canyon (Lake Powell) (Fig. 3), and added USGS coverage of the Hebgen Lake–Yellowstone area. The 1968 "snapshot" misses the presence of scattered Department of Defense, LRSM mobile seismic observatories operated on a temporary basis in the mid 1960s at a few dozen sites throughout the Intermountain region (see Poppe, 1980). The time frame does include, however, operation of a Department of Defense, VELA–Uniform array at the Uinta Basin Observatory (UBO) in northeastern Utah. Figure 8A also includes WWSSN stations installed in 1962 at Dugway (DUG), Utah, and in 1963 west of Bozeman (BOZ), Montana. The latter station operated until 1968 and was moved to Missoula, Montana, in 1973.

By the mid to late 1970s, short-period seismic telemetry networks had become well established in the Intermountain region. Seismographic coverage of the region shown for 1988 (Fig. 8B), with a total of nearly 150 stations, is chiefly a composite of three regional and five local networks (see caption for Fig. 8B). Representative reporting and details for some of the network monitoring are given by Stickney (1988) for Montana, Peyton and Smith (1990) for Yellowstone, King and others (1987) for eastern Idaho, Wood (1988) for western Wyoming–eastern Idaho, Nava and others (1990) for the Utah region, and Rogers and others (1987) for southern Nevada. (See also Wong and Humphrey, 1989, regarding local network monitoring within the Colorado Plateau of southeastern Utah between 1979 and 1987.)

Earthquake catalog

In this chapter we use the catalog through 1985 of Engdahl and Rinehart (1988; this volume), compiled for the 1988 Seismicity Map of North America and hereafter referred to as the DNAG catalog, in order to present an overview of the whole Intermountain region. Original pre-instrumental data are chiefly from sources already described in a preceding section. Sources of instrumental data vary with time, depending on the evolution of seismographic coverage in the region. Instrumental locations for sizable earthquakes in the Intermountain region were made in the

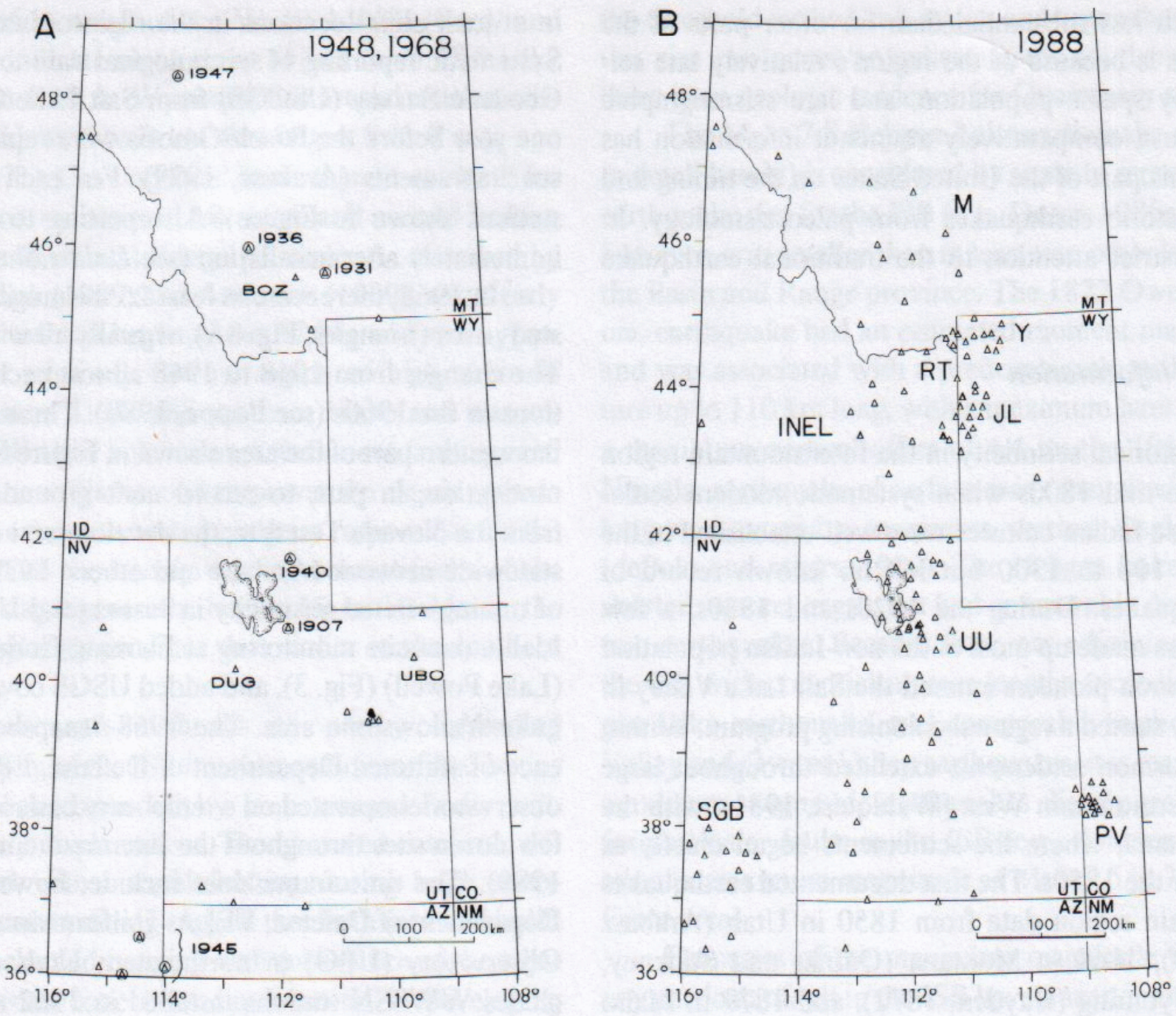

Figure 8. Maps showing representative distribution of seismographic stations in the Intermountain region at three selected times. A, Stations operating in 1948 (circles dated with year of installation) and in 1968 (triangles); circumscribed triangles, both 1948 and 1968. Key: 1907 = Salt Lake City; 1931 = Bozeman; 1936 = Butte; 1940 = Logan; 1945 = Boulder City, Overton, and Pierce Ferry (all surrounding Lake Mead). B, Stations operating in 1988, chiefly as parts of separate seismic networks. Key to seismic networks (from north to south): M = Montana (Montana Bureau of Mines and Geology, 12 sta., from ca. 1980); Y = Yellowstone (U.S. Geological Survey and University of Utah, 16 sta., from 1973); RT = Ricks-Teton (Ricks College, 5 sta., from 1972); JL = Jackson Lake (U.S. Bureau of Reclamation, 16 sta., from 1985); INEL = Idaho National Engineering Laboratory (6 stations, from ca. 1972; UU = University of Utah (57 sta. operated, 82 sta. recorded, from 1974); PV = Paradox Valley (U.S. Bureau of Reclamation, 15 sta., from 1983); SGB = Southern Great Basin (U.S. Geological Survey, 54 sta. [not all within figure], from 1978).

1920s to 1940s by the California Institute of Technology (Gutenberg and Richter, 1954) and routinely after the 1930s by the USCGS and later the U.S. Geological Survey (see *United States Earthquakes*). Figure 8A makes it evident that instrumental locations before the 1960s had to be based on recordings at widely spaced stations in the western U.S.

In mid-1962, the University of Utah began regional instrumental monitoring that later allowed compilation of an important catalog for the Utah region (36.75° to 42.50°N, 108.75° to 114.25°W), predating the installation of a modern (telemetered) regional network in 1974 (Arabasz and others, 1980). These data and subsequent, modern regional-network data make up primary sources of instrumental information in the DNAG catalog for the region (Engdahl and Rinehart, 1988). The latter include data from the University of Utah, the Montana Bureau of Mines and Geology, the Idaho National Engineering Laboratory, and the U.S. Geological Survey (Yellowstone National Park and southern Nevada). Other relevant data sources and compilations are described by Eddington and others (1987).

Time-varying thresholds of completeness since 1900 in the DNAG catalog are suggested by Engdahl and Rinehart (1988; this volume). For the study area, the overall record is best for the Utah region, where the threshold has been about magnitude 2.5 (3.0 in some distal areas) since 1962 and about magnitude 5¾ (Modified Mercalli Intensity VII) for perhaps the entire historic record (Rogers and others, 1976). For the region as a whole, our own subjective judgment indicates catalog completeness above magnitude 5¾ since 1900, above magnitude 5.0 since the 1920s to 1930s, and above magnitude 4.0 since the 1960s. Thresholds of completeness at and below magnitude 2.5 are associated with

the modern regional network recording, but current completeness for the entire Intermountain region based on that recording (Fig. 8B) is at about magnitude 3.0.

The precision of instrumental earthquake locations in the region varies considerably in time and space (see original sources of data). Revised epicenters for instrumentally recorded earthquakes before the 1960s generally have uncertainties of tens of kilometers (e.g., Dewey and others, 1973; Qamar and Hawley, 1979). For earthquakes since the 1960s, epicentral precision reaches ±2 km or better within areas where seismographic spacing is of the order of a few tens of kilometers—as for some of the modern networks (Fig. 8B). Where the station spacing becomes greater, epicentral uncertainties are typically ±5 km, commonly increasing to ±10 km for events outside or in a distal part of the recording network. Reliable focal depths, requiring the presence of a recording station within roughly one focal depth of an earthquake's epicenter, are available for only a small fraction of the earthquakes in the DNAG catalog for the region.

Largest historical earthquakes

For the period from 1900 through 1985, the DNAG catalog contains 49 earthquakes in the Intermountain region with an indicated magnitude of 5.5 or greater, a selected threshold related to the potential for seriously damaging ground motions. These earthquakes are listed in Table 2 and plotted in Figure 9. The conventional magnitudes given in Table 2 are representative estimates, not necessarily the values listed in the DNAG catalog. Locations plotted in Figure 9 are directly from the DNAG catalog; refined locations, where available, are substituted in Table 2. In the following subsections we sequentially describe: (1) two known historical shocks of estimated magnitude 5.5 or greater from the pre-1900 period; (2) the four largest earthquakes in the Intermountain region's recorded history—all later than 1900, all with moment magnitudes greater than 6.5, and all but one with associated surface faulting (Table 2); and (3) other significant earthquakes after 1900 within each of the three main parts of the ISB. The descriptions are necessarily abbreviated, commonly citing one or more relevant summaries in place of original sources. For brevity, MMI signifies Modified Mercalli intensity.

Pre-1900 period. Two significant earthquakes occurred in the Intermountain region during the pre-1900 historical period. An earthquake on November 9, 1884, at 02:00 (local time) was felt strongly in Idaho, Utah, and Wyoming over at least 15,000 km^2 (Williams and Tapper, 1953). Descriptions of damage, MMI = VIII, and reports of at least six shocks felt at Paris, Idaho, in the Bear Lake Valley led Arabasz and McKee (1979) to assign an epicenter at 42.0°N, 111.3°W, arbitrarily on the Idaho-Utah border astride the active East Bear Lake fault, and to estimate a magnitude of 6.3, assuming a relation between MMI and magnitude from Gutenberg and Richter (Richter, 1958). A magnitude of at least 5½ seems likely. On November 4, 1897, at 02:29 (local time) a sizable earthquake occurred in southwestern Montana, with an assigned location of 45.0°N, 113°W, causing damage and resulting in MMI = VI at Dillon, Montana (Coffman and others, 1982). Estimating a felt area of about 500,000 km^2, Qamar and Stickney (1983) assigned a magnitude of 6.4, using an empirical relation between magnitude and felt area for Montana earthquakes.

1925 Clarkston Valley, Montana, earthquake. This 1925 earthquake (No. 11, Table 2), the second largest historical earthquake in Montana, occurred about 50 km northwest of Bozeman in the vicinity of Clarkston Valley, a late Cenozoic intermontane basin bounded on the east by the Clarkston Valley normal fault (Qamar and Hawley, 1979). Despite its significant size (M_{GR} = 6¾, M_W = 6.6, Table 2), the earthquake apparently produced no primary surface faulting, although ground cracks were observed at several localities (Pardee, 1926). The earthquake reached MMI = VIII, was felt over 800,000 km^2, caused major rockfalls, and resulted in considerable damage at nearby towns (Coffman and others, 1982; Qamar and Stickney, 1983). Seismologic data for the main shock (Doser, 1989a; Doser and Smith, 1989) indicate a mainshock focal depth of about 9 km, a subsurface rupture length of about 12 km, and oblique normal slip on a northwesterly-dipping plane with an orientation similar to that of the southern end of the Clarkston Valley fault. The main shock was preceded by at least one sizable foreshock and was followed by aftershocks as large as magnitude 4.8 (Doser, 1990).

1934 Hansel Valley, Utah, earthquake. The 1934 Hansel Valley (Kosmo) earthquake (No. 15, Table 2) remains the largest earthquake in the Utah region since 1850 and the only historical shock in the southern ISB known to have produced surface faulting. The earthquake occurred about 60 km west of the Wasatch fault in a sparsely populated, basin-range setting at the northern end of the Great Salt Lake (Fig. 3-2). The earthquake was felt over an area of 440,000 km^2 and reached MMI = VIII; it caused relatively minor damage (Coffman and others, 1982), although two deaths resulted, one direct and one indirect (Cook, 1972). Richter (1935) used the earthquake as an example in defining his magnitude scale, assigning a magnitude of 7.0 (probably overestimated because of an uncertain distance correction to Pasadena). The conventional magnitude of 6.6 assigned by Gutenberg and Richter (1954) is apparently a surface-wave magnitude and is identical to the earthquake's modern moment magnitude, M_W, of 6.6 calculated by Doser (1989b).

Shenon (1936) provided key documentation of geologic effects of the earthquake, including surface ruptures, rock slides, liquefaction, and other ground-water effects (see Arabasz, 1979, Doser, 1989b, and dePolo and others, 1989, for reference to other original sources). Shenon (1934) mapped four northerly-trending subparallel fractures displacing salt flats and unconsolidated late Quaternary sediments in the southwestern part of Hansel Valley over a zone about 6 km wide and 12 km long (see Doser, 1989b). Displacements were primarily vertical, up to a maximum of 50 cm, but a horizontal offset of 25 cm was also reported (dePolo and others, 1989). The relation of the 1934 surface rupturing to local geologic structure and neotectonics is of

TABLE 2. EARTHQUAKES IN THE INTERMOUNTAIN SEISMIC BELT OF MAGNITUDE 5.5 AND GREATER, 1900 THROUGH 1985

No.	Date (GMT)		Time (GMT) hr mn	Lat. (°N)	Long. (°W)	Magnitude M_{conv}		M_w	Region	References
1.	1900	Aug 01	07:45	40.0	112.1	$(5\frac{1}{2}\pm)$	I/A	---	Eureka, Utah	1, 2, 3L
2.	1901	Nov 14	04:39	38.8	112.1	$(6\frac{1}{2}\pm)$	I/A	---	Southern Utah (Richfield)	1, 2, 3L
3.	1902	Nov 17	19:50	37.4	113.5	$(6\pm)$	I/A	---	Pine Valley, Utah	1, 2, 3L
4.	1905	Nov 11	21:26	42.9	114.5	$(5\frac{1}{2}\pm)$	I/A	---	South central Idaho (Shoshone)	2L, 4
5.	1909	Oct 06	02:50	41.8	112.7	$(6\pm)$	I/A	---	NW Utah (Hansel Valley)	1, 2, 3L
6.	1910	May 22	14:28	40.8	111.9	$(5\frac{1}{2}\pm)$	I/A	---	Salt Lake City, Utah	1, 2, 3L
7.	1912	Aug 18	21:12	36.5	111.5	$(5\frac{1}{2}\pm)$	I/A	---	NE of Williams, Ariz.	2L
8.	1914	May 13	17:15	41.2	112.0	$(5\frac{1}{2}\pm)$	I/A	---	Ogden, Utah	1, 2, 3L
9.	1921	Sep 29	14:12	38.7	112.2	$(6\pm)$	I/A	---	Elsinore, Utah	1, 2, 3L
10.	1921	Oct 01	15:32	38.7	112.2	$(6\pm)$	I/A	---	Elsinore, Utah, 2nd main shock	1, 2, 3L
11.	1925	Jun 28	01:21	46.00	111.50	$6\frac{3}{4}$	M_{GR}	6.6	Clarkston Valley, Mont.	(8, 12)L, (5, 6)S
12.	1928	Feb 29	22:38	46.6	112.0	$(5\frac{1}{2}\pm)$?	I/A	---	Helena, Mont.	7LS, 8S
13.	1929	Feb 16	03:00	46.1	111.3	5.6	I/A	---	Lombard, Mont.	8LS
14.	1930	Jun 12	09:15	42.6	111.0	5.8	REN	---	Grover, Wyo.	2L, 10S
15.	**1934**	**Mar 12**	**15:05**	**41.77**	**112.67**	6.6	M_{GR}	6.6	Hansel Valley, Utah	6S, 9LS
16.	1934	Mar 12	18:20	41.57	112.75	6	M_{GR}	5.9	Hansel Valley, Utah, aftershock	6S, 9LS
17.	1934	Apr 07	02:16	41.5	111.5 ?	5.5	REN	---	Hansel Valley, Utah,aftershock?	1, 7L, 10S
18.	1934	Apr 14	21:26	41.73	112.60	5.6	REN	---	Hansel Valley, Utah, aftershock	9L, 10S
19.	1934	May 06	08:09	41.96	112.82	$5\frac{1}{2}$	M_{GR}	---	Hansel Valley, Utah, aftershock	6S, 9L
20.	1935	Oct 12	07:50	46.62	111.97	5.9	I/A	---	Helena, Mont., swarm event	8LS, 11
21.	1935	Oct 19	04:48	46.80	112.00	$6\frac{1}{4}$	M_{GR}	6.2 ±	Helena, Mont., swarm event	5LS, 6S
22.	1935	Oct 31	18:37	46.62	111.97	6	M_{GR}	6.0 ±	Helena, Mont., swarm event	5LS, 6S
23.	1935	Nov 28	14:41	46.60	112.00	5.5	REN	---	Helena, Mont., swarm event	2L, 10S
24.	1936	May 13	14:06	46.60	112.00	5.7	?	---	Helena, Mont., swarm event	7LS, 8
25.	1936	May 22	02:19	46.60	112.00	5.7	?	---	Helena, Mont., swarm event	7LS, 8
26.	1944	Jul 12	19:30	44.41	115.06	6.1	PAS	---	Central Idaho (Seafoam)	2, 13LS
27.	1945	Feb 14	03:01	44.61	115.09	6.0	PAS	---	Central Idaho (Clayton ?)	2, 13LS
28.	1945	Sep 23	09:57	48.00	114.20	5.5	I/A	---	Flathead Lake, Mont.	2L, 8S
29.	1947	Nov 23	09:46	44.92	111.53	$6\frac{1}{4}$	M_{GR}	6.1	Virginia City, Mont.	6S, 5LS
30.	1952	Apr 01	00:37	48.00	113.80	5.5	I/A	---	Big Fork, Mont.	2L, 8S

TABLE 2. EARTHQUAKES IN THE INTERMOUNTAIN SEISMIC BELT OF MAGNITUDE 5.5 AND GREATER, 1900 THROUGH 1985 (continued)

No.	Date (GMT)	Time (GMT) hr mn	Lat. (°N)	Long. (°W)	Magnitude M_{conv}		M_w	Region	References
31.	1959 Jul 21	17:39	37.00	112.50	5.7	PAS	---	Arizona-Utah border	2L, 7S
32a.	1959 Aug 18	06:37	44.88	111.11	6.3	m_b	6.3	Hebgen Lake, Mont., double event	14LS, 15S
32b.	**1959 Aug 18**	**06:37**	**44.84**	**111.03**	7.5	M_S	7.3	Hebgen Lake, Mont., double event	14L, (15,16)S
33.	1959 Aug 18	07:56	45.00	110.70	$6\frac{1}{2}$	BRK	---	Hebgen Lake, Mont., aftershock	15L, 20S
34.	1959 Aug 18	08:41	45.08	111.80	6	BRK	---	Hebgen Lake, Mont., aftershock	15L, 20S
35.	1959 Aug 18	11:03	44.94	111.80	$5\frac{1}{2}+$	BRK	---	Hebgen Lake, Mont., aftershock	15L, 20S
36.	1959 Aug 18	15:26	44.85	110.70	6.3	M_S	6.3	Hebgen Lake, Mont., aftershock	15LS
37.	1959 Aug 19	04:04	44.76	111.62	6	BRK	6.0	Hebgen Lake, Mont., aftershock	5L, (5, 20)S
38.	1962 Aug 30	13:35	41.92	111.63	5.7	M_S	5.6	Cache Valley (Logan), Utah	17LS
39.	1964 Oct 21	07:38	44.86	111.60	5.8	m_b	5.6	Hebgen Lake, Mont., aftershock	5LS, 7S
40.	1966 Aug 16	18:02	37.46	114.20	6.0	PAS	5.3	Southeast Nevada	7S, 15LS
41.	1966 Aug 18	10:09	37.30	114.20	5.6	m_b	---	Southeast Nevada, aftershock	7LS
42.	1975 Mar 28	02:31	42.06	112.53	6.0	M_S, GS	6.2	Pocatello Valley (Ida.-Utah border)	15S, 18LS
43.	1975 Jun 30	18:54	44.69	110.62	6.1	M_L,GS	---	Yellowstone Park, Wyo.	19LS
44.	1976 Dec 08	14:40	44.76	110.80	5.5	m_b,GS	---	Yellowstone Park, Wyo., aftershock	7LS
45.	**1983 Oct 28**	**14:06**	**43.97**	**113.92**	7.3	M_S,GS	6.9	Borah Peak, Idaho	13LS, 21S
46.	1983 Oct 28	19:51	44.05	113.92	5.8	M_L	5.4	Borah Peak, Idaho, aftershock	13L, (15, 21)S
47.	1983 Oct 29	23:29	44.24	114.06	5.8	M_L	5.5	Borah Peak, Idaho, aftershock	13L, (15, 21)S
48.	1983 Oct 29	23:39	44.24	114.11	5.5	m_b,GS	---	Borah Peak, Idaho, aftershock	13LS
49.	1984 Aug 22	09:46	44.37	114.06	5.8	M_L	5.6	Borah Peak, Idaho, aftershock	13L, (15, 22)S

Explanation:

The local time (Mountain Standard Time) for the earthquakes in this table is found by subtracting seven hours from Greenwich Mean Time. In some cases (War Time, Daylight Savings Time), the difference is six hours. Non-instrumental and instrumental earthquake locations are listed with one- and two-decimal-point accuracy, respectively. **Earthquakes accompanied by surface faulting have their origin time and location in bold print.**

Abbreviations for earthquake magnitude: M_{conv} = conventional magnitude, including M_{GR} (unified magnitude determined by Gutenberg and Richter), M_L (local magnitude), M_S (surface-wave magnitude), and m_b (body-wave magnitude); I/A = estimate of M_L based on intensity and/or felt area (values in parentheses based on authors' judgment here); REN = Reno, empirical estimate of M_{GR}; PAS = Pasadena, unspecified M_S or M_L (except 31 and 40, known to be M_L); BRK = Berkeley (all values here are M_L); GS = U.S. Geological Survey; M_w = moment magnitude (Hanks and Kanamori, 1979).

Key to references, including source of location (L) and size (S): 1. Williams and Tapper (1953); 2. Coffman and others (1982); 3. Arabasz and McKee (1979); 4. Townley and Allen (1939); 5. Doser (1989a); 6. Gutenberg and Richter (1954); 7. Engdahl and Rinehart (this volume); 8. Qamar and Stickney (1983); 9. Doser (1989b); 10. Jones (1975); 11. Doser (1990); 12. Qamar and Hawley (1979); 13. Dewey (1987); 14. Doser (1985); 15. Doser and Smith (1989); 16. Abe (1981); 17. Westaway and Smith (1989b); 18. Arabasz and others (1981); 19. Pitt and others (1979); 20. R. Uhrhammer (personal communication, 1990); 21. Richins and others (1987); 22. Zollweg and Richins (1985).

continuing interest (McCalpin and others, 1987; dePolo and others, 1989), especially in light of recent seismic waveform modeling by Doser (1989b) that indicates a main-shock focal mechanism with nearly pure strike slip, rather than normal slip. The waveform modeling implies a main-shock focal depth of 8 to 10 km, left-lateral slip on a plane striking N38° to 48°E, and a subsurface rupture length of about 11 km (Doser, 1989b). Strong aftershocks were recorded at regional distances (Table 2).

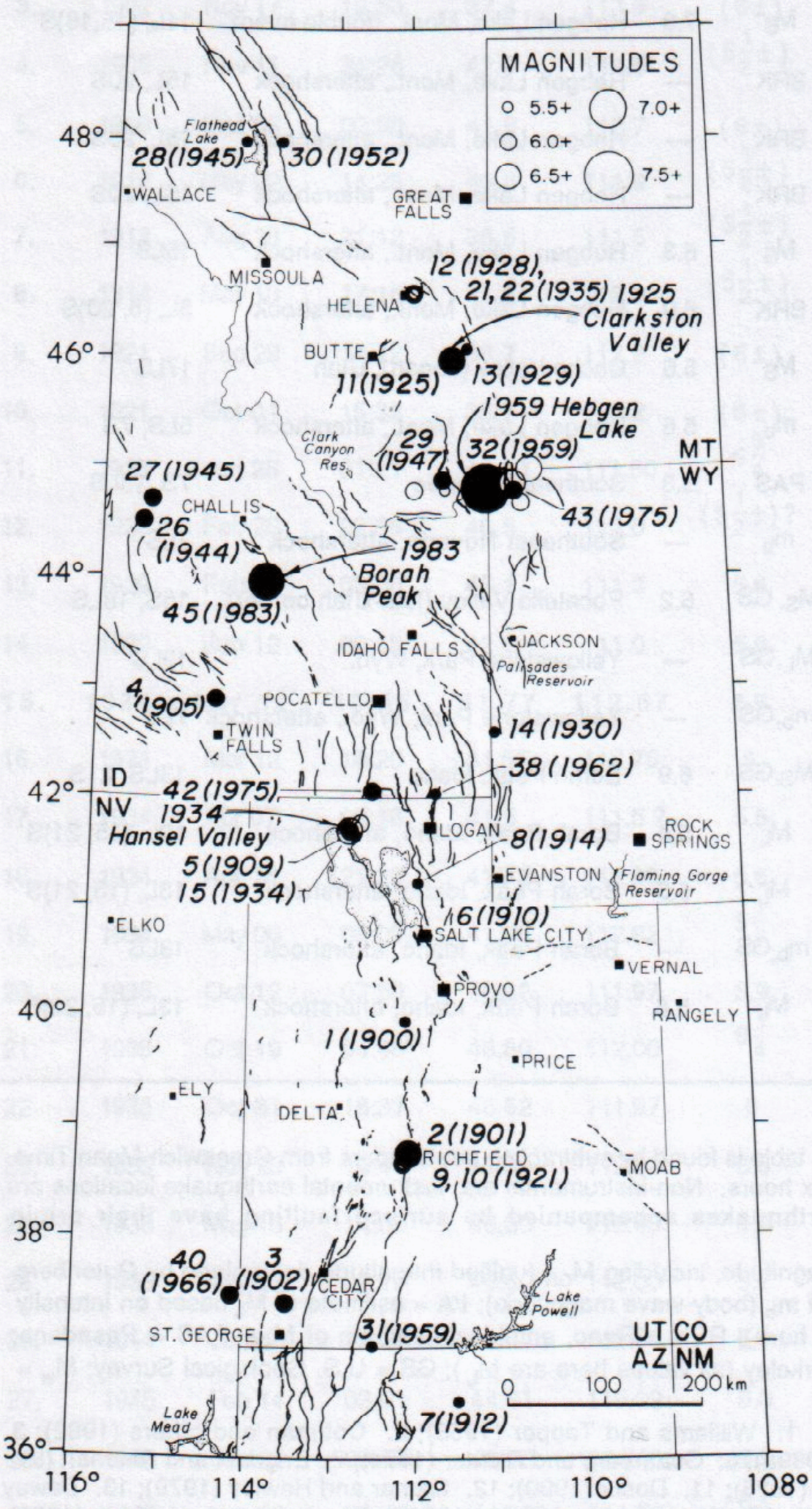

Figure 9. Map showing larger earthquakes in the Intermountain region, 1900–1985, together with selected faults, as in Figure 3. Plot includes main shocks of magnitude 5.5 and greater (solid circles) and aftershocks of magnitude 6.0 and greater (open circles). Numbers and dates for main shocks are keyed to Table 2. Four largest historical shocks known to exceed moment magnitude (M_W) 6.5 are indicated by name.

1959 Hebgen Lake, Montana, earthquake. The 1959 earthquake near Hebgen Lake in southwestern Montana (No. 32a, b, Table 2), directly west of Yellowstone National Park, was the first large normal-faulting earthquake in the Intermountain region in historical time and is distinguished as the largest recorded earthquake in the ISB (see special collection of papers in vol. 52, no. 1, of the *Bulletin of the Seismological Society of America,* 1962). The surface-wave magnitude (M_S) of 7.5 from Abe (1981) is a multistation estimate judged to be more accurate than the earthquake's previously estimated magnitude of 7.1, attributed to Pasadena by Tocher (1962). The occurrence of the M_S = 7.3 Borah Peak, Idaho, earthquake in 1983 (discussed below) prompted immediate comparison between the two large earthquakes. From comparisons of surface faulting (Hall and Sablock, 1985) and recorded seismograms (Bolt, 1984), the larger size of the Hebgen Lake earthquake was evident—confirmed by subsequent comparison of the two earthquakes' source parameters determined both seismically and geodetically (e.g., Barrientos and others, 1987). Restudy of Wood-Anderson seismograms at Berkeley and Pasadena for the 1959 earthquake and comparison with counterpart recordings for the 1983 earthquake led to a revised estimate of 7.7 to 7.8 for the local or Richter magnitude (M_L) of the 1959 earthquake and assignment of 7.2 (M_L) for the 1983 earthquake (Bolt, 1984). This relative size information is valuable. Given the large distances to Berkeley and Pasadena, however, the distance correlations—and hence the absolute values of M_L—are open to question.

The Hebgen Lake earthquake affected an area of 1.5 million km^2, reached MMI = X, caused 28 fatalities, and produced dramatic surficial geologic effects, including spectacular fault scarps, a catastrophic rockslide into the Madison River, basin subsidence of several meters, and hydrogeomorphic features associated with groundwater discharge (Witkind and others, 1962; Coffman and others, 1982). The earthquake produced a 26-km-long complex pattern of west- to northwest-trending normal faulting along the Hebgen and Red Canyon faults near the southern end of the Madison Range, where Laramide faults exert structural control (Witkind, 1964; Doser, 1985b). Trace lengths of surface faulting, including slip on the nearby north-south–trending Madison fault, sum to 61 km (Hall and Sablock, 1985). Maximum vertical displacement is variously cited as 6.7 m by dePolo and others (1989) and 5.5 ± 0.3 m by Bonilla and others (1984). Hall and Sablock (1985) use data from Witkind (1964) to estimate an average vertical displacement of 2.0 m on the Hebgen fault and 2.3 m on the Red Canyon fault.

Notable seismological details of the earthquake sequence (Doser, 1985b, 1989a) include: (1) the occurrence of the main shock as a multiple event, consisting of a shock of m_b = 6.3 at about 10 km depth followed 5 sec later by the principal M_S = 7.3 shock at 15 km depth; (2) nearly pure dip-slip motion during the main shock on one or more planes dipping 40° to 60°SW; and (3) the location of numerous strong aftershocks as large as M_S = 6.3 (Table 2) out to distances of 50 km from the main-shock epicenter. Barrientos and others (1987) recently reanalyzed the

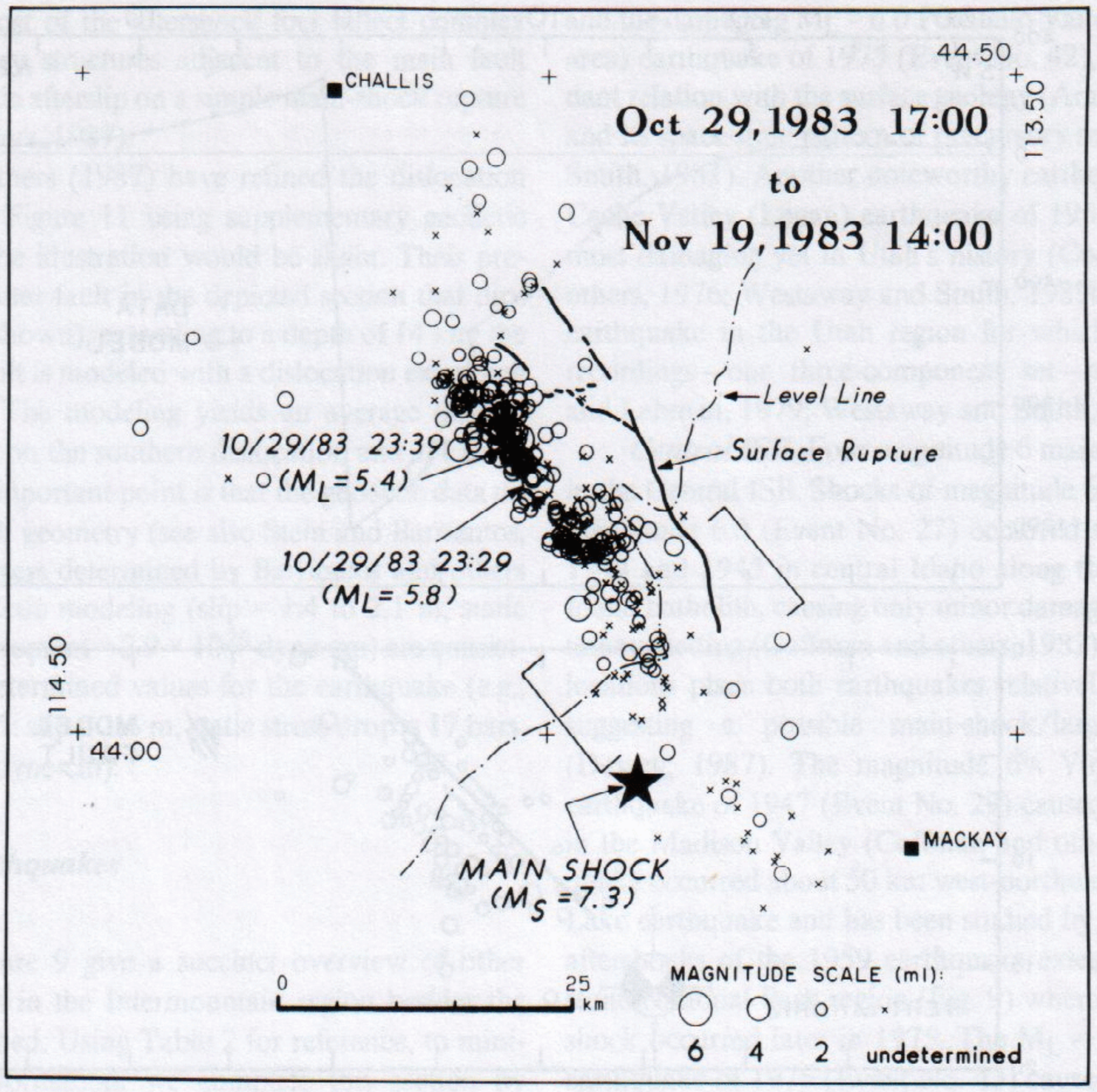

Figure 10. Map (from Richins and others, 1987) showing epicenters of the main shock and early aftershocks of the Borah Peak, Idaho, earthquake sequence, together with the trace of surface rupture. Brackets outline sample area for earthquakes shown in cross section of Figure 11 (middle); dot-dashed line, trace of geodetic level line from which data are displayed in Figure 11 (top).

static deformation field associated with the earthquake using a newly augmented geodetic data set. They interpret a complex source consisting of two en-echelon planes, 15 to 25 km long, which are coincident with the Hebgen and Red Canyon faults at the surface, extend to a depth of 10 to 15 km, dip 45° to 50°SW, and have coseismic dip slip of 7.0 and 7.8 m.

1983 Borah Peak, Idaho, earthquake. This 1983 surface-faulting earthquake (No. 45, Table 2) occurred in east-central Idaho, 60 km northwest of the Snake River Plain, in a sparsely settled area characterized by active late Quaternary basin-range faulting (Scott and others, 1985) but low historic seismicity (Dewey, 1987). The M_S = 7.3 earthquake is the second-largest historical earthquake in the Intermountain region. Importantly, the earthquake allowed abundant modern observations about the mechanics, subsurface rupture geometry, and seismic geology of a large normal-faulting earthquake (see special compendia of papers in U.S. Geological Survey Open-File Report 85-290, 1985, and vol. 77, no. 3, of the Bulletin of the Seismological Society of America, 1987).

The Borah Peak earthquake was felt over 670,000 km^2, reached MMI = VII at the nearby towns of Mackay and Challis (25 km and 65 km distant, respectively, from the main-shock epicenter), caused two deaths in Challis, and resulted in about $12.5 million of damage (Stover, 1985). The earthquake produced 36 km of surface faulting along the southwestern base of the Lost River Range, re-rupturing parts of the 140-km-long Lost River fault that had last broken about mid-Holocene time and a branch fault; vertical displacement along the new fault scarps reached a maximum of 2.7 m (0.8 m average), and net slip averaged 0.17 m of sinistral slip for every 1.00 m of dip slip (Crone and Machette, 1984; Crone and others, 1987). There is substantial information about the segmented behavior of the Lost River fault during the 1983 earthquake and about the fault's paleoseismology (see reviews by Crone and Haller, 1989, and dePolo and others, 1989).

Figure 10 (from Richins and others, 1987) illustrates the map distribution of aftershocks with respect to the main-shock epicenter and surface rupture. The earthquake sequence included sizable aftershocks (Table 2) but no foreshocks (Richins and others, 1987; Dewey, 1987). Seismic-waveform modeling by

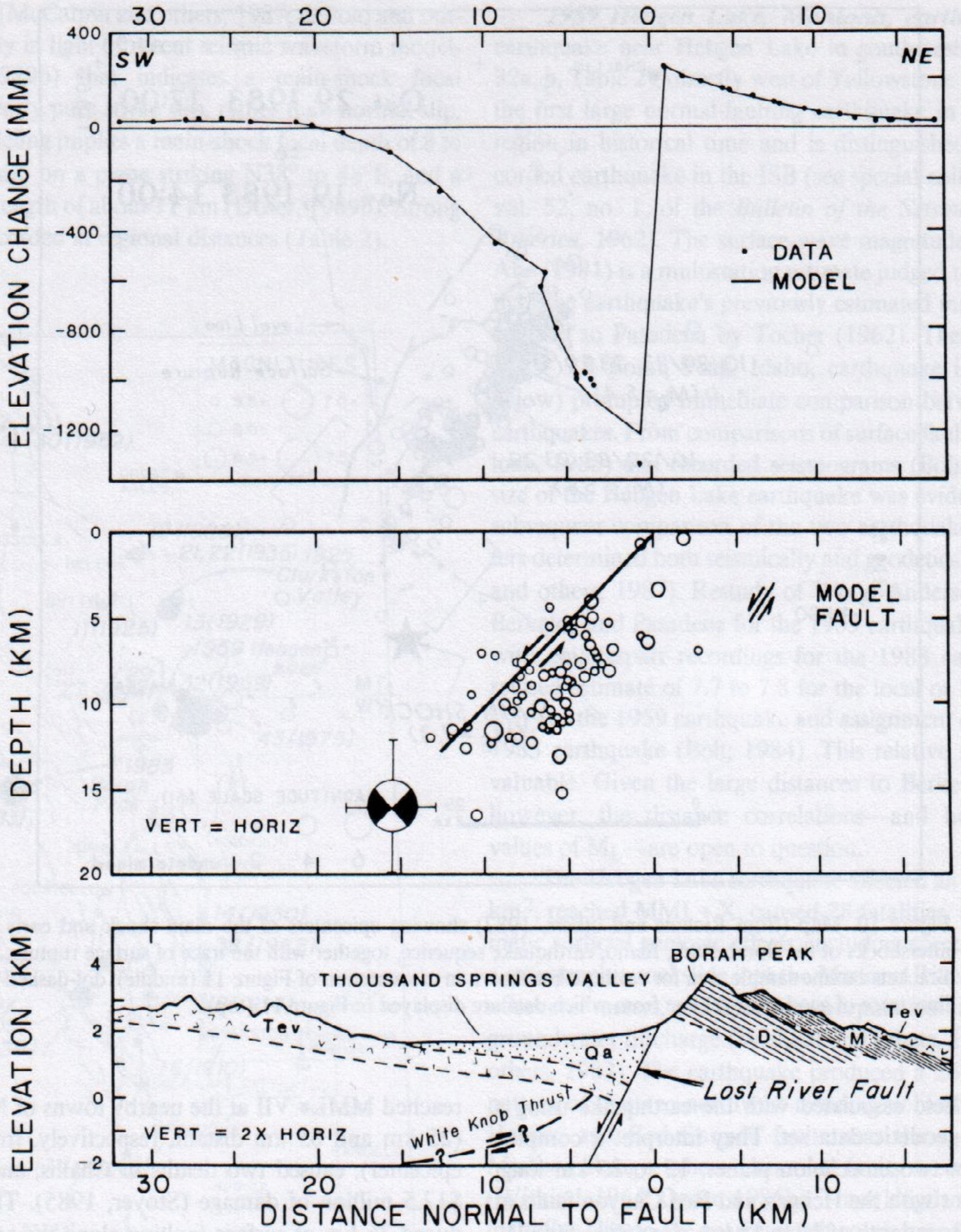

Figure 11. Diagram illustrating the subsurface geometry of faulting associated with the 1983 Borah Peak, Idaho, earthquake (after Stein and Barrientos, 1985). Top, plot of geodetically-observed coseismic elevation changes (dots) and the predicted elevation changes (line) of the coseismic dislocation model. Middle, cross section showing superposition of coseismic dislocation model, aftershock foci from the bracketed area shown in Figure 10, and the projection of the main-shock focus. Bottom, schematic geologic cross section from Bond (1978).

Doser and Smith (1985) indicates the main shock nucleated at a depth of about 16 km and propagated unilaterally northwestward toward the surface along a fault plane dipping 45° to 53° southwest (see Richins and others, 1987, Table 2, for a comparative tabulation of the main shock's source parameters). Figure 11, after Stein and Barrientos (1985), usefully illustrates some of the principal aspects of subsurface fault geometry and deformation. The data are displayed in transverse view to the Lost River fault (bottom) and are keyed to a northeast-southwest geodetic profile of coseismic elevation changes (top) along an irregular leveling route roughly transverse to the fault (Fig. 10). The middle panel shows a cross section of aftershock foci from Richins and others (1985), correlative with the bracketed sample area shown in Figure 10, together with the location and focal mechanism of the main shock and a planar dislocation model that matches the observed surface deformation. Focal mechanisms for 47 after-

shocks suggest that most of the aftershock foci reflect complex fracturing on secondary structures adjacent to the main fault plane rather than seismic afterslip on a simple main-shock rupture plane (Richins and others, 1987).

Barrientos and others (1987) have refined the dislocation model represented in Figure 11 using supplementary geodetic data, but changes to the illustration would be slight. Their preferred model has a planar fault in the depicted section that dips 49° (instead of 47° as shown), extending to a depth of 14 km; the northern part of the fault is modeled with a dislocation extending only to 6 km depth. The modeling yields an average dip-slip displacement of 2.1 m on the southern dislocation and 1.4 m on the northern one. An important point is that the geodetic data do not permit a listric fault geometry (see also Stein and Barrientos, 1985). Source parameters determined by Barrientos and others (1987) from this geodetic modeling (slip = 1.4 to 2.1 m, static stress drop = 30 bars, moment = 2.9×10^{26} dyne-cm) are consistent with seismically-determined values for the earthquake (e.g., Doser and Smith, 1985: slip = 1.4 m, static stress drop = 17 bars, moment = 2.1×10^{26} dyne-cm).

Other significant earthquakes

Table 2 and Figure 9 give a succinct overview of other significant earthquakes in the Intermountain region besides the four largest just described. Using Table 2 for reference, to minimize repetition of information, we complete this section by mentioning the other main shocks of magnitude 6 and some notable smaller shocks.

Southern ISB. The 1901 Southern Utah (Richfield) earthquake (Event No. 2) appears to be the second largest historical shock in the southern ISB, although its equivalent magnitude and precise epicenter are not well known. The earthquake reached MMI = IX, was felt over 130,000 km^2, caused substantial damage at several towns and produced ground cracks (but no documented surface faulting), local liquefaction, and extensive rockslides (Williams and Tapper, 1953). In late 1921, following two and a half weeks of foreshock activity, the Elsinore area, 10 km southwest of Richfield, was struck by two damaging earthquakes of about magnitude 6¼ (Events No. 9 and 10), separated by 50 hours and with an intervening shock of magnitude 5¾ (Pack, 1921; Arabasz and Julander, 1986). Southwestern Utah was significantly affected in 1902 by a damaging earthquake (MMI = VIII) centered in Pine Valley (Event No. 3) and in 1966 by a sizable earthquake (m_b, USGS = 6.1; M_L, Univ. of Utah = 5.6) close to the Nevada-Utah border (Event No. 40) (Arabasz and others, 1979; Coffman and others, 1982). The 1966 event was notable for its strike-slip focal mechanism in a basin-range setting (Smith and Sbar, 1974; Rogers and others, this volume).

Two other magnitude 6 shocks in the southern ISB occurred in the Utah-Idaho border area. This includes a strong (MMI = IX) earthquake in 1909 (Event No. 5), assumed to have originated in the Hansel Valley area (Williams and Tapper, 1953), and the damaging M_L = 6.0 Pocatello Valley (Idaho-Utah border area) earthquake of 1975 (Event No. 42), notable for its discordant relation with the surface geology (Arabasz and others, 1981) and its space-time pattern of precursory seismicity (Arabasz and Smith, 1981). Another noteworthy earthquake is the M_L = 5.7 Cache Valley (Logan) earthquake of 1962 (Event No. 38), the most damaging yet in Utah's history (Cook, 1972; Rogers and others, 1976; Westaway and Smith, 1989b) and the only sizable earthquake in the Utah region for which good strong-motion recordings—one three-component set—currently exist (Smith and Lehman, 1979; Westaway and Smith, 1989a, b).

Central ISB. Four magnitude 6 main shocks have occurred in the Central ISB. Shocks of magnitude 6.1 (Event No. 26) and magnitude 6.0 (Event No. 27) occurred seven months apart in 1944 and 1945 in central Idaho along the eastern flank of the Idaho batholith, causing only minor damage in the remote mountainous setting (Coffman and others, 1982). Revised instrumental locations place both earthquakes relatively close to each other, suggesting a possible main-shock/large-aftershock relation (Dewey, 1987). The magnitude 6¼ Virginia City, Montana, earthquake of 1947 (Event No. 29) caused considerable damage in the Madison Valley (Coffman and others, 1982). The earthquake occurred about 50 km west-northwest of the 1959 Hebgen Lake earthquake and has been studied by Doser (1989a). Large aftershocks of the 1959 earthquake extended into the Yellowstone National Park region (Fig. 9) where an independent main shock occurred later in 1975. The M_L = 6.1 Yellowstone Park earthquake of 1975 (Event No. 43) caused moderate disruption in the national park (Coffman and others, 1982) and provided valuable information on the seismotectonics of the Yellowstone caldera (Pitt and others, 1979). A strong earthquake (MMI = VII), probably in the magnitude 5 range, which caused damage at Shoshone, Idaho, in 1905 (Event No. 4) (Coffman and others, 1982), has an uncertain epicenter but is significant for its possible association with the relatively aseismic Snake River Plain.

Northern ISB. The 1935–1936 Helena earthquakes (Event nos. 20 to 25) were part of a vigorous swarm of more than two thousand felt earthquakes that occurred within 10 to 25 km of Helena, between October 1935 and December 1936, within a poorly defined structural zone extending from Helena northwestward toward Marysville, an area of anomalously high heat flow (Smith and Sbar, 1974; Doser, 1989a). Earthquakes of magnitude 6¼ (Event No. 21) and magnitude 6 (Event No. 22) in October 1935 caused four deaths and severe damage in Helena (Coffman and others, 1982). Some important strong-ground-motion records were recorded locally (Westaway and Smith, 1989a). Other earthquakes in the northern ISB listed in Table 2, which caused only minor damage (Coffman and others, 1982; Qamar and Stickney, 1983), include: a 1928 shock near Helena (Event No. 12), perhaps a precursor to the 1935 swarm; a 1929 shock near Lombard (Event No. 13), 9 km north of Clarkston, possibly a late aftershock of the 1925 Clarkston Valley earthquake; and two shocks in the Flathead Lake region in 1945 (Event No. 28) and 1952 (Event No. 30).

DETAILED SEISMICITY

In earlier sections we gave an overview of the regional-scale patterns of earthquake activity in the ISB (Fig. 1) and described the largest earthquakes that have occurred historically (Fig. 9). In this section, we describe finer details of the spatial distribution of the seismicity portrayed in Figure 1, outlining what is known about the association of the seismicity with geologic structure. Observational data basically come from either long-term monitoring with telemetered seismic networks (Fig. 8B) or focused short-term monitoring using temporary arrays of portable seismographs. Some notable characteristics of observed seismicity throughout the ISB are: (1) the diffuse epicentral scattering of background earthquakes, with weak correlation to major active faults; (2) the conspicuous seismic quiescence of many major faults or fault segments that have been active in Holocene and late Quaternary time; (3) the predominance of focal depths shallower than 20 km; and (4) the prevalence of normal and oblique-normal seismic slip, but with local strike slip and reverse slip.

Southern ISB

Detailed summaries of the instrumental seismicity for major parts of the southern ISB have recently been given by Arabasz and others (1987) for the Wasatch Front area, by Arabasz and Julander (1986) for the Basin and Range–Colorado Plateau transition in central Utah, and by Wong and Humphrey (1989) for the Colorado Plateau. Here, we selectively adapt from and add to those summaries.

The recorded seismic history of the southern ISB has been distinctively characterized by abundant small- to moderate-sized earthquakes (magnitude $\leqslant$ 6.6) without a truly large surface-faulting earthquake, despite the widespread presence of late Pleistocene and Holocene fault scarps. The single instance of historical surface faulting in the southern ISB at Hansel Valley in 1934 (discussed earlier) was for an earthquake only slightly above the threshold of surface faulting. Thus, there is a lack of instrumental information relating to large-scale seismic slip on major faults in this region. Available earthquake observations may chiefly reflect seismic deformation on secondary structures.

The seismicity of the Wasatch Front area shown in Figure 12 displays no simple correlation between the distribution of background earthquakes and the traces of the numerous active faults, except for the general parallelism of this part of the ISB with the Wasatch fault. The depth above which 90 percent of the well-located earthquakes lie varies locally from about 11 to 17 km (Arabasz and others, 1987). Well-located shocks of magnitude 2.0 and greater in this area from 1962 to 1986 have a distinct peak in their depth distribution between 4.5 and 7.5 km (Bjarnason and Pechmann, 1989). An anomalously deep earthquake of M_L = 3.8 occurred at a depth of 90 km beneath northern Utah in 1979 (see Wong and Chapman, 1990).

The seismicity pattern of Figure 12B is representative of instrumental seismicity in the area since 1962 (see Arabasz and others, 1980); spatial clustering is due more to cumulative stationary activity than to isolated temporal bursts. An inverted Y-shaped pattern of clustered earthquakes on the Idaho-Utah border west of the Wasatch fault began to develop several months after the 1975 M_L = 6.0 Pocatello Valley earthquake (No. 42, Fig. 9) and persists to the present. Early aftershocks of the 1975 earthquake occurred mostly north of the Idaho-Utah border (Arabasz and others, 1981). Special studies of post-1975 earthquakes within the inverted Y-pattern (Jones, 1987; Chen, 1988) show that well-located foci are mostly shallower than 8 to 12 km deep, scatter beneath both horsts and grabens of the local basin-range structure, and display diverse seismic slip.

A linear north-south belt of seismicity about 15 to 40 km east of and parallel to the Wasatch fault (Fig. 12) is poorly understood but may be mechanically related to crustal flexure associated with the Wasatch fault and involving non-elastic mechanisms (Zandt and Owens, 1980; Owens, 1983). This seismicity is known to coincide in map view with the eastern leading edges of several Laramide thrust sheets (Smith and Bruhn, 1984). In cross-section view, however, the earthquake foci are diffusely scattered to about 20 km depth (Arabasz and others, 1987; Owens, 1983). In the northern part of the belt, the earthquakes lie east of the west-dipping East Cache and Wasatch faults, perhaps partly on a synthetic fault (Westaway and Smith, 1989b); south of 41°20′N, the epicentral belt follows a series of small, late Cenozoic structural basins within the Middle Rocky Mountains (Sullivan and others, 1988). In the lower right part of Figure 12, the prominent arcuate pattern of seismicity east of the Wasatch fault is mining related (see Induced seismicity).

What about earthquakes along the Wasatch fault itself? In addition to having no historic surface rupture, despite recurrent late Pleistocene and Holocene surface faulting on multiple segments (Machette and others, 1989; Schwartz and Coppersmith, 1984), the Wasatch fault has had little historical seismicity. As many as two, and perhaps no, earthquakes as large as magnitude 5 have occurred on the Wasatch fault in historical time (Arabasz and others, 1987). The most recent surface rupture occurred about 400 years ago (Machette and others, 1989) on a 40-km-long segment immediately north of Nephi (Fig. 12A). In terms of contemporary seismicity, Figure 12B shows a remarkable paucity of microseismicity along most of the Wasatch fault. There are a few local clusters of epicenters along the fault north of Brigham City, and more prominent clusters just west of the fault in the vicinity of Salt Lake City, at the northern end of Utah Valley (~40°20′N), in the vicinity of Goshen Valley (~40°00′N), and in a broadly scattered zone at the southern end of the Wasatch fault. For Goshen Valley and the southern Wasatch fault, hypocenters and corresponding focal mechanisms from portable-array studies show that background earthquakes west of the fault are not occurring on either a listric or a simple planar projection of the fault (Arabasz and Julander, 1986). Elsewhere along the Wasatch fault, cross sections suggest that very few well-located foci could be interpreted to lie on the fault—if one believes that the fault is a planar structure of moderate dip (Arabasz and others,

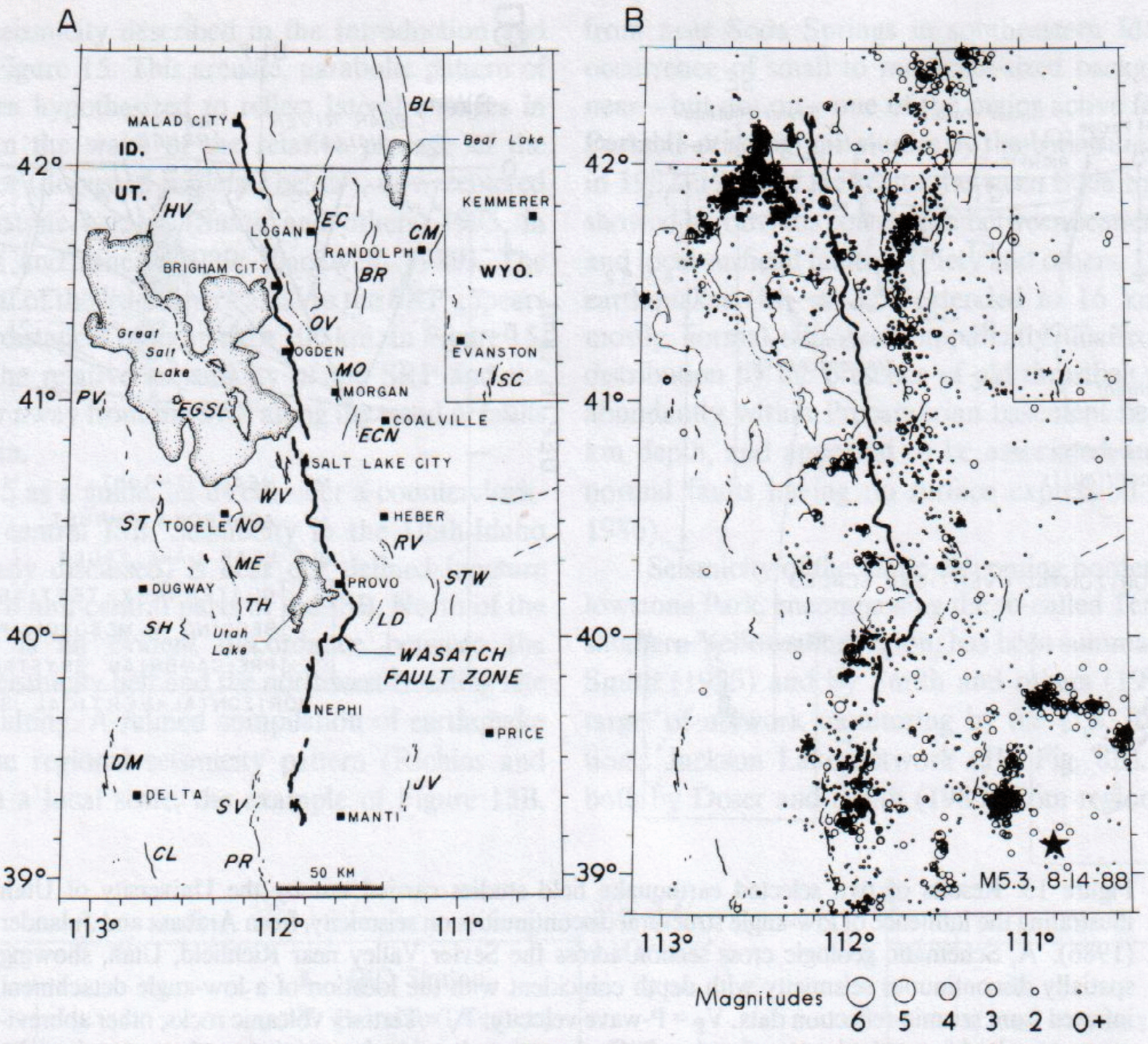

Figure 12. Active faulting and seismicity in the Wasatch Front area, outlined in Figure 3, from Arabasz and others (1987). A, Map showing traces of late Quaternary faulting, abbreviated as follows: BL = Bear Lake; BR = Bear River Range; CL = Clear Lake; CM = Crawford Mts.; DM = Drum Mts.; EC = East Cache; ECN = East Canyon; EGSL = East Great Salt Lake; HV = Hansel Valley; JV = Joes Valley; LD = Little Diamond Creek; ME = Mercur; MO = Morgan; NO = Northern Oquirrh; OV = Ogden Valley; PR = Pavant Range; PV = Puddle Valley; RV = Round Valley; SC = Sulphur Creek; SH = Sheeprock Mts.; ST = Stansbury Mts.; STW = Strawberry Valley; SV = Scipio Valley; TH = Topliff Hill; WV = West Valley. B, Epicenter map of all earthquakes located by the University of Utah Seismograph Stations in the Wasatch Front area, July 1, 1978 to December 31, 1986; star indicates location of 1988 San Rafael Swell, Utah, main shock described in Figure 14.

1987). But the same data are admittedly either inadequate or ambiguous (e.g., Pechmann and Thorbjarnardottir, 1984) for interpreting subsurface association with a listric projection of the fault.

Portable-seismograph studies throughout the transition zone between the Basin and Range and Colorado Plateau provinces in central and southwestern Utah reveal that low-angle structural discontinuities appear to play a fundamental role in separating locally intense upper-crustal seismicity above 6 to 8 km depth from less frequent background earthquakes at greater depth (Arabasz and Julander, 1986). This is illustrated in Figure 13A, where spatially discontinuous seismicity with depth beneath the Sevier Valley near Richfield, Utah, coincides with a low-angle detachment inferred from seismic-reflection data. The earthquakes beneath the northwestern side of the valley are background events recorded in 1981; those beneath the southeastern side are aftershocks of an M_L = 4.0 earthquake in May 1982. Companion results from a portable-seismograph study of an earthquake swarm sequence ($M_L \leqslant 4.7$) in October 1982 near Soda Springs, Idaho (Fig. 13B), similarly show a depth distribution of upper-crustal earthquakes apparently influenced by preexisting low-angle structures. Instead of being associated, as expected, with late Cenozoic basin-range faulting along the active Bear Lake fault, the seismicity is associated with secondary faults within a northwest-trending near-vertical zone in the hanging-wall block. Marked changes in the vertical distribution of foci coincide with pre-Neogene thrust faults. Focal mechanisms sampled from both above and below the Meade thrust indicate a predominance of strike slip on northwest-trending, steeply-dipping fault planes, with no evidence for seismic slip on a low-angle plane (see Arabasz and Julander, 1986).

East of the southern ISB, scattered seismicity within the Colorado Plateau (Figs. 1 and 2), described by Wong and Humphrey (1989), occasionally reaches the magnitude 6 range

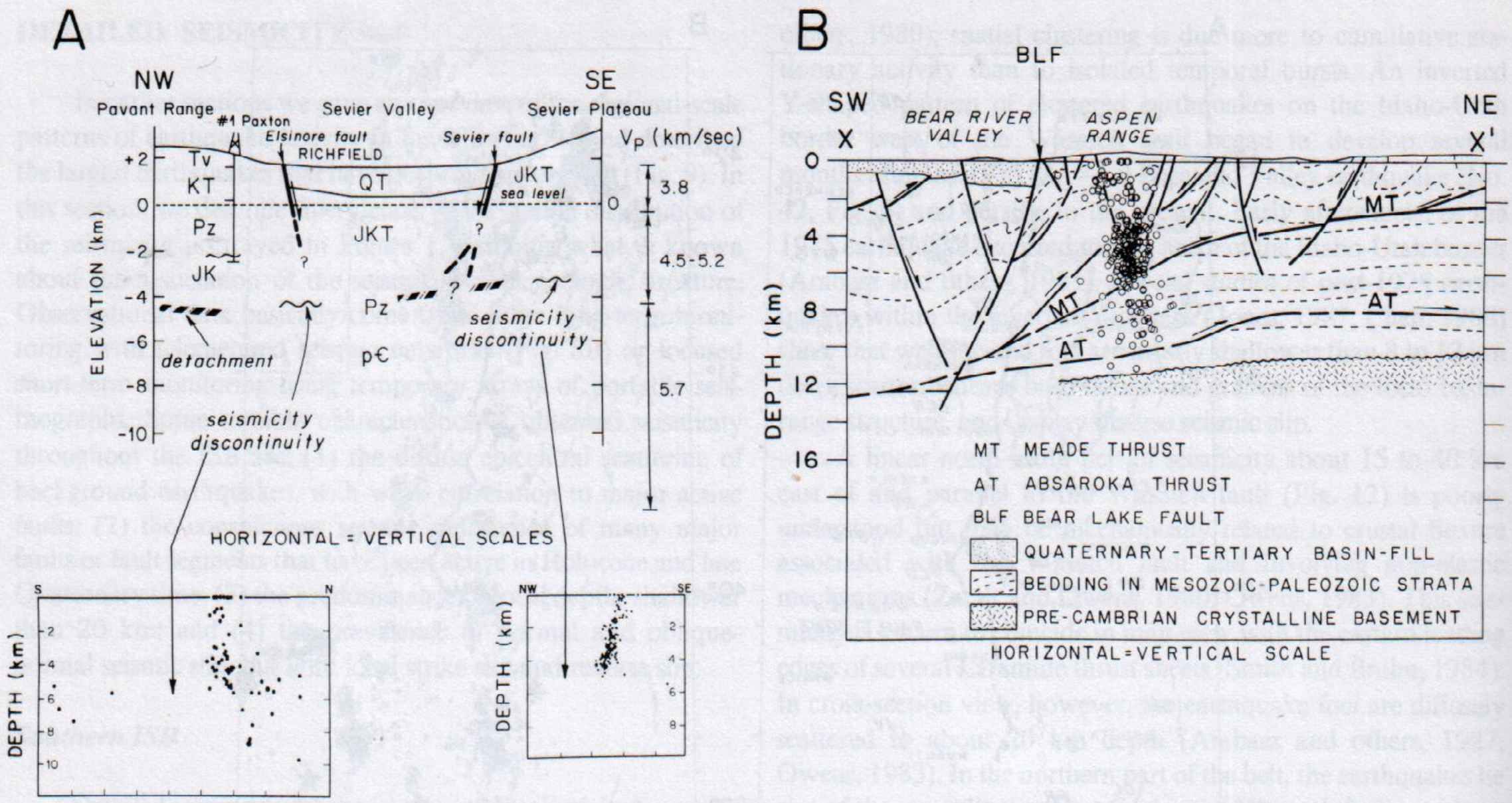

Figure 13. Results of two selected earthquake field studies carried out by the University of Utah illustrating the influence of low-angle structural discontinuities on seismicity, from Arabasz and Julander (1986). A, Schematic geologic cross section across the Sevier Valley near Richfield, Utah, showing spatially discontinuous seismicity with depth coincident with the location of a low-angle detachment inferred from seismic-reflection data. V_P = P-wave velocity; T_V = Tertiary volcanic rocks; other abbreviations, standard for geologic ages of rocks. B, Cross section showing the association of swarm seismicity in late 1982 near Soda Springs, Idaho, with geologic structure; earthquake data from Richins and others (1983) are superposed on a generalized geologic cross section from Dixon (1982) based on seismic-reflection profiling.

and appears chiefly to reflect normal to lateral seismic slip on buried Precambrian basement faults without evident surface expression. Focal depths predominate above 15-20 km, but the Colorado Plateau is distinctive in having observed seismicity in the lower crust, and locally 40 to 60 km deep in the uppermost mantle (Wong and Humphrey, 1989; Wong and Chapman, 1990). Figure 14 illustrates details of what may be a typical, moderate-sized crustal earthquake within the Colorado Plateau. The August 1988 San Rafael Swell earthquake (M_L = 5.3) involved oblique-normal slip on a buried Precambrian basement fault in an area of minimal historical seismicity where there are no active faults mapped in the overlying 3-km-thick sedimentary cover rocks of Mesozoic and Paleozoic age (Nava and others, 1988). Figure 14 also usefully illustrates some prerequisites for associating seismicity with geologic structure: (1) local seismographic control for hypocentral resolution, especially for precise focal depths; (2) sufficient seismicity for defining the spatial geometry of one or more active structures; and (3) a reliable focal mechanism for correlating with the geometry and sense of slip inferred from the seismicity.

Noteworthy microearthquake studies in the southern Utah–northern Arizona area have been reported by Johnson and Sbar (1987) and Kruger-Knuepfer and others (1985). Both studies present valuable focal-mechanism information relevant to regional stress orientations. Other key studies that summarize and discuss significant focal-mechanism information for the southern ISB include those by Bjarnason and Pechmann (1989), Wong and Humphrey (1989), Arabasz and Julander (1986), Zoback (1983), Arabasz and others (1980), Smith and Lindh (1978), and Smith and Sbar (1974). Besides implications for stress state (discussed earlier), the focal mechanisms also provide information on fault kinematics. Seismic slip predominates on fault segments of moderate (>30°) to steep dip. There is yet no convincing evidence, in the form of clustered earthquake foci and corroborating focal mechanisms, for seismic slip on either a downward-flattening or a low-angle normal fault in this region.

Central ISB

The central part of the ISB is distinctive in two regards. First, it has had two large surface-faulting earthquakes in historical time—the 1959 Hebgen Lake and 1983 Borah Peak earthquakes. Second, its seismicity reflects the apparent influence of the Y-SRP volcanic system. In map view this is illustrated by the

arcuate pattern of seismicity described in the Introduction and shown in detail in Figure 15. This arcuate, parabolic pattern of earthquakes has been hypothesized to reflect lateral changes in deviatoric stresses in the wake of the relative passage of the Yellowstone hot spot (discussed in detail below), now centered beneath the Yellowstone caldera (Smith and others, 1985, in preparation; Anders and others, 1989; Blackwell, 1989). The seismogenic potential of the lithosphere axial to the SRP appears to be affected out to distances of more than 100 km. In Figure 15, for example, note the relative aseismicity of the SRP and the increase in seismicity away from the SRP along the trend of faults transverse to the plain.

Using Figure 15 as a guide, let us consider a counterclockwise circuit of the central ISB. Seismicity in the Utah-Idaho border region (already discussed) is near our defined juncture between the southern and central parts of the ISB. North of the Utah border there is an evident discordance between the northeast-trending seismicity belt and the northwest-trending late Cenozoic normal faulting. A refined compilation of earthquake locations verifies the regional seismicity pattern (Richins and Arabasz, 1985). On a local scale, the example of Figure 13B, from near Soda Springs in southeastern Idaho, illustrates the occurrence of small to moderate-sized background earthquakes near—but not on—one of the major active faults in this region. Portable-seismograph studies by the U.S. Bureau of Reclamation, in 1982–1983, of the region between Soda Springs and Jackson showed no obvious correlation between scattered microseismicity and local surficial faulting (Piety and others, 1986). Well-located earthquakes ($M_L \leqslant 3.0$) extended to 16 km depth, exhibited mostly normal slip, were apparently unaffected in their depth distribution by the presence of old thrustbelt structure, occurred abundantly within Precambrian basement below about 5 to 10 km depth, and appeared to be associated, in part, with buried normal faults having no surface expression (Piety and others, 1986).

Seismicity of the Idaho-Wyoming border area south of Yellowstone Park, encompassing the so-called Teton–Jackson Hole–southern Yellowstone region, has been summarized by Doser and Smith (1983) and by Smith and others (1990a, b) and is the target of network monitoring by the U.S. Bureau of Reclamation's Jackson Lake network (JL, Fig. 8B). Results described both by Doser and Smith (1983) from regional monitoring and

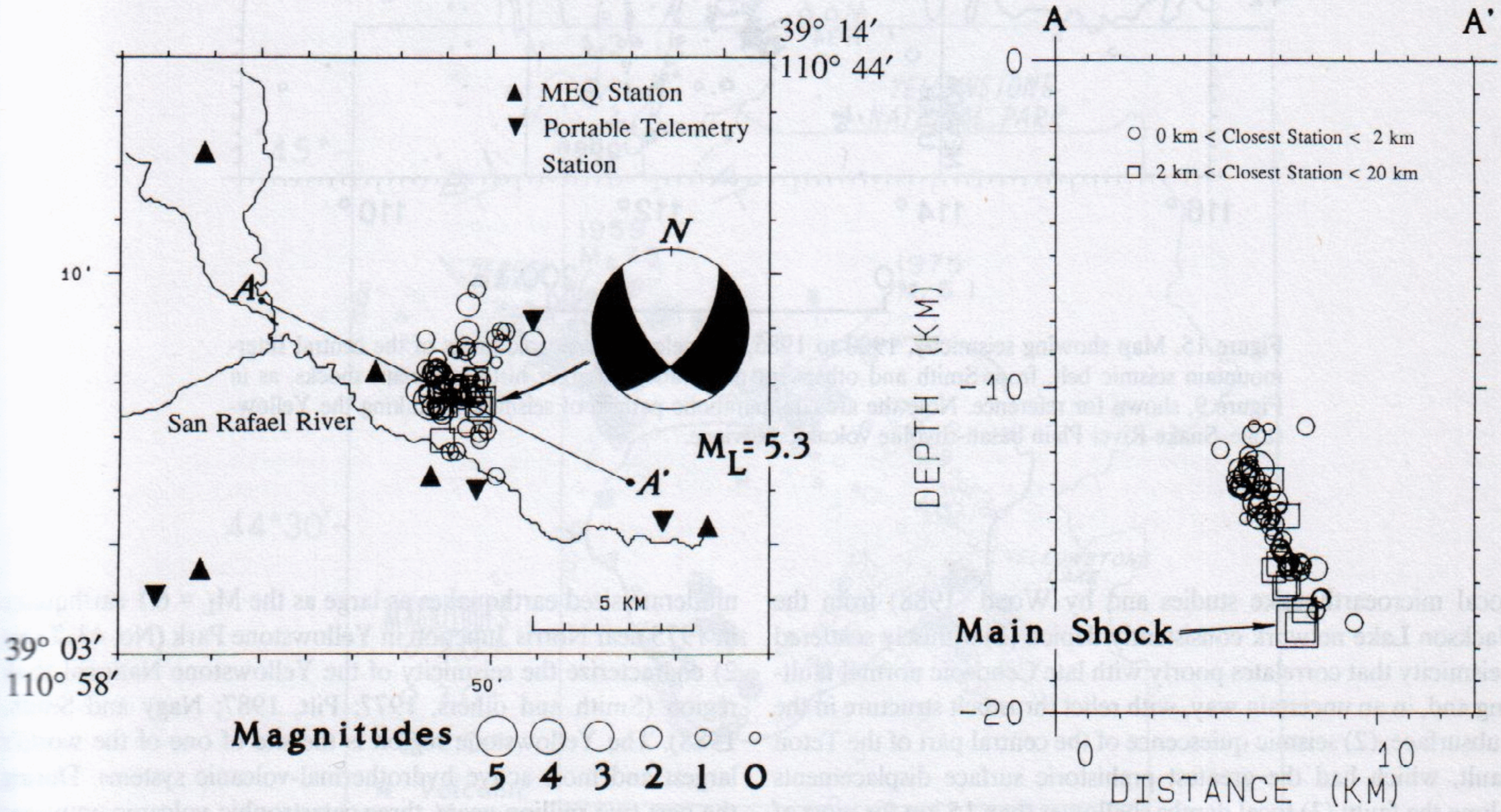

Figure 14. Details of the San Rafael Swell, Utah, earthquake sequence, August 14, 1988 to March 31, 1989, whose location is shown in Figure 12, adapted from Nava and others (1988) using revised, unpublished data from J. C. Pechmann and S. J. Nava, University of Utah. Left, map showing epicenters of the 66 best-located earthquakes in the sequence together with the main-shock focal mechanism (lower-hemisphere, compressional quadrant black). Right, cross section of earthquake foci projected onto the plane of line A-A′ (left), the projection for which planar clustering was best defined; the earthquakes define a zone dipping 60° ± 5° SE, with a downdip extent of 6 km. The main-shock focal mechanism has a corresponding nodal plane striking N39°E and dipping 62°SE, with a slip-vector rake of 29° (down to the NE); uncertainties for that plane range from N20°E to N42°E in strike, 44° to 80° in dip to the SE, and 21° to 59° in slip-vector rake.

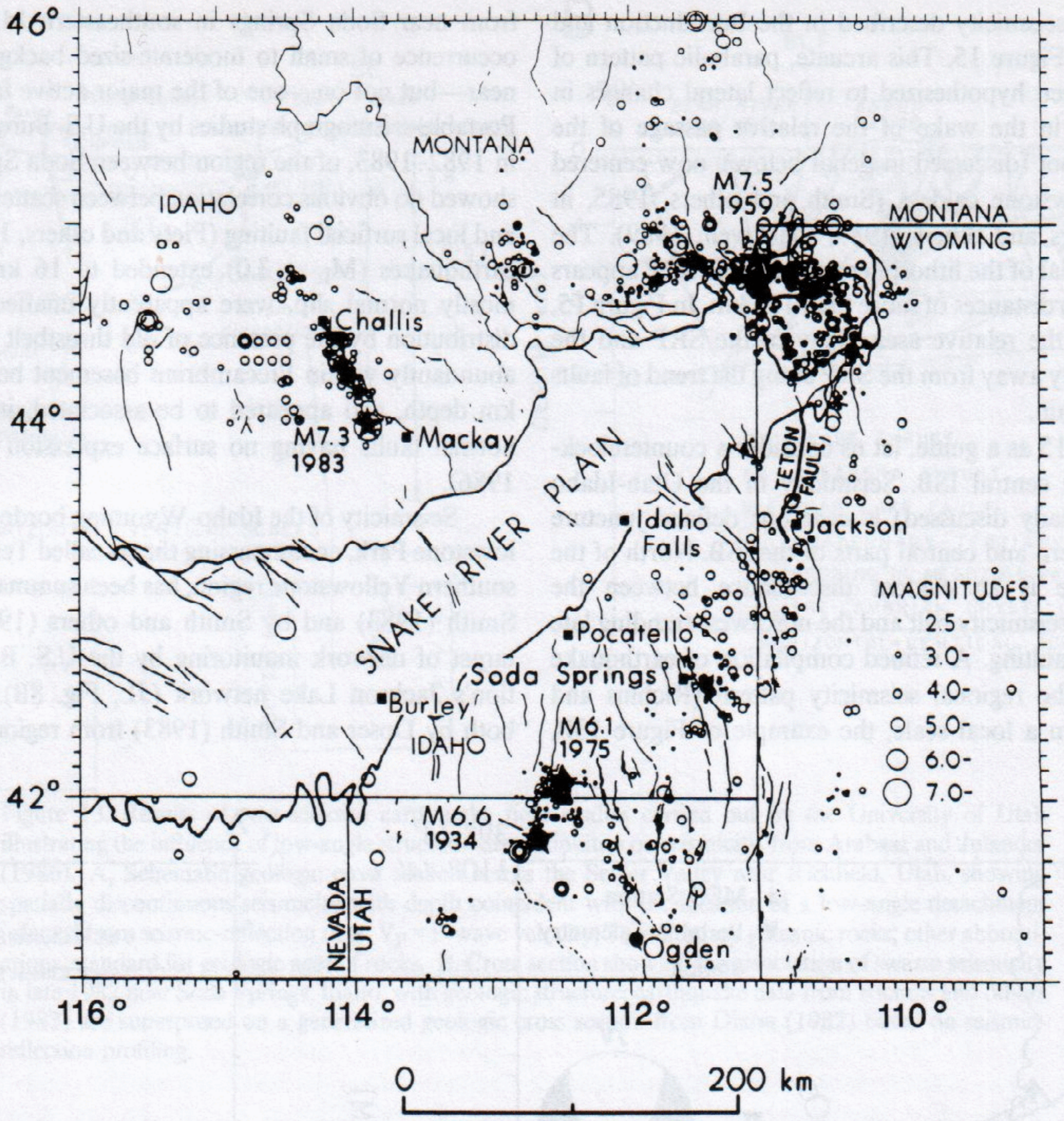

Figure 15. Map showing seismicity, 1900 to 1985, and selected Cenozoic faults of the central Intermountain seismic belt, from Smith and others (in preparation). Larger historical main shocks, as in Figure 9, shown for reference. Note the arcuate, parabolic pattern of seismicity flanking the Yellowstone–Snake River Plain basalt-rhyolite volcanic province.

local microearthquake studies and by Wood (1988) from the Jackson Lake network consistently depict: (1) diffusely scattered seismicity that correlates poorly with late Cenozoic normal faulting and, in an uncertain way, with relict thrustbelt structure in the subsurface; (2) seismic quiescence of the central part of the Teton fault, which had the greatest prehistoric surface displacements along the fault; (3) focal depths shallower than 15 km for most of the local earthquakes; and (4) fault-plane solutions with normal to strike slip reflecting general east-west extension. On a regional scale, perhaps the most noteworthy feature of the Teton region is its appearance as a distinct seismic gap in the ISB (Fig. 1), accentuated by the presence of the large and active Teton fault, which has had up to 50 m of late Quaternary displacement (Smith and others, 1990a, b).

Intense swarms of shallow earthquakes and occasional moderate-sized earthquakes as large as the M_L = 6.1 earthquake in 1975 near Norris Junction in Yellowstone Park (No. 43, Table 2) characterize the seismicity of the Yellowstone National Park region (Smith and others, 1977; Pitt, 1987; Nagy and Smith, 1988). The Yellowstone region is the site of one of the world's largest and most active hydrothermal-volcanic systems. During the past two million years, three catastrophic volcanic eruptions have expelled more than 3,500 km^3 of rhyolitic ashflow tuffs forming three calderas, and another 3,000 km^3 of similar material were extruded between explosive eruptions (Christiansen, 1984). A preponderance of geophysical evidence suggests that the seismicity of the Yellowstone region is directly influenced by the presence of magmas, partial melts, and hydrothermal activity at mid- to upper-crustal depths (Smith and others, 1974, 1977; Smith and Braile, 1984). Seismic slip on the boundaries of small

upper-crustal blocks may reflect a combination of deformation caused by local transport of magma and hydrothermal fluid and by the regional tectonic stress field.

Figure 16 shows a representative view of background seismicity in the Yellowstone–Hebgen Lake region, together with an outline of the youngest, 600,000-year-old caldera. Earthquake clusters extend eastward from Hebgen Lake, Montana, along an east-west trend into Yellowstone National Park where they take on a northwest trend along distinct seismic zones about 25 km long that cross the caldera boundary. Within the caldera, earthquakes have not exceeded magnitude (M_L) 5.0 and generally have scattered epicenters; in the western part of the caldera, northwest-trending clusters of epicenters, together with aligned volcanic vents, may be related to buried, but still active, Quaternary faults (Christiansen, 1984). In several cases, there are good correlations between earthquake swarms and major changes in hydrothermal activity (Pitt and Hutchinson, 1982). Local faulting along the west side of Yellowstone Lake has Holocene displacements and appears to be seismically active. South of this area, seismicity has a general north-south trend as it extends southward into the Teton region. Older basin-range structure is inferred to have influenced the Quaternary tectonics of the Yellowstone region. Parts of the Gallatin and Teton normal fault systems, which generally have a northerly trend outside the Yellowstone region, presumably lie beneath the area now covered by the Quaternary volcanics of the Yellowstone Plateau.

Focal depths show conspicuous variations across the Yellowstone caldera (Fig. 17). Maximum focal depths outside the caldera are generally less than 15 to 20 km, and mostly less than 5 km beneath the inner caldera (Smith and others, 1977; Nagy and Smith, 1988). This pattern of earthquake shallowing suggests a thin layer of seismogenic brittle upper crust beneath the thermally active inner caldera. Rheologic considerations (e.g., Smith and Bruhn, 1984) imply that below about 5 km, the crust is in a quasi-plastic ductile state at temperatures in excess of 350°C, incapable of supporting large stresses. Note that the M_L = 6.1 earthquake in 1975 occurred along the caldera's northwest boundary.

Continuing our circuit of the central ISB in Figure 15, we next move westward from the Yellowstone region—following an

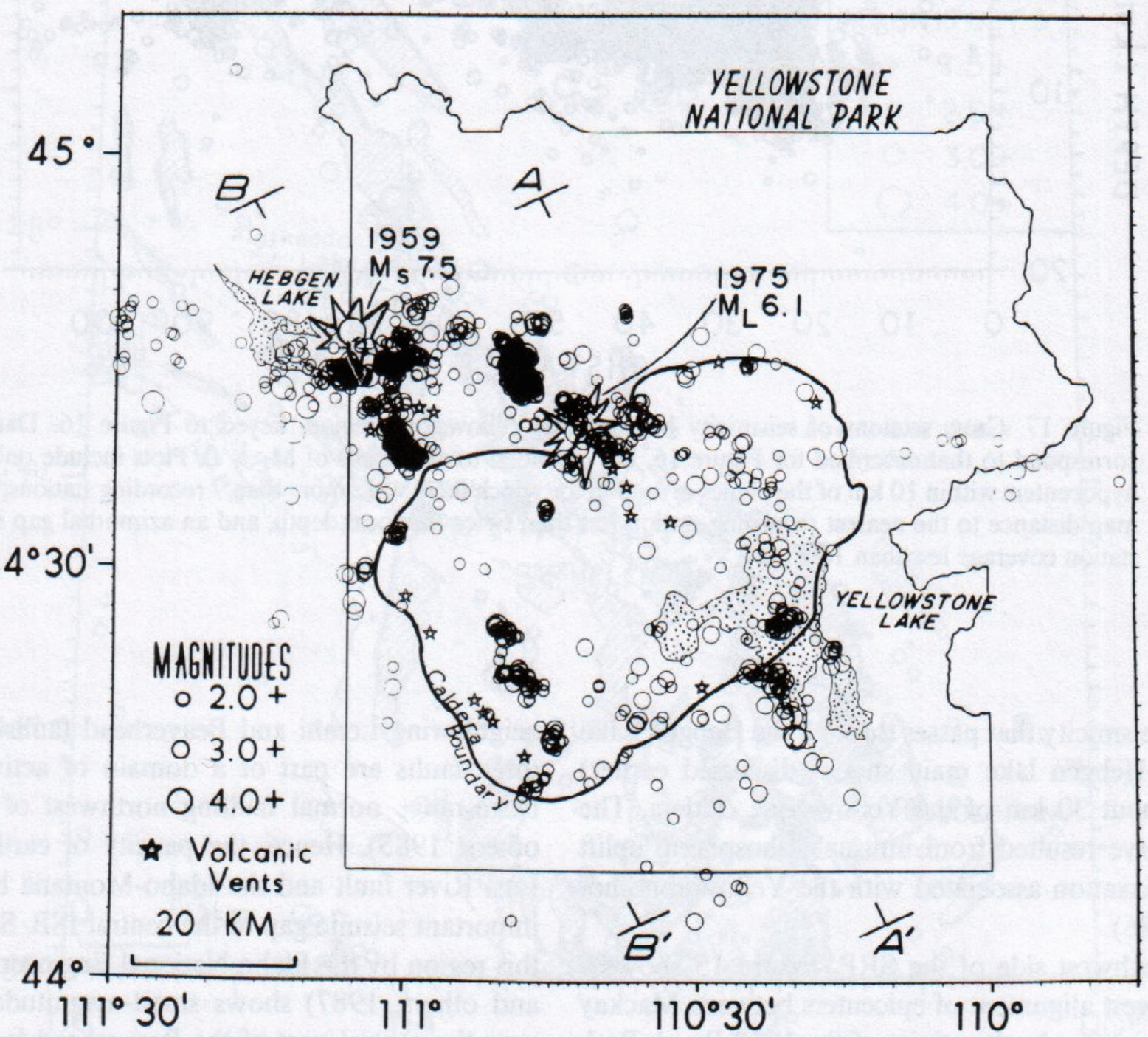

Figure 16. Map showing representative seismicity in the Yellowstone region of magnitude (M_L) 2.0 or greater, from compilations by the U.S. Geological Survey for 1973 to 1981 (Pitt, 1987) and by the University of Utah for 1984 to 1989 (e.g., Peyton and Smith, 1990). A-A′ and B-B′ define the locations of cross sections shown in Figure 17. Boundary of the Yellowstone caldera and epicenters of 1959 and 1975 main shocks (starbursts), as in Figure 9, shown for reference.

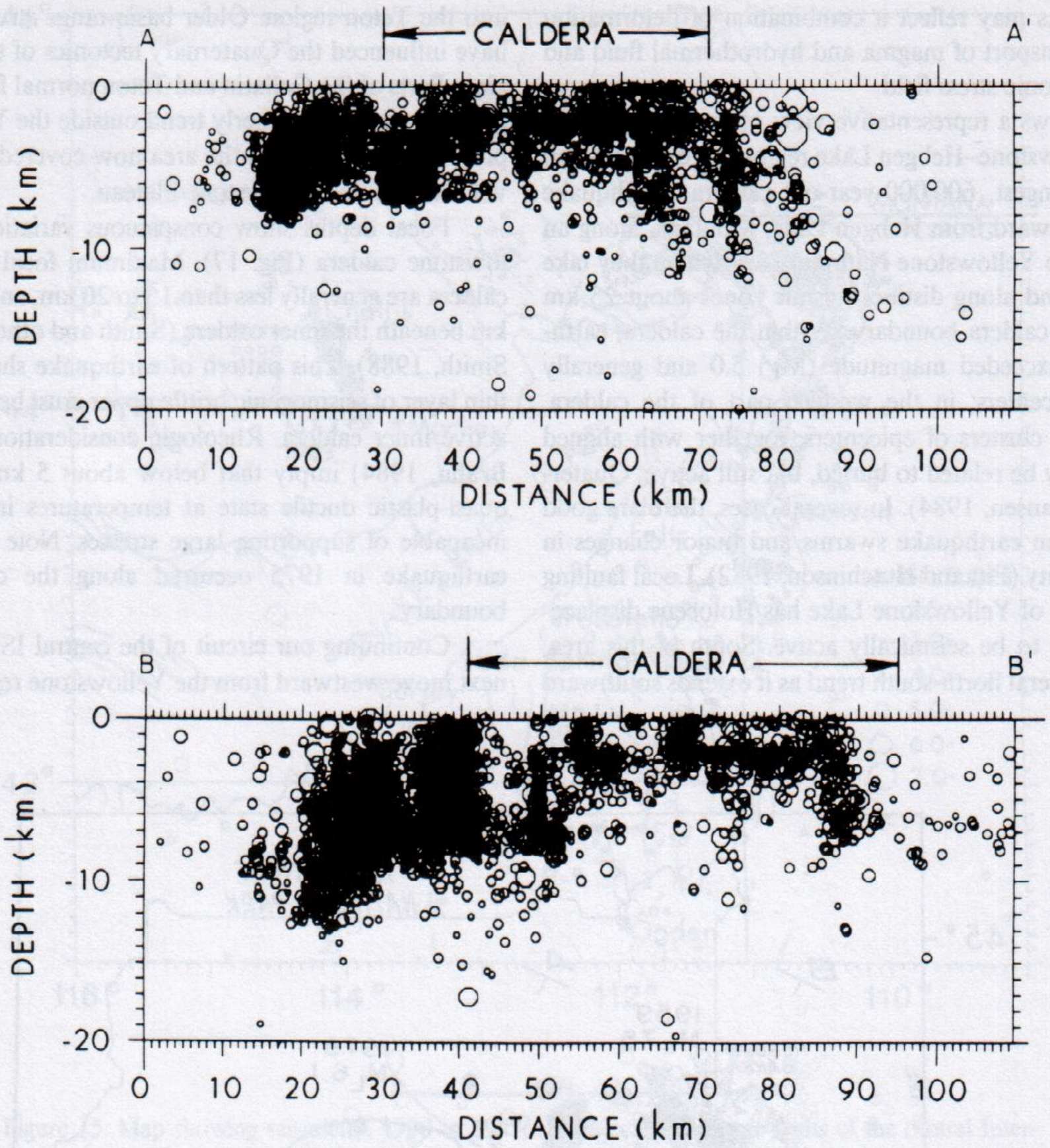

Figure 17. Cross sections of seismicity beneath the Yellowstone region, keyed to Figure 16. Data correspond to that described for Figure 16, but extended to all shocks of $M_L > 0$. Plots include only hypocenters within 10 km of the planes of section for which there were more than 7 recording stations, a map distance to the nearest recording station less than twice the focal depth, and an azimuthal gap in station coverage less than 180°.

east-west band of seismicity that passes through the Hebgen Lake region. The 1959 Hebgen lake main shock (discussed earlier) occurred within about 30 km of the Yellowstone caldera. The earthquake may have resulted from unusual lithospheric uplift and viscoelastic relaxation associated with the Yellowstone hot spot (Reilinger, 1986).

Along the northwest side of the SRP, Figure 15 shows a pronounced northwest alignment of epicenters between Mackay and Challis, which is aftershock activity of the 1983 Borah Peak earthquake on the Lost River fault. This pattern contrasts with the scatter of what we have called background seismicity elsewhere in the central ISB. The "turning on" of earthquakes on the Lost River fault emphasizes the relative seismic quiescence of the neighboring Lemhi and Beaverhead faults to the northeast. All three faults are part of a domain of active, latest Quaternary basin-range normal faulting northwest of the SRP (Scott and others, 1985). Hence, the paucity of earthquakes between the Lost River fault and the Idaho-Montana border marks another important seismic gap in the central ISB. Seismic surveillance of this region by the Idaho National Engineering Laboratory (King and others, 1987) shows small-magnitude earthquake activity near the central part of the Beaverhead fault, but very minimal microseismicity along the Lemhi fault. Central Idaho west of the Borah Peak earthquake zone (Fig. 15) is characterized by diffuse earthquake activity (Dewey, 1987; Smith and Sbar, 1974), earthquake swarms (Pennington and others, 1974; Smith, 1977),

and extensive hot spring activity. Microearthquake studies reported by Smith (1977) suggest maximum focal depths of 10 to 15 km.

Northern ISB

The northern ISB, as we have delimited it north of the Hebgen Lake–Yellowstone region, lies entirely within western Montana (Fig. 1). The region has had no historical surface faulting, and the largest historical earthquake reached magnitude 6¾ (Fig. 9, Table 2). Here, we expand upon a recent summary of seismicity and faulting in western Montana–eastern Idaho by Stickney and Bartholomew (1987) to describe some detailed aspects of the northern ISB. For illustration, Figure 18 combines available information on Cenozoic faulting with a representative seven-year sample of instrumental seismicity from the Montana regional seismic network (M, Fig. 8B).

The area of Figure 18 contains at least three fundamentally different domains of Cenozoic basin-bounding extensional faults (see Fig. 3 for names): (1) large north-northwest–trending faults in northwestern Montana, (2) west-northwest–trending faults marking the Lewis and Clark Zone (LCZ), and (3) faults of variable trend south of the LCZ. Significantly, none of these domains include faulting of Holocene age; Holocene faulting in Montana is restricted to a belt along the northwest flank of the SRP (the Centennial Tectonic Belt of Stickney and Bartholomew, 1987), which we have described as part of the central ISB. Large faults in northwestern Montana have exerted strong control on Cenozoic topography, probably including significant Quaternary displacements (Pardee, 1950), but the current seismic potential of these faults is uncertain (Qamar and others, 1982). The LCZ is a pre-Cenozoic structural lineament about 400 km long, perhaps dating from the Proterozoic, that has been interpreted to reflect a fundamental intraplate boundary (see Stickney and Bartholomew, 1987). Major transcurrent shearing has been postulated for the LCZ, but the zone is not noted for any such slip in late Cenozoic time (Eardley, 1962). In its modern expression, the LCZ is considered to be a transitional zone, up to 50 km wide, that "divides a region of uniformly northwest-trending Laramide thrusts and folds and Tertiary normal faults to the north from a

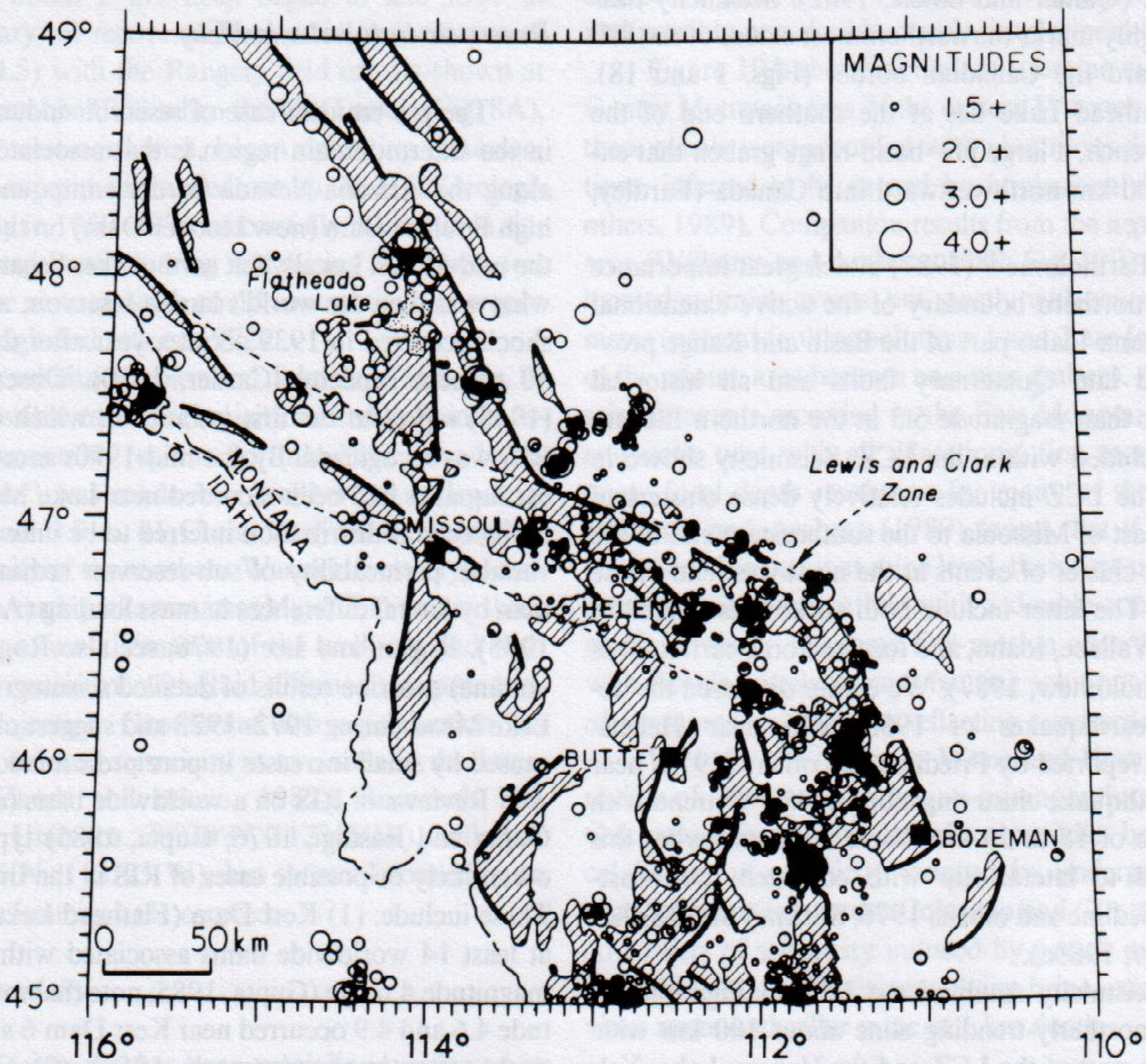

Figure 18. Seismicity map of the northern Intermountain seismic belt. Map shows all earthquakes of magnitude 1.5 and greater located by the Montana Bureau of Mines and Geology from 1982 through 1987 (M. C. Stickney, personal communication, 1990). Base map shows Cenozoic basins (hachured), basin-bounding extensional faults (heavy lines), and the outline of the Lewis and Clark Zone (short-dashed line) after Stickney and Bartholomew (1987).

region of batholithic intrusions and shorter Basin and Range structures with diverse trends to the south" (Stickney and Bartholomew, 1987).

The background seismicity shown in Figure 18 defines a belt about 200 km wide that follows the regional northwest trend of extensional basins in western Montana without definite association with the mapped faults. We describe features of this seismicity in each of the three domains of faulting outlined above. In northwestern Montana, historical seismicity has not exceeded magnitude 5.5 (Fig. 9) and has been dominant in the vicinity of Flathead Lake (Figs. 1, 9, 18), where significant earthquake swarms occurred in 1945, 1952, 1964, 1969, 1971, and 1975 (Qamar and others, 1982). A possible relation between seismicity and reservoir loading at Flathead Lake has been suggested by Dunphy (1972). Results from short-term seismographic recording near Flathead Lake in 1971 by Stevenson (1976; see also Sbar and others, 1972) showed clustering of small earthquakes on the west side of the lake, with focal depths extending from 5 to 12 km depth and foci defining a planar zone dipping 70° to the east-northeast. Diverse focal mechanisms in the vicinity of Flathead Lake appear mostly to reflect east-west to northwest-southeast extension (Qamar and others, 1982). Seismicity near Flathead Lake roughly marks the northernmost extent of the ISB as it dies out toward the Canadian border (Figs. 1 and 18). Coincidentally, Flathead Lake lies at the southern end of the Rocky Mountain trench, a large pre–basin-range graben that extends more than 800 km northwestward into Canada (Eardley, 1962; Pardee, 1950).

Stickney and Bartholomew (1987) attach great importance to the LCZ as the northern boundary of the active extensional regime of the Montana-Idaho part of the Basin and Range province. All identified late Quaternary faults and all historical earthquakes greater than magnitude 5.5 in the northern ISB are south of, or are included within, the LCZ. Seismicity shown in Figure 18 within the LCZ includes relatively dense clusters of earthquakes from east of Missoula to the southeastern end of the LCZ and a distinct cluster of events at the northwest end of the LCZ in the figure. The latter include both rockbursts related to deep mining near Wallace, Idaho, and local tectonic earthquakes (Stickney and Bartholomew, 1987). We earlier discussed the destructive swarm earthquakes of 1935–1936 near Helena. Earthquake studies reported by Friedline and others (1976) near Helena indicate earthquake clustering along a N50°W trend with focal-depth maxima of 15 to 20 km. Focal mechanisms for this area imply normal to lateral slip with consistent northeast-trending T-axes (Friedline and others, 1976; Stickney and Bartholomew, 1987; Doser, 1989a).

Background seismicity south of the LCZ in Figure 18 is concentrated in a northerly-trending zone about 100 km wide between the eastern part of the LCZ and the Hebgen Lake–Yellowstone region to the south. Recall that the Helena-Bozeman area has had the largest historical earthquakes in the northern ISB (Fig. 9). Densely clustered seismicity about 50 km northwest of Bozeman is in the Clarkston Valley area, one of the most persistently active earthquake zones in the northern ISB since the occurrence of the M = 6¾ Clarkston Valley earthquake in 1925 (Stickney and Bartholomew, 1987). Special studies of seismic activity in the Clarkston Valley area have been reported by Qamar and Hawley (1979), who document relatively shallow (<10 km) focal depths and both normal and strike-slip focal mechanisms with T-axes trending 55° to 95°—different from the trend of 127° for the 1925 main-shock mechanism (Doser, 1989a).

INDUCED SEISMICITY

Human activities have demonstrably triggered small to moderate earthquakes ($M \leqslant 5.0$) in the Intermountain region, both within the main active zone of the ISB and in marginal, less seismically active areas. This includes documented cases of each of the three principal types of induced seismicity—associated, respectively, with reservoir impoundment, fluid injection, and mining. We proceed to summarize examples (see also Dewey and others, 1989, Table 1), referring to localities identified in Figure 3.

Reservoir-induced seismicity

The pre-eminent case of reservoir-induced seismicity (RIS) in the Intermountain region is that associated with Lake Mead along the Arizona-Nevada border—impounded by the 221-m-high Boulder Dam (now Hoover Dam) on the Colorado River in the mid-1930s. Locally felt earthquakes began soon after filling of what was then the world's largest reservoir, and a magnitude 5.0 shock occurred in 1939 about a year after the reservoir reached 80 percent capacity (Carder, 1970). Observations by Carder (1945) represent the first instance in which the phenomenon of RIS was recognized. By the mid-1970s more than 10,000 local earthquakes had been recorded near Lake Mead, with an irregular epicentral distribution inferred to be influenced chiefly by the variable permeability of sub-reservoir sedimentary rocks rather than by lateral differences in mass loading (Anderson and Laney, 1975). Rogers and Lee (1976; see also Rogers and others, this volume) describe results of detailed seismographic monitoring at Lake Mead during 1972–1973 and suggest observed RIS there is caused by small increases in pore pressure along existing faults.

Reviews of RIS on a worldwide basis (e.g., Simpson, 1976; Gupta and Rastogi, 1976; Gupta, 1985) typically mention five other likely or possible cases of RIS in the Intermountain region. These include: (1) Kerr Dam (Flathead Lake), Montana, one of at least 14 worldwide dams associated with earthquakes in the magnitude 4 range (Gupta, 1985; note that earthquakes of magnitude 4.6 and 4.9 occurred near Kerr Dam 6 and 13 years, respectively, after impoundment in 1958); (2) Glen Canyon (Lake Powell) and (3) Flaming Gorge dams in Utah, where there is uncertain evidence for impoundment-related *decreases* in seismicity (Simpson, 1976); and possible cases of RIS at (4) Clark Canyon Dam, Montana, and Palisades Dam, Idaho (Gupta,

1985; Simpson, 1976). The common occurrence of earthquake swarms throughout the region immediately surrounding Palisades Reservoir confounds arguments for causally relating such seismicity with the reservoir (see review by Piety and others, 1986). There, as elsewhere in the Intermountain region, adequacy of seismographic control is a critical issue in correlating small-magnitude earthquakes with reservoir impoundment. LaForge (1988), for example, rigorously tested for RIS in connection with 14 dams, 38 to 81 m high, built by the U.S. Bureau of Reclamation in north-central Utah and found no evidence for RIS. However, all but one of the reservoirs was filled before 1967 when seismographic control in the region was still relatively poor.

Fluid injection

After the U.S. Army accidentally triggered earthquakes by deep fluid injection near Denver, Colorado, in the early 1960s, the U.S. Geological Survey carried out a controlled experiment in the Rangely oil field in northwestern Colorado to study the effects of pore-pressure changes at depth on the triggering of small earthquakes (Raleigh and others, 1972). Water injection into a sandstone reservoir about 2 km deep began in late 1957 at Rangely for secondary oil recovery. The spatial coincidence of earthquakes ($M \leqslant 4.5$) with the Rangely field can be shown at least as early as November 1962 when the UBO array (Fig. 8A), 50 to 80 km to the west-northwest, began operating (Munson, 1970). The detailed experiment carried out by the U.S. Geological Survey at Rangely in 1969–1970 successfully measured in situ stress state and showed how lowering and raising fluid pressures in a seismically active zone at depth could control the occurrence of earthquakes (Raleigh and others, 1972).

Arabasz (1984; see also Arabasz and Julander, 1986, Fig. 8) describes another possible case of seismicity related to fluid injection in the Intermountain region. In mid-1982 an "acid-breakdown hydrofrac" was made in a wellbore at a depth of about 5 km (Chevron U.S.A. #1 Chriss Canyon, total depth = 5,344 m) in the vicinity of the southern Wasatch fault. Hypocentral clustering of two earthquake swarms ($M_L \leqslant 2.1$) two to three months later, within a few kilometers of the wellbore and with distance-delay times consistent with fluid diffusion, suggests triggering by the fluid injection. Geothermal steam production has been monitored for induced seismicity at two sites in the Intermountain region (Zandt and others, 1982): Roosevelt Hot Springs–Cove Fort, Utah (ca. 38°30′N, 112°45′W), and Raft River, Idaho (42°06′N, 113°23′W), but to our knowledge no significant induced seismicity has occurred.

Mining-related seismicity

Mining-related seismicity has been specially investigated in two parts of the Intermountain region—the northern and northwestern Colorado Plateau, chiefly in association with underground coal mining, and near Wallace, Idaho, in association with deep vein mines of the Couer d'Alene mining district. In the latter area, seismographic studies have focused on rockbursts (e.g., McLaughlin and others, 1976); however, sizable shocks up to magnitude 4 suggest tectonic stress release as well (Stickney and Bartholomew, 1987).

Seismicity in east-central Utah defines an inverted U-shaped pattern (Figs. 1 and 12B) coinciding with areas of extensive underground coal mining along an arcuate erosional escarpment of the eastern Wasatch Plateau and Book Cliffs. The association of both rockbursts and earthquakes ($M_L \leqslant 4.5$) with sites of major coal extraction in this area has been evident since the late 1950s. Wong and Humphrey (1989) and Williams and Arabasz (1989; see also Smith and others, 1974) give good overviews of varied seismological investigations indicating that: (1) much of the seismicity appears to be mining induced, resulting from stress redistribution from both room-and-pillar and longwall coal extraction in mine workings down to 900 m below the surface; (2) abundant seismicity occurs *beneath* the mines to depths of 2 to 3 km; (3) time-varying rates of extraction at individual mines have influenced seismicity changes detected by regional seismic monitoring; and (4) source mechanisms appear variously to reflect extensional subsidence above mine workings and a mixture, at and below mine level, of seismic slip on prestressed reverse faults and possibly non-double-couple, implosional failures.

Figure 19A shows abundant submine events located in the Gentry Mountain area of the eastern Wasatch Plateau. Nearly all these events were recorded with ubiquitous dilatational first motions, inferred to be caused by implosional failure (Wong and others, 1989). Companion results from the nearby East Mountain area (Williams and Arabasz, 1989; Fig. 19B) also show reliably-located submine events, but mostly with reverse-faulting mechanisms (normal-faulting solutions 1 and 2 are for earthquakes west of the mining area beneath an active graben). About a third of the seismic events recorded in the East Mountain area were of the enigmatic type with all dilatational first motions. Given inadequate focal-depth resolution for many of these shallow events, Williams and Arabasz (1989) found that if these events were constrained to occur at mine level, their first-motion distributions were indeed incompatible with a double-couple source mechanism. However, the same first-motion observations could be fit with double-couple normal-faulting solutions if the sources were *above* mine level, perhaps reflecting overburden subsidence.

We refer the reader to Wong and Humphrey (1989) for a review of other varied work on mining-induced seismicity in the Colorado Plateau. This includes (1) studies by the U.S. Geological Survey of seismicity induced by underground coal mining near Somerset in western Colorado and (2) studies by Wong and coworkers of seismicity induced by potash mining in the north-central Colorado Plateau involving brine extraction from a previous room-and-pillar mine at 1 km depth.

PATTERNS OF EARTHQUAKE OCCURRENCE

Observations about patterns of earthquake occurrence in the ISB are fundamental both for scientific understanding of earthquake behavior in the region as well as for basic evaluations of

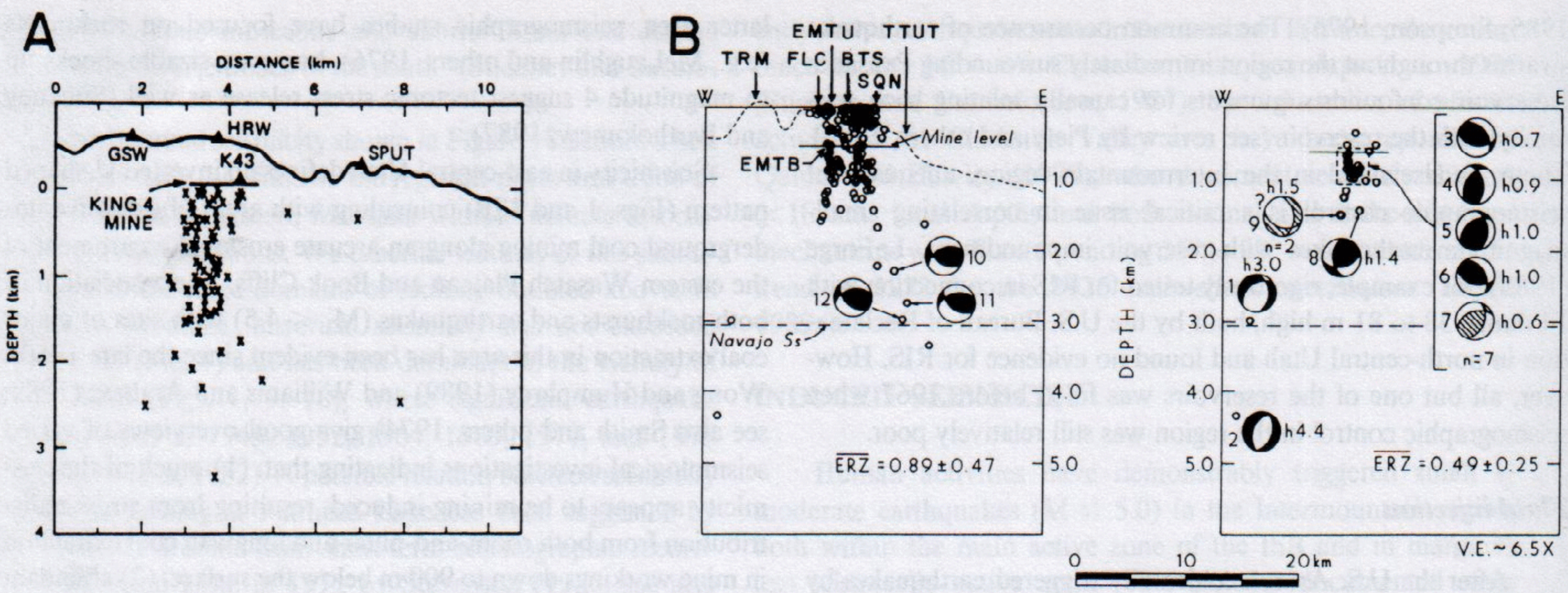

Figure 19. Mining-related seismicity in the eastern Wasatch Plateau, Utah. A, Cross section from a special study in the Gentry Mountain area (from Wong and others, 1989) showing ground surface (heavy line), seismic events (x's) within 500 m of the plane of section, and closest seismographs (triangles). B, Cross sections from the East Mountain area, about 20 km south of Gentry Mountain (from Williams and Arabasz, 1989) showing ground surface (short-dashed line), seismic events (small circles) within 5 km of the plane of section, seismograph locations (letter codes) within 1 km of the plane of section, and schematic equatorial-plane projection of 12 focal mechanisms—dilatational quadrants are white and compressional quadrants either black (for single-event solutions) or hachured (for composite solutions); the left panel of B includes events located with standard errors in focal depth (ERZ) less than 2.0 km; the right panel includes only the "best" located events meeting rigorous criteria for reliability of focal depth, h.

earthquake hazards and risk. In this section we briefly summarize relevant information on (1) earthquake swarms, (2) earthquake recurrence, and (3) the space-time distribution of earthquakes in the ISB.

Earthquake swarms

Earthquake swarm activity, the clustering of earthquakes of similar size in space and time without an outstanding main shock, is a common feature in parts of the ISB. Such earthquake swarms tend to occur in and near areas of Quaternary volcanism or high heat flow. Smith and Sbar (1974) present a good general discussion, describing notable areas of historical swarm activity in the ISB. These include: Flathead Lake and Helena, Montana, in the northern ISB; Yellowstone, central Idaho, and southeastern Idaho in the central ISB; and areas in western and southwestern Utah in the southern ISB. We have already described sources of information for most of these areas in preceding sections. Additional information on earthquake swarm activity is given by Arabasz and Julander (1986) for southwestern Utah and by Piety and others (1986) for southeastern Idaho. The destructive earthquake swarm near Helena, Montana, in 1935–1936 (described earlier) that included shocks of magnitude 6 and 6¼ (Table 2) is the most outstanding example of swarm seismicity in the ISB. Elsewhere in the ISB, the largest earthquakes in individual swarms have been in the upper magnitude 4 range or smaller.

Earthquake recurrence in the ISB

Earthquake recurrence specifies the distribution of earthquake sizes (e.g., magnitudes or intensities) and their frequency of occurrence on a fault or in a specified area. Here, we basically want to describe how often moderate to large earthquakes occur in the ISB and point the interested reader to more specific information for recurrence modeling. Modern methods for quantifying earthquake recurrence using information from observational seismology and from geologic studies of the age, frequency, and rupture characteristics of prehistoric earthquakes are summarized by McGuire and Arabasz (1990) and Schwartz and Coppersmith (1986) (see also Doser and Smith, 1982).

The most commonly used relations to describe the relative number of earthquakes as a function of size is the well-known Gutenberg-Richter relation (Richter, 1958): $\log_{10}N(m) = a - bm$, where $N(m)$ is the number of earthquakes of magnitude m or greater per unit time (and ideally per unit area) and a and b are constants. The average inter-event time or recurrence interval for earthquakes of a particular magnitude m or greater is given by $1/N(m)$. There is growing recognition that the Gutenberg-Richter relation may appropriately apply to a region but not necessarily to an individual fault (e.g., Schwartz and Coppersmith, 1986). It is also recognized that the historical and instrumental earthquake record cannot confidently be extrapolated to estimate the frequency of occurrence of large surface-faulting earthquakes in the

ISB and that information from late Quaternary faulting is therefore essential (Schwartz and Coppersmith, 1984; Arabasz and others, 1987). Thus, historical and instrumental records of seismicity in the ISB are important for modeling the recurrence of earthquake sizes up to the threshold of surface faulting, and paleoseismology is needed for estimating how often large surface-faulting earthquakes will occur.

A rough estimate of the recurrence interval of sizable earthquakes for the *whole* ISB can be made from Table 2. Neglecting aftershocks and secondary events, 27 independent main shocks of approximate magnitude 5.5 and greater occurred in the ISB from 1900 through 1985, which gives an average inter-event time of 3 years for such shocks somewhere in the ISB. Corresponding estimates from Table 2 for thresholds of approximate magnitude 6.0 and 6.5 are about 6 years and 17 years, respectively. For earthquakes of magnitude 7.0 or greater, we simply note that two such events occurred during the 85-year observation period, insufficient for meaningful modeling of inter-event times. Recurrence intervals vary, of course, with the particular region and the total area being considered. For example, for the 85,000 km^2 of the Wasatch Front area (Fig. 12), rigorous recurrence modeling of instrumental seismicity for 1962 through 1985 (Arabasz and others, 1987) yields average recurrence intervals of 24 years for $M_L \geqslant 5.5$, 54 years for $M_L \geqslant 6.0$, 120 years (extrapolated) for $M_L \geqslant 6.5$, and 280 years (extrapolated) for $M_L \geqslant 7.0$. For other examples of recurrence modeling in parts of the ISB, we refer the reader to Youngs and others (1987), Doser and Smith (1982), Piety and others (1986), Stickney and Bartholomew (1987), and Algermissen and others (1982). Comparison of seismicity parameters among these and other published reports for the ISB must be made with care, checking whether the parameters were determined with sufficient rigor, whether the parameters are intrinsically comparable, and whether the parameters describe the occurrence only of independent main shocks or of all earthquakes (see McGuire and Arabasz, 1990).

Average slip rates on normal faults in the ISB are one to two orders of magnitude lower than for those on major plate-boundary faults, typically being about 1 mm/yr for the most active faults like the Wasatch fault (Schwartz and Coppersmith, 1984; Machette and others, 1987) and the Teton fault (Byrd and Smith, 1990), and a few tenths of a millimeter or less on faults elsewhere in the region (e.g., Schwartz, 1987; Youngs and others, 1987; Scott and others, 1985; Stickney and Bartholomew, 1987). Corresponding recurrence intervals for surface rupture on an individual fault segment are about 2,000 yr on the most active parts of the Wasatch fault, are uncertain on the Teton fault, and are typically several thousand or tens of thousands of years on other faults. The issue of uniform versus time-varying recurrence (see Schwartz, 1988) has become an important consideration for estimating expected rates of occurrence of large earthquakes in the ISB. On the Wasatch fault, for example, the record of surface-faulting earthquakes during the past 6,000 yr leads to an average recurrence interval of 415 yr for a large surface-faulting earthquake somewhere on the fault, but an accelerated rate of faulting between about 400 and 1,500 yr ago implies such an earthquake once every 220 yr (Machette and others, 1989). Comparably detailed paleoseismological data do not exist for other faults in the ISB.

How do rates of intraplate faulting and earthquake activity in the ISB compare to those along the North American plate boundary in California? Recurrence intervals of thousands of years for surface rupture on individual fault segments in the ISB compare to much shorter intervals of hundreds of years for large earthquakes on the most active parts of the San Andreas fault system (Schwartz and Coppersmith, 1984). Maximum-size earthquakes of about magnitude 7¾ in the ISB compare to a value of about 8½ on the San Andreas fault. We remarked earlier that deformation rates for most of the intraplate ISB are one to two orders of magnitude lower than along the western North America plate boundary. Comparison between seismicity in the ISB and California can be made using seismicity rates determined in a uniform way by Algermissen and others (1982, Table 1) for source zones throughout the United States, normalizing those values per unit area. The mean rate of earthquakes equivalent in size to MMI = V (about magnitude 4) per year per 1,000 km^2 is approximately 8×10^{-2} for the 41 seismic source zones depicted by Algermissen and others (1982, Fig. 2) in the main seismically active part of California. The mean value of that same rate for their seismic zones making up the main ISB is approximately 2×10^{-2}. Thus, normalized seismicity in the ISB, on average, is lower by about a factor of 4 compared to that along the plate boundary in California.

Space-time patterns of seismicity in the ISB

To get an overview of variations of earthquake activity along the ISB as a function of space and time, as captured by the DNAG catalog, we have plotted those data in a conventional space-time format and show the results in Figure 20. The same DNAG catalog data used for Figure 1 were sorted for the four sample areas shown in Figure 20A, prescribing a magnitude threshold of 3.0 and the time period from 1930 through 1985. We chose 1930, judging that epicentral precision had become sufficient by that time to make meaningful spatial comparisons, and the date precedes the occurrence of sizable earthquakes in the ISB in the mid-1930s and 1940s. The sorted earthquakes are plotted in Figure 20B with latitude as the space coordinate, given the general north-south trend of the ISB, recognizing the limitation that the northern and southernmost parts of the ISB trend obliquely to the latitude ordinate. Data for central Idaho had to be excluded to prevent confusion in projection.

As usual, there are evident artifacts that must be accounted for in space-time plots of this type, the most obvious being those due to catalog incompleteness. Increases in numbers of earthquakes in the early 1960s and locally in the mid-1970s correspond to improvements in seismographic coverage that we described in the section on instrumental recording and seismic networks. Despite recognizable problems, Figure 20 reveals some

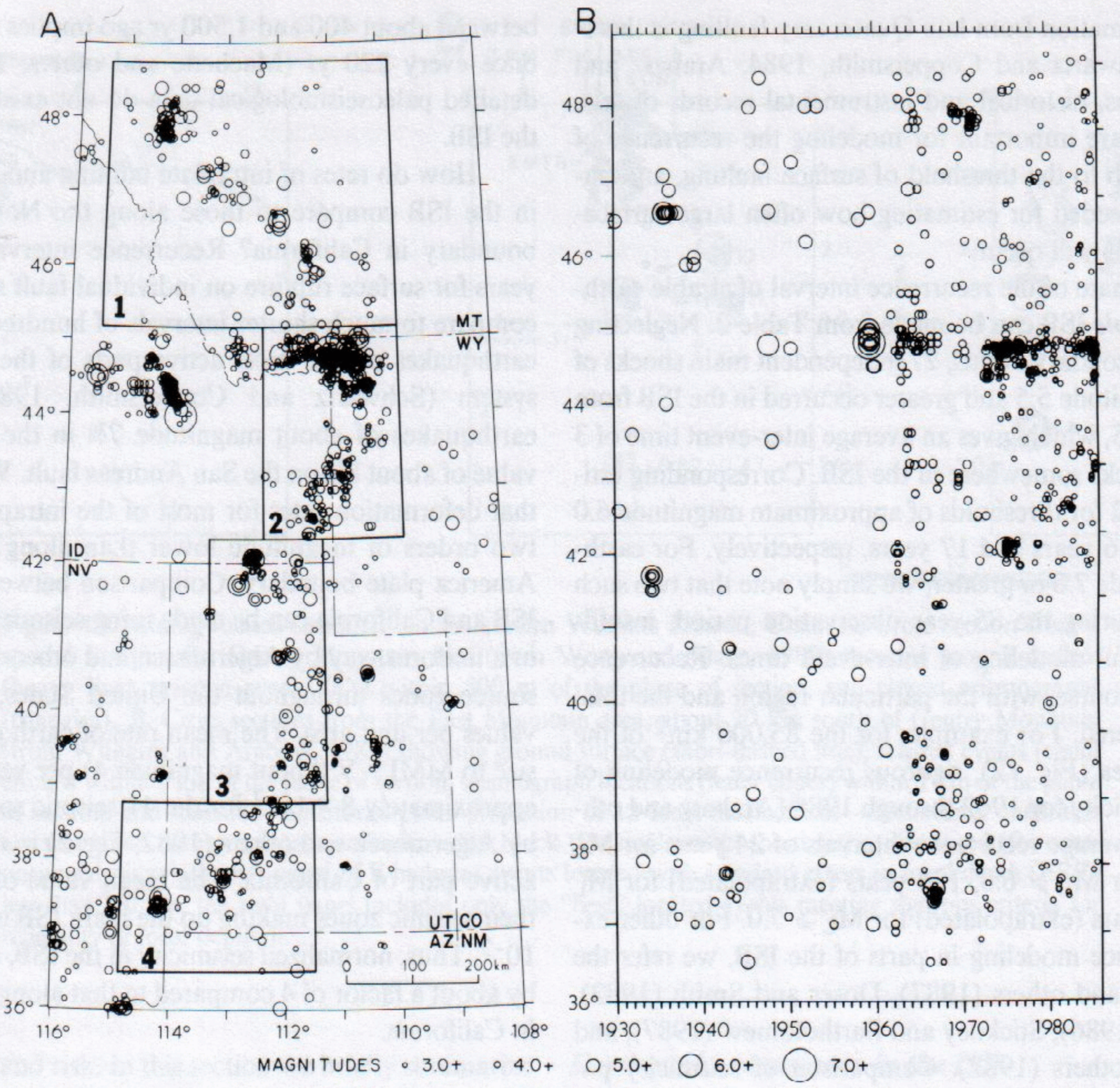

Figure 20. Space-time seismicity of the Intermountain seismic belt, 1930 to 1985. A, Map showing earthquakes from Figure 1 of magnitude 3.0 and greater since 1930, together with sample boxes used for the space-time plot in B. B, Space-time plot of earthquakes as a function of time (abscissa) and latitude (ordinate), keyed to A.

important observations that warrant attention. We proceed from north to south, using the boxes numbered from 1 to 4 for reference.

For the northern ISB, the space-time projection of earthquakes in Box 1 shows an understandable increase in smaller-magnitude earthquakes after about the mid-1960s, but there is a noticeable decrease in the number of larger earthquakes ($M \geq 5$) after that time, compared to earlier decades. Seismicity in the Hebgen Lake–Yellowstone region dominates the picture for the part of the central ISB bounded by Box 2. The projection of the Hebgen Lake–Yellowstone seismicity reveals the most intense earthquake activity in the ISB. There was a marked increase in the detection of small earthquakes following the installation of the Yellowstone seismic network in 1973, but similarly sensitive networks elsewhere in the ISB do not show the same level of seismicity. The $M_S = 7.5$ Hebgen Lake earthquake of 1959 is the largest shock at that latitude. Nearby prior occurrence of the M = 6¼ Virginia City earthquake 12 years earlier in 1947 suggests that earthquake may have been a preshock (Doser, 1989a). Both the map and space-time plot emphasize the existence of the Teton seismic gap, more than 50 km long, immediately south of the Yellowstone region. As earlier described, there is a similarly prominent gap northwest of the SRP between the Borah Peak earthquake zone and the Idaho-Montana border (Fig. 20A).

Box 3 essentially covers the Wasatch Front area. The $M_L = 6.0$ Pocatello Valley earthquake of 1975, at about 42°N, was preceded by seismic quiescence within 50 km that began 6.4 years before the main shock (Arabasz and Smith, 1981). One of the most striking features of the space-time projection of the earthquakes of Box 3 is the sparseness of earthquakes ($M \geq 3.0$) since the mid-1960s along a zone more than 200 km long between about 39.5°N and 41.5°N, corresponding to the most geologically active part of the Wasatch fault (Fig. 12). Note that there has been effective seismographic coverage of the Wasatch Front area since the early 1960s (Fig. 8B). Smith (1972) first noted the relative contemporary quiescence of the Wasatch Front area compared to neighboring segments of the ISB, and Arabasz and Smith (1981, Fig. 8; see also Griscom, 1980) portrayed the

relative quiescence in space-time view. The apparent decrease in background seismicity in the Wasatch Front area beginning in the mid-1960s compared to prior decades was statistically tested by Arabasz (1984), who found that one could not reject at the 95-percent confidence level the hypothesis that the apparent decrease was simply random. The pattern of earthquake clustering in the Wasatch Front area, however, does have significant features. Based on a statistical analysis of the Utah earthquake catalog for 1962 through 1985 by Shimizu (1987), Veneziano and others (1987) observed that, compared to earthquake behavior in neighboring areas, there is a distinct paucity of secondary events, relative to the number of main events, in the vicinity of the Wasatch fault between 39.5°N and 41.5°N. We refer the reader to Arabasz and others (1987, Fig. 17) for a detailed space-time plot of microseismicity within a 30-km-wide zone along the Wasatch fault for 1962 through 1986.

The space-time plot of earthquakes in Box 4 at the southern end of the ISB shows a somewhat similar pattern to that for Box 1. Despite a marked improvement in seismographic coverage for the area of Box 4 in the mid-1970s, background seismicity has been noticeably lower since that time, compared to activity during the 1962 through 1975 period. Earthquake sizes in the Utah region have been measured instrumentally in a uniform way since 1962 (Arabasz and others, 1979). Although not rigorously analyzed here, the space-time overview of the entire ISB in Figure 20 points out general patterns that need to be addressed. The occurrence of the 1983 Borah Peak earthquake in an area of prior low seismicity and prehistoric surface faulting, which should have been recognized as a seismic gap, serves as a useful reminder.

CONCLUDING REMARKS

The mechanics and subsurface geometry of normal faulting are topics of great current interest and importance, especially for assessing ground deformation and peak ground motions associated with large normal-faulting earthquakes. The observation in parts of the Basin and Range province of steep planar faults (dips $> 45°$) associated with large normal-faulting earthquakes in the same structural setting where late Tertiary to Quaternary low-angle and listric normal faults are present in the subsurface poses a quandary. In this final section, we discuss observations and hypotheses relating to large normal-faulting earthquakes and to the diffuse background seismicity that dominates the earthquake record of the Intermountain region. We also consider implications of earthquake focal depths for rheology and the possible influence of the Yellowstone hot spot on the seismotectonics of the ISB, including its influence on Quaternary faulting of the SRP and surrounding region. Discussion of earthquakes in the Yellowstone region also provides insights into the relation between magma transport and seismicity.

Correlation of seismicity and geologic structure

A recurring observation in the ISB is the lack of distinct correlation between scattered background seismicity and mapped Cenozoic faulting. Numerous descriptions of background seismicity in the region published during the last decade include remarks to this effect. The problematic correlation has been discussed at length for the southern ISB by Arabasz and Julander (1986; see also Arabasz and Smith, 1981; Zoback, 1983; Smith and Bruhn, 1984). As outlined by Arabasz and Julander (1986), and generalized to the ISB as a whole, the basic problems include: (1) uncertain subsurface structure, which typically is more complex along the main seismic belt than is apparent from the surface geology, commonly because of the superposition of basin-range faulting upon older thrust-belt structure; (2) observations of discordance between surface fault patterns and seismic slip at depth; (3) limited opportunity to observe large-scale seismic slip because of only three cases of historic surface faulting; and (4) inadequate hypocentral resolution commonly resulting from regional seismic monitoring. In order to correlate seismicity with structure, there is a critical need (aptly illustrated by Fig. 14) for local seismographic control, especially for good focal-depth resolution, sufficient seismicity for defining the spatial geometry of active structures, and reliable focal mechanisms for correlating observed seismicity with fault geometry and the sense of slip. Focal mechanisms also allow assessment of the principal stress directions.

On the basis of special earthquake studies in mostly the southern ISB, a working hypothesis was offered by Arabasz (1984; see also Arabasz and Julander, 1986) to explain observations of diffuse background seismicity. Background seismicity, it was suggested, is fundamentally influenced by variable mechanical behavior and internal structure of individual plates within the seismogenic upper crust. Diffuse epicentral patterns appear to result from the superposition of relatively intense shallow seismicity within upper-crustal plates and less frequent background earthquakes at greater depth. Favorable conditions for block-interior rather than block-boundary microseismic slip may also contribute to the epicentral scatter. Some aspects of the working hypothesis are shown schematically in Figure 21A, which depicts (following Arabasz and Julander, 1986): (a) a predominance locally of seismicity within a lower plate; (b) nucleation of a large normal-faulting earthquake near the base of the seismogenic layer, hypothetically on an old thrust ramp, and with linkage to a shallow structure; (d) occurrence of a moderate-sized earthquake and aftershocks on a secondary fault where an underlying detachment restricts deformation to the upper plate; (e) diffuse block-interior microseismicity predominating within an upper plate—perhaps responding to extension enhanced by gravitational backsliding on an underlying detachment; and (f) diffuse block-interior microseismicity within a lower plate where frequency of occurrence is markedly lower than in the overlying plate.

While Figure 21A suitably illustrates many features of background seismicity in the southern ISB, particularly central Utah, it is not adequately general for the whole ISB. One shortcoming of the sketch in Figure 21A is that it does not explicitly depict the spatial relation of seismicity to Precambrian basement. In some parts of the ISB, Precambrian basement was faulted by

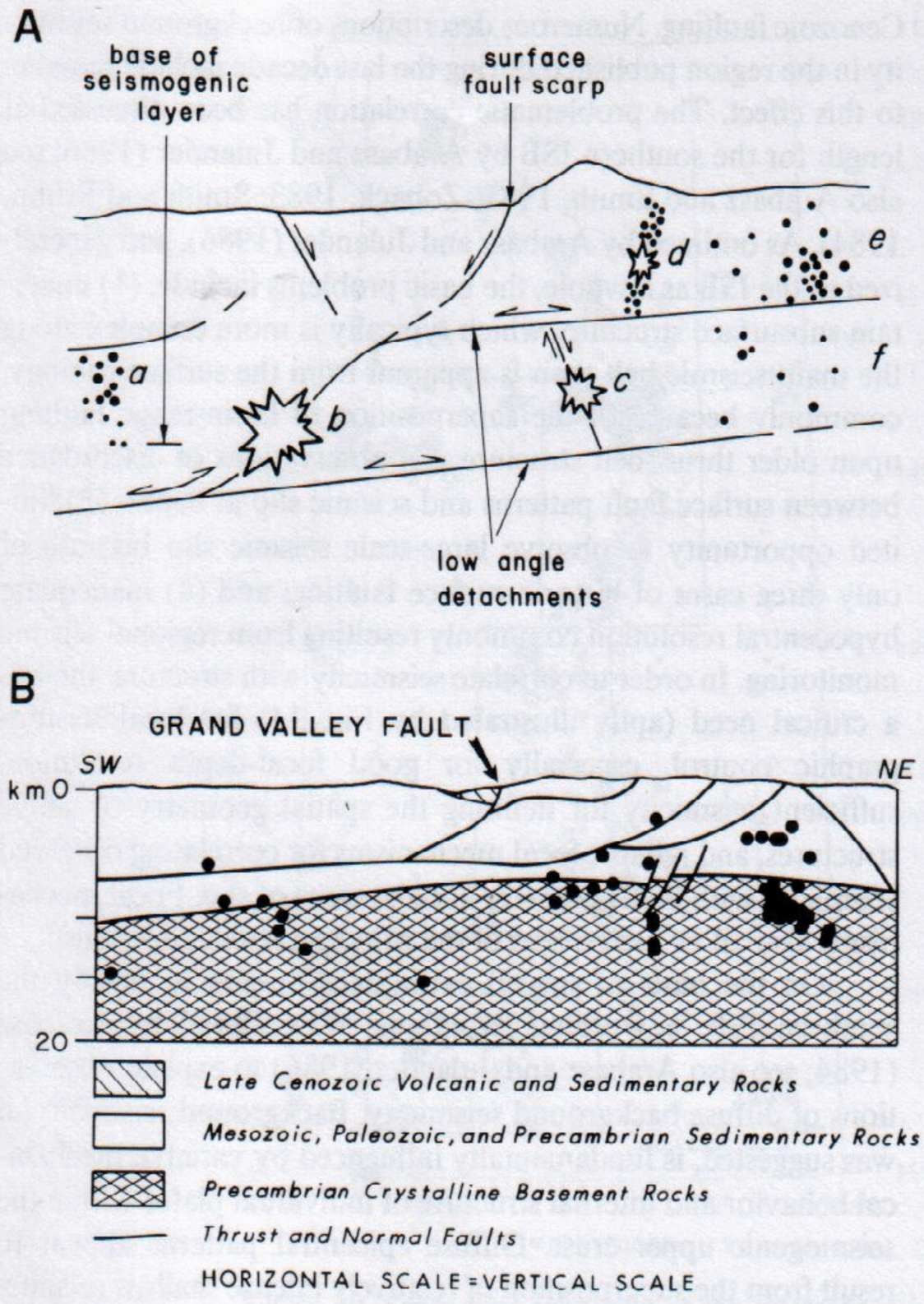

Figure 21. A, Schematic geologic cross section of the upper crust illustrating the inferred association of seismicity with geologic structure in the southern Intermountain seismic belt (from Arabasz and Julander, 1986). Starbursts indicate hypothesized foci of moderate-to-large earthquakes; small circles, microseismicity; lines in subsurface, faults; two-directional arrows, extensional backsliding on pre-existing low-angle faults possibly formed as thrust faults. Letters identify examples referred to in text. Base of seismogenic layer is approximately 10 to 15 km depth. B, Cross section (from Piety and others, 1986) showing distribution of well-located background earthquakes (circles), together with generalized geology from interpretations of seismic-reflection data by Dixon (1982), across the Grand Valley fault in the central Intermountain seismic belt. Line of section trends N60°E and crosses the northern end of Palisades Reservoir (Fig. 3).

pre-Neogene thrusting and is allochthonous, as in parts of the Wasatch Front area (Smith and Bruhn, 1984); in others areas, such as that studied by Piety and others (1986) in the central ISB, Precambrian crystalline basement rocks lie beneath a basal detachment and are autochthonous. For the latter area we noted that relatively abundant background microseismicity was located by Piety and others (1986), as shown in Figure 21B, within the Precambrian crystalline basement, and they observed no marked change in the vertical distribution of foci that could be associated with the basal detachment.

The present thickness of sedimentary cover rocks, the extent of involvement of Precambrian basement in older compressional deformation and subsequent extension, and whether normal faulting penetrates the entire crust (Zandt and Owens, 1980) all are likely to be important local factors governing the pattern of background seismicity. The influence of these respective factors throughout the ISB is not yet understood, but there are accumulating observations, such as seismic slip on discrete Precambrian basement faults at depth (Fig. 14), the broad involvement of Precambrian basement in contemporary extension (Fig. 21B), and perhaps the regional, flexural(?) deformation of Precambrian basement on the eastern, footwall side of the Wasatch fault (Fig. 12B).

Earthquake focal depths and rheology

Since the mid-1970s, accurate hypocenter data have been acquired by regional and portable seismic networks in the Intermountain region that permit the construction of reliable focal-depth histograms. Using some of these data, Sibson (1982) and Smith and Bruhn (1984) hypothesized seismogenic models based on theoretical depths for peaks in maximum shear stress at the boundary between the brittle upper crust and a quasi-plastic layer. These models in a general way account for the maximum depths of nucleation of large normal faulting earthquakes and for the maximum depths of background seismicity, corresponding to the base of the seismogenic layer. The models involve a temperature-dependent, depth-varying power law for creep combined with a linear brittle-behavior criterion (see representative plot in Fig. 22). In Smith and Bruhn's (1984) model for extensional normal-faulting regimes, the maximum focal depths of large normal-faulting earthquakes correlate approximately with the 80th percentile of focal depths for smaller background earthquakes, similar to the findings of Sibson (1982) for the San Andreas fault system. Scholz (1990) predicts the thickness of the seismogenic layer, and hence the maximum focal depths of earthquakes, using both a similar temperature criterion as that described above and additional fault-velocity constraints.

Qualitative arguments of Sibson (1982) and Smith and Bruhn (1984) suggest that the theoretically derived transition depth from brittle to quasi-plastic flow for silica-rich rocks is controlled primarily by a critical temperature of approximately 350°C to 450°C and occurs at or near the depth of maximum shear stress (Figure 22). At this depth, short-term strain rates greater than 10^{-4}/sec are necessary to achieve brittle failure during earthquakes within the more ductile, intermediate-depth crustal material. In theory, this is the critical depth for nucleation of the largest magnitude earthquakes.

On the basis of the observed heat flow and extrapolated thermal gradients of the ISB, Smith and Bruhn (1984) inferred that this critical depth of earthquake nucleation would not exceed ~10 km, but large stress drops for magnitude-7 earthquakes could produce locally higher strain rates allowing their nucleation at mid-crustal depths of about 15 km ± 5 km. In the cooler

lithosphere of the Colorado Plateau and Rocky Mountains east of the ISB, where background heat flow is less than 65 mW m^{-2}, maximum focal depths exceed 30 to 40 km and are attributed to deeper depths for the critical isotherms (Wong and Chapman, 1990).

The influence of shallow, high temperatures on earthquake depth distributions was described for the Yellowstone caldera (Fig. 17), which is characterized by an extremely high heat flow of 1500 mW m^{-2}. The observed lateral variation in focal-depth maxima reflects the combined influence of conductive and convective heat flow, hypothesized to produce the abrupt shallowing of the critical 350°C to 450°C isotherm beneath the inner caldera

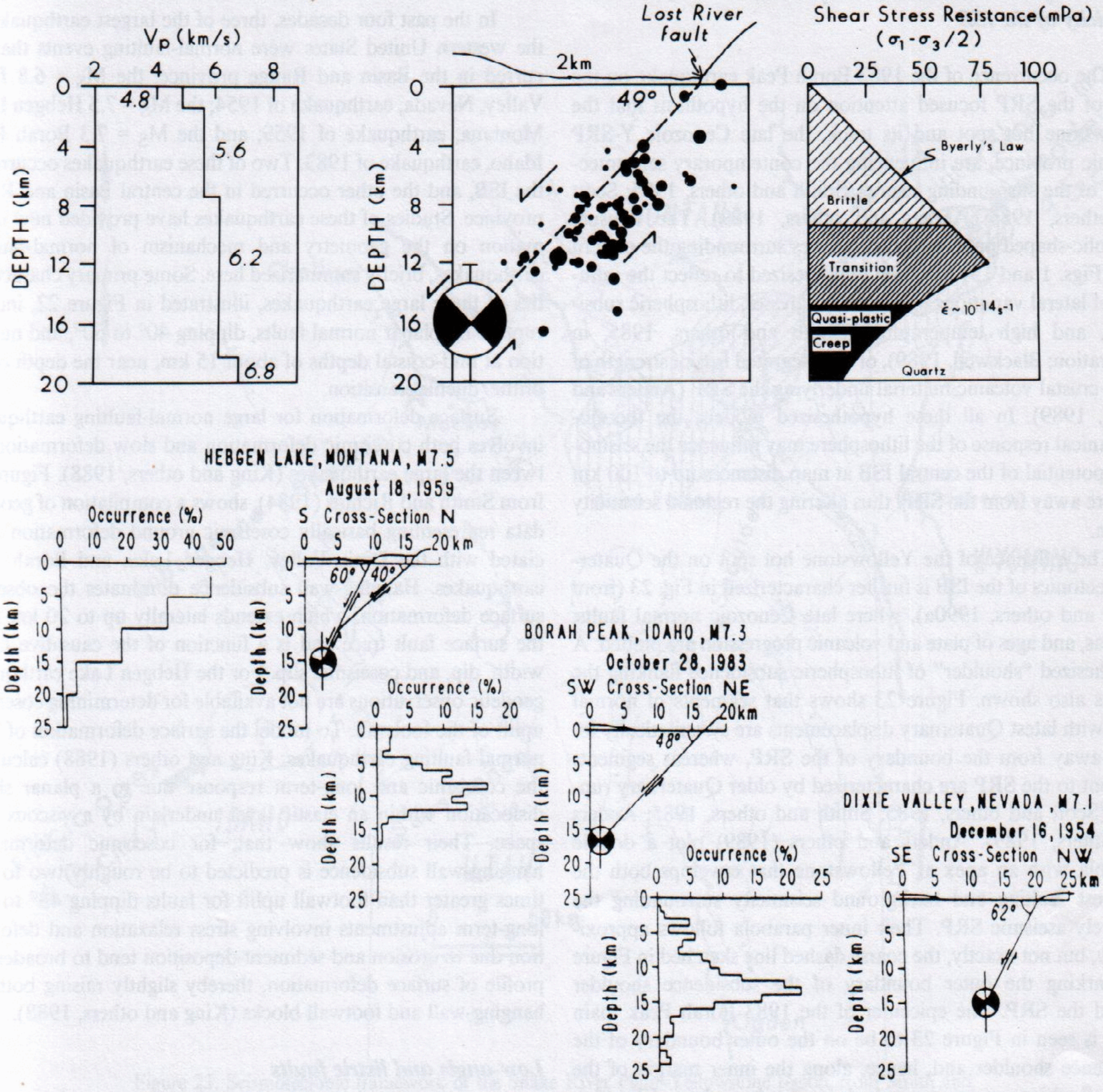

Figure 22. Hypothetical model for large (M >7.0) Basin and Range earthquakes, from Smith and others (1985). Upper, P-wave velocity model and subsurface fault geometry associated with the 1983, M_S = 7.3, Borah Peak, Idaho, earthquake (after Richins and others, 1985), together with a rheological model for the upper crust showing shear stress versus depth for a quartz rheology (after Smith and Bruhn, 1984). Lower, Fault-plane geometries and corresponding focal-depth histograms for three large historical earthquakes in the Basin and Range province; sources of data: Doser (1985b) and a compilation of microearthquake focal depths from University of Utah student theses, for the Hebgen Lake earthquake; Doser and Smith (1985) and Richins and others (1985), for the Borah Peak earthquake; and Okaya and Thompson (1985) and Doser (1986), for the Dixie Valley earthquake.

(Smith, 1989). Possibilities for the mechanisms controlling earthquake depth distributions include crystallization of rhyolite and basaltic melts, hydrothermal fluid flow into the shallow crust of the caldera, and the shallowing of superheated brines above a magma source (Pelton and Smith, 1982; Dzurisin and others, 1990).

Influence of the Yellowstone hot spot on the seismicity of the ISB

The occurrence of the 1983 Borah Peak earthquake on the flank of the SRP focused attention on the hypothesis that the Yellowstone hot spot and its track, the late Cenozoic Y-SRP volcanic province, are influencing the contemporary seismotectonics of the surrounding region (Smith and others, 1985; Scott and others, 1985; Anders and others, 1989). The unusual parabolic-shaped pattern of earthquakes surrounding the eastern SRP (Figs. 1 and 15) has been hypothesized to reflect the influence of lateral variations in deviatoric stresses, lithospheric subsidence, and high temperatures (Smith and others, 1985, in preparation; Blackwell, 1989), or an integrated loss of strength of upper-crustal volcanic material underlying the SRP (Anders and others, 1989). In all these hypothesized models, the thermomechanical response of the lithosphere may influence the seismogenic potential of the central ISB at map distances up to 100 km or more away from the SRP, thus altering the regional seismicity pattern.

The influence of the Yellowstone hot spot on the Quaternary tectonics of the ISB is further characterized in Fig. 23 (from Smith and others, 1990a), where late Cenozoic normal faults, calderas, and ages of plate and volcanic progression are plotted. A hypothesized "shoulder" of lithospheric subsidence flanking the SRP is also shown. Figure 23 shows that segments of normal faults with latest Quaternary displacements are systematically located away from the boundary of the SRP, whereas segments adjacent to the SRP are characterized by older Quaternary ruptures (Scott and others, 1985; Smith and others, 1985; Anders and others, 1989). Anders and others (1989) plot a double parabola with an apex at Yellowstone that envelops both the youngest faulting and background seismicity surrounding the relatively aseismic SRP. Their inner parabola follows approximately, but not exactly, the coarse dashed line sketched in Figure 23 marking the outer boundary of the subsidence shoulder around the SRP. The epicenter of the 1983 Borah Peak main shock is seen in Figure 23 to be on the outer boundary of the subsidence shoulder and, hence, along the inner margin of the SRP's flanking seismicity and along the boundary delimiting older and younger faulting.

Brott and others (1981) and Blackwell (1989) have shown that there is up to 700 m of systematic topographic subsidence southwestward along the SRP, away from the Yellowstone caldera along the 800-km-long track of the Yellowstone hot spot, that matches the cooling curve for the passage of a crustal heat source. These observations and the parabolic pattern of seismicity of the central ISB suggest that a thermal anomaly due to passage of the Yellowstone hot spot extends laterally beyond the SRP, systematically influencing regional seismicity in northern Utah, eastern Idaho, and western Wyoming.

Models for large Basin-and-Range-type normal-faulting earthquakes

In the past four decades, three of the largest earthquakes in the western United States were normal-faulting events that occurred in the Basin and Range province: the M_S = 6.8 Dixie Valley, Nevada, earthquake of 1954; the M_S = 7.5 Hebgen Lake, Montana, earthquake of 1959; and the M_S = 7.3 Borah Peak, Idaho, earthquake of 1983. Two of these earthquakes occurred in the ISB, and the other occurred in the central Basin and Range province. Studies of these earthquakes have provided new information on the geometry and mechanism of normal-faulting earthquakes, briefly summarized here. Some primary characteristics of these large earthquakes, illustrated in Figure 22, include rupture on planar normal faults, dipping 40° to 60°, and nucleation at mid-crustal depths of about 15 km, near the depth of the brittle/ductile transition.

Surface deformation for large normal-faulting earthquakes involves both coseismic deformation and slow deformation between the large earthquakes (King and others, 1988). Figure 24, from Smith and Richins (1984), shows a compilation of geodetic data representing basically coseismic ground deformation associated with the Dixie Valley, Hebgen Lake, and Borah Peak earthquakes. Hanging-wall subsidence dominates the observed surface deformation, which extends laterally up to 20 km from the surface fault trace and is a function of the causative fault's width, dip, and coseismic slip. For the Hebgen Lake earthquake, geodetic observations are not available for determining coseismic uplift of the footwall. To model the surface deformation of large normal-faulting earthquakes, King and others (1988) calculated the coseismic and long-term response due to a planar shear-dislocation within an elastic layer underlain by a viscous half-space. Their results show that, for coseismic deformation, hanging-wall subsidence is predicted to be roughly two to four times greater than footwall uplift for faults dipping 45° to 60°; long-term adjustments involving stress relaxation and deformation due to erosion and sediment-deposition tend to broaden the profile of surface deformation, thereby slightly raising both the hanging-wall and footwall blocks (King and others, 1988).

Low-angle and listric faults

The working model outlined in Figure 22 and described above for large normal-faulting earthquakes is not simply compatible with observations from seismic-reflection data and geologic mapping that document Quaternary listric and low-angle normal faulting in many subsurface locations in the central and eastern Basin and Range province (Royse and others, 1975; Anderson and others, 1983; Smith and Bruhn, 1984; Smith and oth-

ers, 1989). These structures typically flatten at maximum depths of 4 to 6 km, at similar depths to much of the Sevier Desert detachment of western Utah, described in the section on seismotectonic framework.

The question of the seismogenic capability of shallow dipping faults in the ISB has been addressed by various workers by scrutinizing compilations of focal mechanisms (e.g., Zoback, 1983; Arabasz and Julander, 1986; Bjarnason and Pechmann, 1989; Doser and Smith, 1989), and all have similarly found the predominance of seismic slip on planes of moderate (> 30°) to steep dip, with mean dips in the range of 45° to 60°. Some fault-plane solutions can be found with one low-angle nodal plane; however, in those cases there is no corroborating evidence in the form of clustered earthquake foci on either a downward-flattening or planar low-angle normal fault to support selection of the low-angle nodal plane as the plane of seismic slip (Arabasz

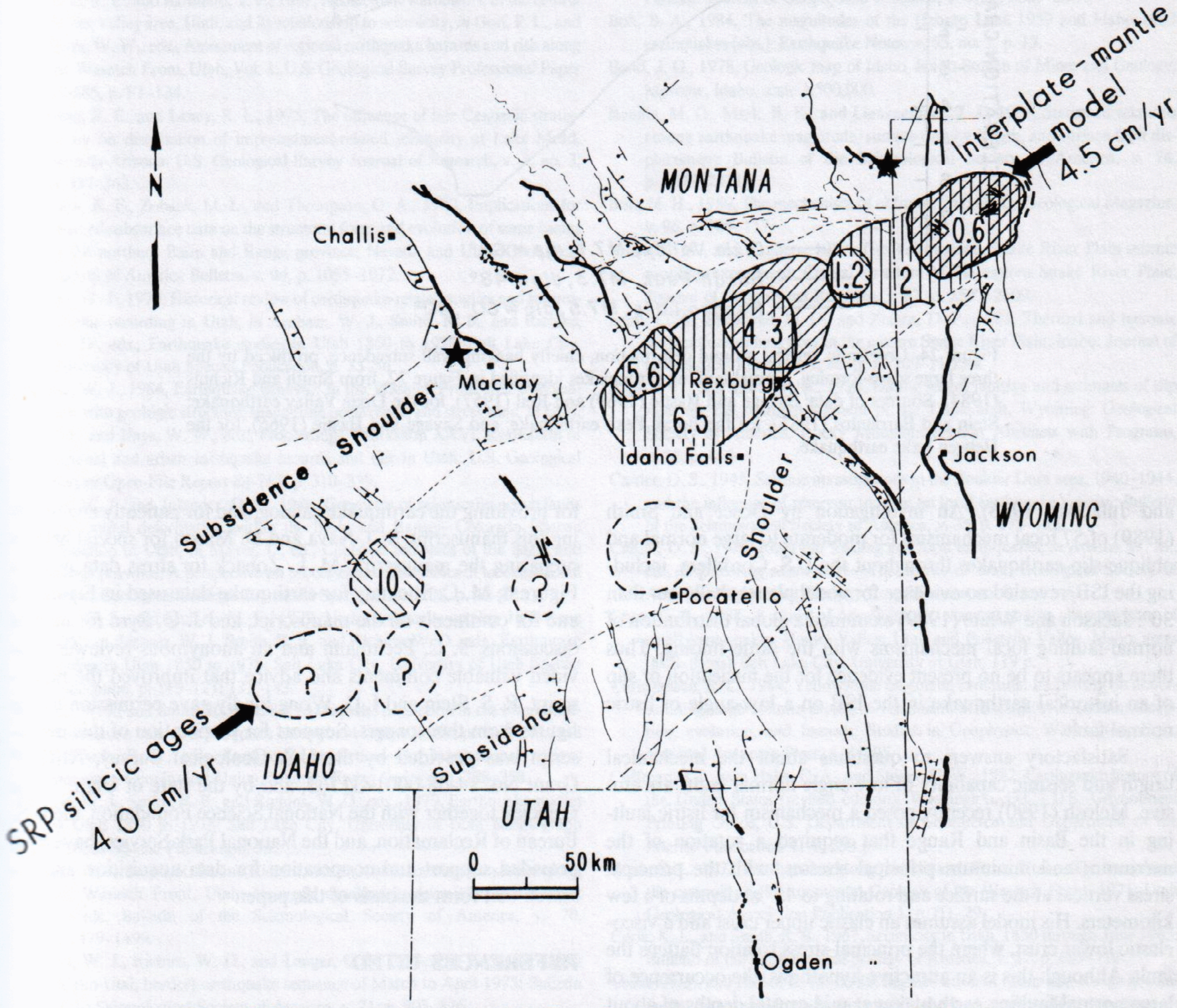

Figure 23. Seismotectonic framework of the Snake River Plain–Yellowstone region, from Smith and others (1990a). Map shows the northeastward decreasing age, in millions of years, of volcanic calderas (hachured) along the eastern Snake River Plain (ESRP), associated with passage of the Yellowstone hot spot, together with the boundary of an hypothesized shoulder of lithospheric subsidence (coarse dashed line), and late Quaternary normal faulting (marked by a heavy line weight where most recent displacement is Holocene). Arrow at Yellowstone (upper right) shows the direction of motion of the North American plate over the Yellowstone hot spot at a relative velocity of 4.5 cm/yr—in agreement with the northeastward space-time progression of calderas at a rate of 4.0 cm/yr. Fine dashed line indicates boundary of the Snake River Plain volcanic province; stars, the epicenters of the 1959 Hebgen Lake and 1983 Borah Peak earthquakes, as in Figure 9.

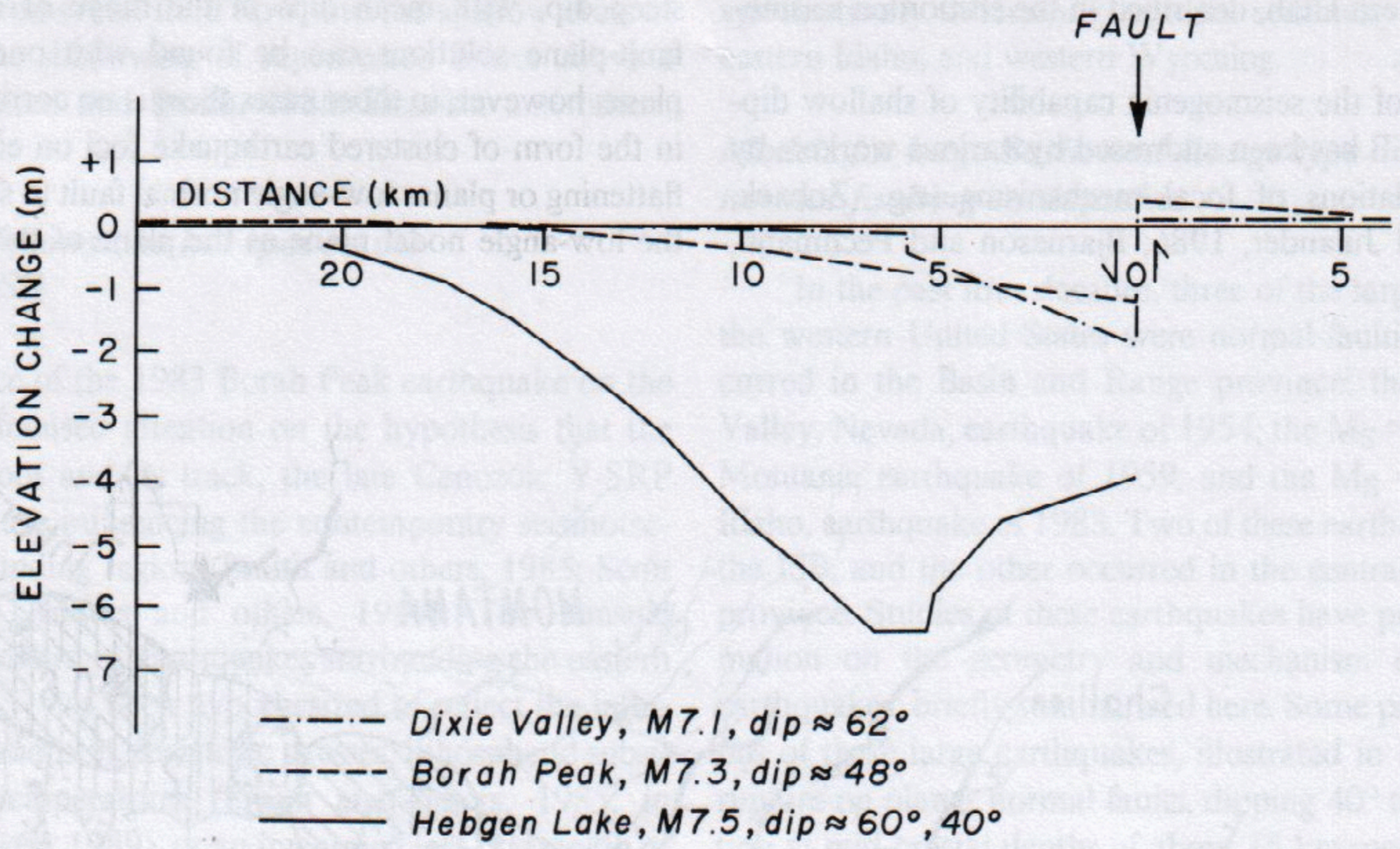

Figure 24. Coseismic vertical ground deformation, chiefly hanging-wall subsidence, produced by the three large scarp-forming, normal-faulting earthquakes identified in Figure 22, from Smith and Richins (1984). Sources of data: Savage and Hastie (1969) and Reil (1957), for the Dixie Valley earthquake; Stein and Barrientos (1985), for the Borah Peak earthquake; and Savage and Hastie (1966), for the Hebgen Lake earthquake.

and Julander, 1986). An investigation by Doser and Smith (1989) of 57 focal mechanisms for moderate to large normal and oblique-slip earthquakes throughout the U.S. Cordillera, including the ISB, revealed no evidence for nodal planes shallower than 30°. Jackson and White (1989) examined a global distribution of normal-faulting focal mechanisms with the same finding. Thus there appears to be no present evidence for the nucleation or slip of an historical earthquake in the ISB on a low-angle or listric normal fault.

Satisfactory answers to questions about the mechanical origin and seismic capability of low-angle normal faults are elusive. Melosh (1990) recently posed a mechanism for listric faulting in the Basin and Range that required a rotation of the maximum and minimum principal stresses, with the principal stress vertical at the surface and rotating to 45° at depths of a few kilometers. His model assumes an elastic upper crust and a viscoelastic lower crust, where the principal-stress rotation flattens the fault. Although this is an attractive hypothesis, the occurrence of large normal-faulting earthquakes at mid-crustal depths of about 15 km on planar faults dipping 45° to 60° argues for a homogeneous stress field to at least the maximum depth of crustal earthquakes in the Intermountain region.

ACKNOWLEDGMENTS

We are indebted to many colleagues who through the years have shared with us their data and ideas about the geology and geophysics of the Intermountain region. We thank E. R. Engdahl for providing the earthquake catalog, and for patiently encouraging this manuscript; S. J. Nava and D. Mason for special help in preparing the manuscript; M. L. Zoback for stress data used in Figure 6; M. C. Stickney for earthquake data used in Figure 18 and for comments on the manuscript; and J. O. Byrd for helpful discussions. J. C. Pechmann and an anonymous reviewer provided valuable comments and advice that improved the manuscript. R. S. Stein and I. G. Wong kindly gave permission to use figures from their papers. Support for preparation of this manuscript was provided by the U.S. Geological Survey, NEHRP Grant No. 14-08-0001-G1762, and by the state of Utah. These agencies, together with the National Science Foundation, the U.S. Bureau of Reclamation, and the National Park Service, have long provided support and cooperation for data acquisition and research that form the basis of this paper.

REFERENCES CITED

Abe, K., 1981, Magnitudes of large shallow earthquakes from 1904 to 1980: Physics of the Earth and Planetary Interiors, v. 27, p. 72–92.

Algermissen, S. T., Perkins, D. M., Thenhaus, P. C., Hanson, S. L., and Bender, B. L., 1982, Probabilistic estimates of maximum acceleration and velocity in the contiguous United States: U.S. Geological Survey Open-File Report 82-1033, 99 p.

Allmendinger, R. W., and 7 others, 1983, Cenozoic and Mesozoic structure of the eastern Basin and Range province, Utah from COCORP seismic reflection data: Geology, v. 11, p. 532–536.

Anders, M. H., Geissman, J. W., Piety, L. A., and Sullivan, J. T., 1989, Parabolic

distribution of circumeastern Snake River Plain seismicity and latest Quaternary faulting: Migratory pattern and association with the Yellowstone hotspot: Journal of Geophysical Research, v. 94, p. 1589–1621.

Anderson, L. W., and Miller, D. G., 1979, Quaternary fault map of Utah, *in* Fugro, Inc., Consulting Engineers & Geologists Technical Report: Long Beach, California, 35 p., scale 1:500,000.

Anderson, R. E., 1989, Tectonic evolution of the Intermontane system; Basin and Range, Colorado Plateau, and High Lava Plains, *in* Pakiser, L. C., and Mooney, W. D., eds., Geophysical framework of the continental United States: Geological Society of America Memoir 172, p. 163–176.

Anderson, R. E., and Barnhard, T. P., 1987, Neotectonic framework of the central Sevier Valley area, Utah, and its relationship to seismicity, *in* Gori, P. L., and Hays, W. W., eds., Assessment of regional earthquake hazards and risk along the Wasatch Front, Utah, Vol. 1: U.S. Geological Survey Professional Paper 87-585, p. F1–134.

Anderson, R. E., and Laney, R. L., 1975, The influence of late Cenozoic stratigraphy on distribution of impoundment-related seismicity at Lake Mead, Nevada-Arizona: U.S. Geological Survey Journal of Research, v. 3, no. 3, p. 337–343.

Anderson, R. E., Zoback, M. L., and Thompson, G. A., 1983, Implications for selected subsurface data on the structural form and evolution of some basins in the northern Basin and Range province, Nevada and Utah: Geological Society of America Bulletin, v. 94, p. 1055–1072.

Arabasz, W. J., 1979, Historical review of earthquake-related studies and seismographic recording in Utah, *in* Arabasz, W. J., Smith, R. B., and Richins, W. D., eds., Earthquake studies in Utah 1850 to 1978: Salt Lake City, University of Utah Special Publication, p. 33–56.

Arabasz, W. J., 1984, Earthquake behavior in the Wasatch Front area: Association with geologic structure, space-time occurrence, and stress state, *in* Gori, P. L. and Hays, W. W., eds., Proceedings, Workshop XXVI, Evaluation of regional and urban earthquake hazards and risk in Utah: U.S. Geological Survey Open-File Report 84-763, p. 310–339.

Arabasz, W. J., and Julander, D. R., 1986, Geometry of seismically active faults and crustal deformation within the Basin and Range—Colorado Plateau transition in Utah, *in* Mayer, L., ed., Cenozoic tectonics of the Basin and Range province: A perspective on processes and kinematics of an extensional origin: Geological Society of America Special Paper 208, p. 43–74.

Arabasz, W. J., and McKee, M. E., 1979, Utah earthquake catalog 1850-June 1962, *in* Arabasz, W. J., Smith, R. B., and Richins, W. D., eds., Earthquake studies in Utah 1850 to 1978: Salt Lake City, University of Utah Special Publication, p. 119–121; 133–143.

Arabasz, W. J., and Smith, R. B., 1981, Earthquake prediction in the Intermountain seismic belt—An intraplate extensional regime, *in* Simpson, D. W., and Richards, P. G., eds., Earthquake prediction—An international review: American Geophysical Union, Maurice Ewing Series 4, p. 238–258.

Arabasz, W. J., Smith, R. B., and Richins, W. D., eds., 1979, Earthquake studies in Utah 1850 to 1978: Salt Lake City, University of Utah Seismograph Stations Special Publication, 552 p.

Arabasz, W. J., Smith, R. B., and Richins, W. D., 1980, Earthquake studies along the Wasatch Front, Utah: Network monitoring, seismicity, and seismic hazards: Bulletin of the Seismological Society of America, v. 70, p. 1479–1499.

Arabasz, W. J., Richins, W. D., and Langer, C. J., 1981, The Pocatello Valley (Idaho-Utah border) earthquake sequence of March to April 1975: Bulletin of the Seismological Society of America, v. 71, p. 803–826.

Arabasz, W. J., Pechmann, J. C., and Brown, E. D., 1987, Observational seismology and the evaluation of earthquake hazards and risk in the Wasatch Front area, Utah, *in* Gori, P. L., and Hays, W. W., eds., Assessment of regional earthquake hazards and risk along the Wasatch Front, Utah, Vol. 1: U.S. Geological Survey Professional Paper 87-585, p. D1–39 (revised, 1991, U.S. Geological Survey Professional Paper 1500-D [in press]).

Barazangi, M., and Dorman, J., 1969, World seismicity maps compiled from ESSA, Coast and Geodetic Survey, epicenter data, 1961–1967: Bulletin of the Seismological Society of America, v. 59, p. 369–380.

Barrientos, S. E., Stein, R. S., and Ward, S. N., 1987, Comparison of the 1959 Hebgen Lake, Montana and the 1983 Borah Peak, Idaho, earthquakes from geodetic observations: Bulletin of the Seismological Society of America, v. 77, p. 784–808.

Bjarnason, I. T., and Pechmann, J. C., 1989, Contemporary tectonics of the Wasatch front region, Utah, from earthquake focal mechanisms: Bulletin of the Seismological Society of America, v. 79, p. 731–755.

Blackwell, D. D., 1989, Regional implications of heat flow of the Snake River Plain, northwestern United States: Tectonophysics, v. 164, p. 323–343.

Bodell, J. M., and Chapman, D. S., 1982, Heat flow in the north-central Colorado Plateau: Journal of Geophysical Research, v. 87, p. 2869–2884.

Bolt, B. A., 1984, The magnitudes of the Hebgen Lake 1959 and Idaho 1983 earthquakes [abs.]: Earthquake Notes, v. 55, no. 1, p. 13.

Bond, J. G., 1978, Geologic map of Idaho, Idaho Bureau of Mines and Geology, Moscow, Idaho, scale 1:500,000.

Bonilla, M. G., Mark, R. K., and Lienkaemper, J. J., 1984, Statistical relations among earthquake magnitude, surface rupture length, and surface fault displacement: Bulletin of the Seismological Society of America, v. 74, p. 2379–2411.

Bott, M. H., 1959, The mechanism of oblique slip faulting: Geological Magazine, v. 96, p. 109–117.

Braile, L. W., and 9 others, 1982, The Yellowstone–Snake River Plain seismic profiling experiment: Crustal structure of the eastern Snake River Plain: Journal of Geophysical Research, v. 87, p. 2597–2609.

Brott, C. A., Blackwell, D. D., and Ziagos, D. P., 1981, Thermal and tectonic implications of heat flow in the eastern Snake River Plain, Idaho: Journal of Geophysical Research, v. 86, p. 11,709–11,734.

Byrd, J. O., and Smith, R. B., 1990, Dating recent faulting and estimates of slip rates for the southern segment of the Teton fault, Wyoming: Geological Society of America, Rocky Mountain Section Abstracts with Programs, v. 22, p. 4–5.

Carder, D. S., 1945, Seismic investigations in the Boulder Dam area, 1940–1944, and the influence of reservoir loading on local earthquake activity: Bulletin of the Seismological Society of America, v. 35, p. 175–192.

Carder, D. S., 1970, Reservoir loading and local earthquakes, *in* Adams, W. M., ed., Engineering seismology—The works of man: Geological Society of America, Engineering Geology Case Histories, no. 8, p. 51–61.

Chen, G. J., 1988, A study of seismicity and spectral source characteristics of small earthquakes: Hansel Valley, Utah and Pocatello Valley, Idaho, areas [M.S. thesis]: Salt Lake City, University of Utah, 119 p.

Christiansen, R. L., 1984, Yellowstone magmatic evolution: Its bearing on understanding large-volume explosive volcanism, *in* Explosive volcanism: Inception, evolution, and hazards: Studies in Geophysics: Washington, D.C., National Academy Press, p. 84–95.

Coffman, J. L., von Hake, C. A., and Stover, C. W., 1982, Earthquake history of the United States (revised edition): Washington, D.C., U.S. Government Printing Office, U.S. Department of Commerce and Department of the Interior Publication 41-1, 258 p.

Cook, K. L., 1972, Earthquakes along the Wasatch Front, Utah—The record and the outlook, *in* Environmental Geology of the Wasatch Front, 1971: Utah Geological Association Publication 1, p. H1–29.

Cook, K. L., and Smith, R. B., 1967, Seismicity in Utah, 1850 through June 1965: Bulletin of the Seismological Society of America, v. 57, p. 689–718.

Crone, A. J., and Haller, K. M., 1989, Segmentation of Basin-and-Range normal faults: Examples from east-central Idaho and southwestern Montana, *in* Schwartz, D. P., and Sibson, R. H., eds., Proceedings, Conference XLV, Fault segmentation and controls of rupture initiation and termination, Palm Springs: U.S. Geological Survey Open-File Report 89-315, p. 110–130.

Crone, A. J., and Harding, S. T., 1984, Relationship of late Quaternary fault scarps to subjacent faults, eastern Great Basin, Utah: Geology, v. 12, p. 292–295.

Crone, A. J., and Machette, M. N., 1984, Surface faulting accompanying the Borah Peak earthquake, central Idaho: Geology, v. 12, p. 664–667.

Crone, A. J., and others, 1987, Surface faulting accompanying the Borah Peak

earthquake and segmentation of the Lost River fault, central Idaho: Bulletin of the Seismological Society of America, v. 77, p. 739–770.

dePolo, C. M., Clark, D. G., Slemmons, D. B., and Aymard, W. H., 1989, Historical Basin and Range province surface faulting and fault segmentation, *in* Schwartz, D. P., and Sibson, R. H., eds., Proceedings, Conference XLV, Fault segmentation and controls of rupture initiation and termination, Palm Springs: U.S. Geological Survey Open-File Report 89-315, p. 131–162.

Dewey, J. W., 1987, Instrumental seismicity of central Idaho: Bulletin of the Seismological Society of America, v. 77, p. 819–836.

Dewey, J. W., Dillinger, W. H., Taggart, J., and Algermissen, S. T., 1973, A technique for seismic zoning: Analysis of earthquake locations and mechanisms in northern Utah, Wyoming, Idaho, and Montana, *in* Harding, S. T., ed., Contributions to seismic zoning: NOAA Technical Report ERL 267-ESL 30, p. 29–48.

Dewey, J. W., Hill, D. P., Ellsworth, W. L., and Engdahl, E. R., 1989, Earthquakes, faults, and the seismotectonic framework of the contiguous United States, *in* Pakiser, L. C., and Mooney, W. D., eds., Geophysical framework of the continental United States: Geological Society of America Memoir 172, p. 541–575.

Dixon, J. S., 1982, Regional structural synthesis, Wyoming salient of western overthrust belt: American Association of Petroleum Geologists Bulletin, v. 66, p. 1560–1580.

Doser, D. I., 1985a, The 1983 Borah Peak, Idaho and 1959 Hebgen Lake Montana earthquakes: Models for normal fault earthquakes in the Intermountain seismic belt, *in* Stein, R. S., and Bucknam, R. C., eds., Proceedings, Workshop XXVIII, On the Borah Peak, Idaho, Earthquake, Vol. A: U.S. Geological Survey Open-File Report 85-290, p. 368–384.

Doser, D. I., 1985b, Source parameters and faulting processes of the 1959 Hebgen Lake, Montana, earthquake sequence: Journal of Geophysical Research, v. 90, p. 4537–4555.

Doser, D. I., 1986, Earthquake processes in the Rainbow Mountain–Fairview Peak–Dixie Valley, Nevada region, 1954–1959: Journal of Geophysical Research, v. 91, p. 12,572–12,586.

Doser, D. I., 1989a, Source parameters of Montana earthquakes (1925–1964) and tectonic deformation in the northern Intermountain seismic belt: Bulletin of the Seismological Society of America, v. 79, p. 31–50.

Doser, D. I., 1989b, Extensional tectonics in northern Utah–southern Idaho, U.S.A., and the 1934 Hansel Valley sequence: Physics of the Earth and Planetary Interiors, v. 54, p. 120–134.

Doser, D. I., 1990, Foreshocks and aftershocks of large (M ≥5.5) earthquakes within the western Cordillera of the United States: Bulletin of the Seismological Society of America, v. 80, p. 110–128.

Doser, D. I., and Smith, R. B., 1982, Seismic moment rates in the Utah region: Bulletin of the Seismological Society of America, v. 72, p. 525–551.

Doser, D. I., and Smith, R. B., 1983, Seismicity of the Teton–southern Yellowstone region, Wyoming: Bulletin of the Seismological Society of America, v. 73, p. 1369–1394.

Doser, D. I., and Smith, R. B., 1985, Source parameters of the 28 October 1983 Borah Peak, Idaho, earthquake from body wave analysis: Bulletin of the Seismological Society of America, v. 75, p. 1041–1051.

Doser, D. I., and Smith, R. B., 1989, An assessment of source parameters of earthquakes in the Cordillera of the western United States: Bulletin of the Seismological Society of America, v. 79, p. 1383–1409.

Dunphy, G. J., 1972, Seismic activity of the Kerr Dam—S.W. Flathead Lake area, Montana, *in* Earthquake research in NOAA: U.S. Department of Commerce, NOAA Technical Report ERL236-ESL121, p. 59–61.

Dzurisin, D., Savage, J. C., and Fournier, R. O., 1990, Recent crustal subsidence at Yellowstone caldera, Wyoming: Journal of Volcanology, v. 52, p. 247–270.

Eaton, G. P., 1982, The Basin and Range province: Origin and tectonic significance: Annual Review of Earth and Planetary Science, v. 10, p. 409–440A.

Eaton, G. P., Wahl, R. R., Prostka, H. J., Mabey, D. R., and Kleinkopf, M. D., 1978, Regional gravity and tectonic patterns: Their relation to late Cenozoic epeirogeny and lateral spreading in the western Cordillera, *in* Smith, R. B. and Eaton, G. P., eds., Cenozoic tectonics and regional geophysics of the western Cordillera: Geological Society of America Memoir 152, p. 51–92.

Eardley, A. J., 1962, Structural geology of North America (second edition): New York, Harper and Row, 743 p.

Eddington, P. K., Smith, R. B., and Renggli, C., 1987, Kinematics of Basin and Range intraplate extension, *in* Coward, M. P., Dewey, J. F., and Hancock, P. L., eds., Continental extensional tectonics: Geological Society of London Special Publication 28, p. 371–392.

Engdahl, E. R., and Rinehart, W. A., 1988, Seismicity map of North America, Continent-Scale Map-004, Decade of North American geology, Geological Society of America, scale 1:5,000,000, 4 sheets.

Freidline, R. A., Smith, R. B., and Blackwell, D. D., 1976, Seismicity and contemporary tectonics of the Helena, Montana area: Bulletin of the Seismological Society of America, v. 66, p. 81–95.

Gilbert, J. D., Ostenna, D., and Wood, C., 1983, Seismotectonic study of Jackson Lake Dam and Reservoir, Minidoka project, Idaho-Wyoming: U.S. Bureau of Reclamation, 123 p.

Griscom, M., 1980, Space-time seismicity patterns in the Utah region and an evaluation of local magnitude as the basis of a uniform earthquake catalog [M.S. thesis]: Salt Lake City, University of Utah, 134 p.

Gupta, H. K., 1985, The present status of reservoir induced seismicity investigations with special emphasis on Koyna earthquakes: Tectonophysics, v. 118, p. 257–279.

Gupta, H. K., and Rastogi, B. K., 1976, Dams and earthquakes: Amsterdam, Elsevier, 229 p.

Gutenberg, B., and Richter, C. F., 1954, Seismicity of the earth and associated phenomena (second edition): Princeton, New Jersey, Princeton University Press, 310 p.

Hall, W. B., and Sablock, P. E., 1985, Comparison of the geomorphic and surficial fracturing effects of the 1983 Borah Peak, Idaho earthquake with those of the 1959 Hebgen Lake, Montana earthquake, *in* Stein, R. S., and Bucknam, R. C., eds., Proceedings, Workshop XXVIII, The Borah Peak, Idaho, earthquake, Vol. A: U.S. Geological Survey Open-File Report 85-290, p. 141–152.

Haller, K. M., 1988, Segmentation of the Lemhi and Beaverhead faults, east-central Idaho, and Red Rock fault, southwest Montana, during the Late Quaternary [M.S. thesis]: University of Colorado, Boulder, 141 p.

Hayden, F. V., 1872, Preliminary report of the United States Geological Survey of Montana and portions of adjacent territories: U.S. Geological and Geographical Survey of the Territories Fifth Annual Report (for 1871), p. 82.

Heck, N. H., 1938, Earthquakes and the western mountain region: Bulletin of the Geological Society of America, v. 49, p. 1–22.

Jackson, J. A., and White, N. J., 1989, Normal faulting in the upper continental crust: Observations from regions of active extension: Journal of Structural Geology, v. 11, no. 1/2, p. 15–36.

Johnson, P. A., and Sbar, M. L., 1987, A microearthquake study of southwest Utah - northwest Arizona: Transition between the Basin and Range province and Intermountain seismic belt: Bulletin of the Seismological Society of America, v. 77, p. 579–596.

Jones, A. E., 1975, Recordings of earthquakes at Reno, 1916–1951: Bulletin of the Seismological Laboratory, Mackay School of Mines, University of Nevada, Reno, 199 p.

Jones, C. H., 1987, A geophysical and geological investigation of extensional structures, Great Basin, western United States [Ph.D. dissertation]: Cambridge, Massachusetts Institute of Technology, 226 p.

King, G. C., Stein, R. S., and Rundle, J. B., 1988, The growth of geological structures by repeated earthquakes, 1. Conceptual framework: Journal of Geophysical Research, v. 93, p. 13,307–13,318.

King, J. J., Doyle, T. E., and Jackson, S. M., 1987, Seismicity of the eastern Snake River plain region, Idaho, prior to the Borah Peak, Idaho, earthquake: October 1972–October 1983: Bulletin of the Seismological Society of America, v. 77, p. 809–818.

Kostrov, V. V., 1974, Seismic moment and energy of earthquakes, and seismic flow of rock: Izvestiya, Academy of Sciences, USSR, Physics of the Solid

Earth (English edition), No. 1, p. 13–21.

Kruger-Knuepfer, J. L., Sbar, M. L., and Richardson, R. M., 1985, Microseismicity of the Kaibab Plateau, northern Arizona and its tectonic implications: Bulletin of the Seismological Society of America, v. 75, p. 491–505.

LaForge, R. C., 1988, An analysis of reservoir-induced seismicity in the back valleys of the Wasatch Mountains, *in* Sullivan, J. T., Martin, R. A., and Foley, L. L., Seismotectonic study for Jordanelle Dam, Bonneville unit, Central Utah Project, Utah: U.S. Bureau of Reclamation, Seismotectonic Report no. 88-6, Appendix B.

Levy, M., and Christie-Blick, N., 1989, Pre-Mesozoic palinspastic reconstruction of the eastern Great Basin (western United States): Science, v. 245, p. 1454–1462.

Loeb, D. T., and Pechmann, J. C., 1986, The P-wave velocity structure of the crust-mantle boundary beneath Utah from network travel time measurements [abs.]: Earthquake Notes, v. 57, no. 1, p. 10.

Love, J. D., and Reed, J. C., Jr., 1971, Creation of the Teton landscape, the geological story of Grand Teton National Park: Jackson, Wyoming, Grand Teton Natural History Association, 120 p.

Machette, M. N., Personius, S. F., and Nelson, A. R., 1987, Quaternary geology along the Wasatch fault zone: segmentation, recent investigations, and preliminary conclusions *in* Gori, P. L., and Hays, W. W., eds., Assessment of regional earthquake hazards and risk along the Wasatch Front, Utah, Vol 1: U.S. Geological Survey Open-File Report 87-585, p. A1–72.

Machette, M. N., Personius, S. F., Nelson, A. R., Schwartz, D. P., and Lund, W. R., 1989, Segmentation models and Holocene movement history of the Wasatch fault zone, Utah, *in* Schwartz, D. P., Sibson, R. H., eds., Proceedings, Conference XLV, Fault segmentation and controls of rupture initiation and termination, Palm Springs: U.S. Geological Survey Open-File Report 89-315, p. 229–245.

McCalpin, J., Robison, R. M., and Garr, J. D., 1987, Neotectonics of the Hansel Valley–Pocatello Valley corridor, northern Utah and southern Idaho, *in* Gori, P. L., and Hays, W. W., eds., Assessment of regional earthquake hazards and risk along the Wasatch Front, Utah, Vol. 1: U.S. Geological Survey Open-File Report 87-585, p. G1–44.

McGuire, R. K., and Arabasz, W. J., 1990, An introduction to probabilistic seismic hazard analysis, *in* Ward, S. H., ed., Geotechnical and environmental geophysics, Volume 1: Review and tutorial: Society of Exploration Geophysics, Investigations in Geophysics No. 5, p. 333–353.

McLaughlin, W. C., Waddell, G. G., and McCaslin, J. G., 1976, Seismic equipment used in rock-burst control in the Coeur d'Alene mining district, Idaho: U.S. Bureau of Mines Report of Investigation 8138, 29 p.

Melosh, H. J., 1990, Mechanical basis for low-angle normal faulting in the Basin and Range province: Nature, v. 343, p. 331–335.

Morgan, P., and Gosnold, W. D., 1989, Heat flow and thermal regimes in the continental United States, *in* Pakiser, L. C., and Mooney, W. D., eds., Geophysical framework of the continental United States: Geological Society of America Memoir 172, p. 493–522.

Munson, R. C., 1970, Relationship of effect of waterflooding of the Rangely oil field on seismicity, *in* Adams, W. M., ed., Engineering seismology—The works of man: Geological Society of America, Engineering Geology Case Histories, no. 8, p. 39–49.

Nagy, W. C., and Smith, R. B., 1988, Seismotectonic implications of the 1985–86 Yellowstone earthquake swarm from velocity and stress inversion [abs.]: Seismological Research Letters, v. 59, no. 1, p. 20.

Nava, S. J., Pechmann, J. C., and Arabasz, W. J., 1988, A Swell earthquake in the Colorado Plateau [abs.]: Seismological Research Letters, v. 60, n. 1, p. 30.

Nava, S. J., and 7 others, 1990, Earthquake catalog for the Utah region: January 1, 1986 to December 31, 1988: Salt Lake City, University of Utah Seismograph Stations Special Publication, 96 p.

Okaya, D. A., and Thompson, G. A., 1985, Geometry of Cenozoic extensional faulting: Dixie Valley, Nevada: Tectonics, v. 4, p. 107–126.

Owens, T. J., 1983, Normal faulting and flexure in an elastic-perfectly plastic plate: Tectonophysics, v. 93, p. 129–150.

Pack, F. J., 1921, The Elsinore earthquakes in central Utah, September 29 and October 1, 1921: Bulletin of the Seismological Society of America, v. 11, p. 155–165.

Pakiser, L. C., 1989, Geophysics of the Intermontane system, in Pakiser and Mooney, *in* Pakiser, L. C., and Mooney, W. D., eds., Geophysical framework of the continental United States: Geological Society of America Memoir 172, p. 235–248.

Pardee, J. T., 1926, The Montana earthquake of June 27, 1925: U.S. Geological Survey Professional Paper 147-B, 17 p.

Pardee, J. T., 1950, Late Cenozoic block faulting in western Montana: Bulletin of the Geological Society of America, v. 51, p. 359–406.

Parry, W. T., and Bruhn, R. L., 1986, Pore fluid and seismogenic characteristics of fault rock at depth on the Wasatch Fault, Utah: Journal of Geophysical Research, v. 91, p. 730–744.

Parry, W. T., and Bruhn, R. L., 1987, Fluid inclusion evidence for minimum 11 km vertical offset on the Wasatch fault, Utah: Geology, v. 15, p. 67–70.

Pechmann, J. C., and Thorbjarnardottir, B., 1984, Investigation of an M_L 4.3 earthquake in the western Salt Lake Valley using digital seismic data, *in* Gori, P. L., and Hays, W. W., eds., Proceedings, Workshop XXVI, Evaluation of regional and urban earthquake hazards and risk in Utah: U.S. Geological Survey Open-File Report 84-763, p. 340–365.

Pelton, J. R., and Smith, R. B., 1982, Contemporary vertical surface displacements in Yellowstone National Park: Journal of Geophysical Research, v. 87, p. 2745–2761.

Pennington, W., Smith, R. B., and Trimble, A. B., 1974, A microearthquake survey of parts of the Snake River Plain and Central Idaho: Bulletin of the Seismological Society of America, v. 64, p. 307–312.

Peyton, S. L., and Smith, R. B., 1990, Earthquake catalog for the Yellowstone National Park region: January 1, 1989 through December 31, 1989: Salt Lake City, University of Utah Special Publication, 33 p.

Piety, L. A., Wood, C. K., Gilbert, J. D., Sullivan, J. T., and Anders, M. H., 1986, Seismotectonic study for Palisades Dam and Reservoir, Palisades project: U.S. Bureau of Reclamation, Engineering and Research Center, Seismotectonic Division, Denver, Colorado, and Pacific Northwest Region Geology Branch, Boise, Idaho, Seismotectonic Report no. 86-3, 198 p.

Pitt, A. M., 1987, Catalog of earthquakes in the Yellowstone National Park-Hebgen Lake region, Wyoming, Montana, and Idaho for the years 1973 to 1981: U.S. Geological Survey Open File Report, p. 87–61.

Pitt, A. M., and Hutchinson, R. A., 1982, Hydrothermal changes related to earthquake activity at Mud Volcano, Yellowstone National Park, Wyoming: Journal of Geophysical Research, v. 87, p. 2762–2766.

Pitt, A. M., Weaver, C. S., and Spence, W., 1979, The Yellowstone Park earthquake of June 30, 1975: Bulletin of the Seismological Society of America, v. 69, p. 187–205.

Planke, S., and Smith, R. B., 1991, Cenozoic extension and evolution of the Sevier Desert Basin, Utah, from seismic reflection, gravity, and well log data: Tectonics, v. 10, p. 345–365.

Poppe, B. B., 1980, Directory of world seismograph stations: U.S. Department of Commerce Report SE-25, Part 1, v. 1, 465 p.

Qamar, A., and Hawley, B., 1979, Seismic activity near the Three Forks Basin, Montana: Bulletin of the Seismological Society of America, v. 69, p. 1917–1929.

Qamar, A. I., and Stickney, M. C., 1983, Montana earthquakes, 1869–1979—Historical seismicity and earthquake hazard: Montana Bureau of Mines and Geology Memoir 51, 80 p.

Qamar, A., Kogan, J., and Stickney, M. C., 1982, Tectonics and recent seismicity near Flathead Lake, Montana: Bulletin of the Seismological Society of America, v. 72, p. 1591–1599.

Raleigh, C. B., Healy, J. H., and Bredehoeft, J. D., 1972, Faulting and crustal stress at Rangely, Colorado, *in* Flow and Fracture of Rocks, Monograph 16: American Geophysical Union, p. 275–284.

Reil, O. E., 1957, The Dixie Valley–Fairview Peak, Nevada, earthquakes of December 16, 1954: Damage to Nevada highways: Bulletin of the Seismological Society of America, v. 47, p. 349–352.

Reilinger, R., 1986, Evidence for postseismic viscoelastic relaxation following the 1959 M = 7.5 Hebgen Lake, Montana, earthquake: Journal of Geophysical Research, v. 91, p. 9488–9494.

Richins, W. D., and Arabasz, W. J., 1985, Seismicity of southeastern Idaho based on seismic monitoring using regional and temporary local networks [abs.]: Geological Society of America Rocky Mountain Section Meeting Abstracts with Programs, v. 17, n. 4, p. 261.

Richins, W. D., Arabasz, W. J., and Langer, C. J., 1983, Episodic earthquake swarms ($M_L \leq 4.7$) near Soda Springs, Idaho, 1981–82: Correlation with local structure and regional tectonics [abs.]: Earthquake Notes, v. 54, no. 1, p. 99.

Richins, W. D., Smith, R. B., Langer, C. J., Zollweg, J. E., King, J. J., and Pechmann, J. C., 1985, The 1983 Borah Peak, Idaho, earthquake: Relationship of aftershocks to the main shock, surface faulting, and regional tectonics, *in* Stein, R. S., and Bucknam, R. C., eds., Proceedings, Workshop XXVIII, On the Borah Peak, Idaho, earthquake, Vol. A: U.S. Geological Survey Open-File Report 85-290, p. 285–310.

Richins, W. D., and 6 others, 1987, The 1983 Borah Peak, Idaho, earthquake and its aftershocks: Bulletin of the Seismological Society of America, v. 77, p. 694–723.

Richter, C. F., 1935, An instrumental earthquake magnitude scale: Bulletin of the Seismological Society of America, v. 25, p. 1–32.

Richter, C. F., 1958, Elementary seismology: San Francisco, W. H. Freeman and Company, 768 p.

Rogers, A. M., and Lee, W. H., 1976, Seismic study of earthquakes in the Lake Mead, Nevada-Arizona region: Bulletin of the Seismological Society of America, v. 66, p. 1657–1681.

Rogers, A. M., Algermissen, S. T., Hays, W. W., and Perkins, D. M., 1976, A study of earthquake losses in the Salt Lake City, Utah, area: U.S. Geological Survey Open-File Report 76-89, 357 p.

Rogers, A. M., Harmsen, S. C., and Meremonte, M. E., 1987, Evaluation of the seismicity of the southern Great Basin and its relationship to the tectonic framework of the region: U.S. Geological Survey Open-File Report 87-408, 196 p.

Royse, F., Warner, M. A., and Reese, D. L., 1975, Thrust belt structural geometry and related stratigraphic problems, Wyoming–Idaho–Northern Utah, *in* Bolyare, D. W., ed., Deep drilling frontiers in the central Rocky Mountains: Rocky Mountain Association of Geologists, Denver, p. 41–54.

Ryall, A., Slemmons, D. B., and Gedney, L. S., 1966, Seismicity, tectonism, and surface faulting in the western United States during historic time: Bulletin of the Seismological Society of America, v. 56, p. 1105–1135.

Savage, J. C., and Hastie, L. M., 1966, Surface deformation associated with dip-slip faulting: Journal of Geophysical Research, v. 71, p. 4897–4904.

Savage, J. C., and Hastie, L. M., 1969, A dislocation model for the Fairview Peak, Nevada, earthquake: Bulletin of the Seismological Society of America, v. 59, p. 1937–1948.

Savage, J. C., Lisowski, M., and Prescott, W. H., 1985, Strain accumulation in the Rocky Mountain states: Journal of Geophysical Research, v. 90, p. 10,310–10,320.

Sbar, M. L., and Barazangi, M., 1970, Tectonics of the Intermountain seismic belt, western United States, Part I—Microearthquake seismicity and composite fault plane solutions: Geological Society of America Abstracts with Programs, v. 2, p. 675.

Sbar, M. L., Barazangi, M., Dorman, J., Scholz, C. H., and Smith, R. B., 1972, Tectonics of the Intermountain seismic belt, western United States: Microearthquake seismicity and composite fault plane solutions: Geological Society of America Bulletin, v. 83, p. 13–28.

Scarborough, R. B., Manges, C. M., and Pearthree, P. A., 1986, Map of Late Pliocene–Quaternary (post 4 m.y.) faults, folds, and volcanic rocks in Arizona: Tucson, Arizona Bureau of Geology and Mineral Technology, Geological Survey Branch, Map 22, scale 1:1,000,000.

Scholz, C. H., 1990, The mechanics of earthquakes and faulting, Cambridge University Press, 439 p.

Schwartz, D. P., 1987, Earthquakes of the Holocene: Reviews of Geophysics, v. 25, p. 1197–1202.

Schwartz, D. P., 1988, Geological characterization of seismic sources: Moving into the 1990s, *in* Von Thun, J. L., ed., Earthquake engineering and soil dynamics II—Recent advances in ground motion evaluation: American Society of Civil Engineers, Geotechnical Special Publication 20, p. 1–42.

Schwartz, D. P., and Coppersmith, K. J., 1984, Fault behavior and characteristic earthquakes: examples from the Wasatch and San Andreas fault zones: Journal of Geophysical Research, v. 89, p. 5681–5698.

Schwartz, D. P., and Coppersmith, K. J., 1986, Seismic hazards: New trends in analysis using geologic data, *in* Active tectonics: Washington, D.C., National Academy Press, p. 215–230.

Scott, W. E., Pierce, K. L., and Hait, M. H., Jr., 1985, Quaternary tectonic setting of the 1983 Borah Peak earthquake, central Idaho: Bulletin of the Seismological Society of America, v. 75, p. 1053–1066.

Shenon, P. J., 1934, Hansel Valley earthquake, March 12, 1934 (unpublished report): U.S. Geological Survey.

Shenon, P. J., 1936, The Utah earthquake of March 12, 1934 (extracts from unpublished report), *in* Neuman, F., United States earthquakes 1934: U.S. Department of Commerce, Coast and Geodetic Survey, ser. 593, p. 43–48.

Shimizu, Y., 1987, Earthquake clustering in the Utah region [M.S. thesis]: Cambridge, Massachusetts Institute of Technology, 149 p.

Sibson, R. H., 1982, Fault zone models, heat flow, and the depth distribution of earthquakes in the continental crust of the United States: Bulletin of the Seismological Society of America, v. 72, p. 151–163.

Simpson, D. W., 1976, Seismicity changes associated with reservoir loading: Engineering Geology, v. 10, p. 123–150.

Slemmons, D. B., 1977, State-of-the-art for assessing earthquake hazards in the United States, Report 6: Faults and earthquake magnitude: U.S. Army Engineer Waterways Experiment Station Miscellaneous Paper S-73-1, 129 p.

Smith, R. B., 1972, Contemporary seismicity, seismic gaps, and earthquake recurrences of the Wasatch Front; *in* Cook, K. L., ed., Environmental geology of the Wasatch Front, 1971: Utah Geological Association, Publication 1, p. I1–19.

Smith, R. B., 1977, Intraplate tectonics of the western North American Plate: Tectonophysics, v. 37, p. 323–336.

Smith, R. B., 1978, Seismicity, crustal structure, and intraplate tectonics of the interior of the western Cordillera, *in* Smith, R. B., and Eaton, G. P., eds., Cenozoic tectonics and regional geophysics of the western Cordillera: Geological Society of America Memoir 152, p. 111–144.

Smith, R. B., 1989, Kinematics and dynamics of the Yellowstone hotspot [abs.]: EOS American Geophysical Union Transactions, v. 70, p. 1356.

Smith, R. B., and Braile, L. W., 1984, Crustal structure and evolution of an explosive silicic volcanic system at Yellowstone National Park, *in* Explosive volcanism: Inception, evolution, and hazards: Studies in Geophysics: Washington, D.C., National Academy Press, p. 96–111.

Smith, R. B., and Bruhn, R. L., 1984, Intraplate extensional tectonics of the eastern Basin-Range: Inferences on structural style from seismic reflection data, regional tectonics, and thermal-mechanical models of brittle-ductile deformation: Journal of Geophysical Research, v. 89, p. 5733–5762.

Smith, R. B., and Lehman, J. A., 1979, Ground response spectra from M_L 5.7 Logan (Cache Valley) earthquake of 1962, *in* Arabasz, W. J., Smith, R. B., and Richins, W. D., eds., Earthquake Studies in Utah 1850 to 1978: Salt Lake City, University of Utah Seismograph Stations Special Publication, p. 487–495.

Smith, R. B., and Lindh, A. G., 1978, Fault-plane solutions of the western United States; A compilation, *in* Smith, R. B., and Eaton, G. P., eds., Cenozoic tectonics and regional geophysics of the western Cordillera: Geological Society of America Memoir 152, p. 107–109.

Smith, R. B., and Richins, W. D., 1984, Seismicity and earthquake hazards of Utah and the Wasatch Front: Paradigm and paradox, *in* Gori, P. L., and Hays, W. W., eds., Proceedings, Workshop XXVI, Evaluation of regional and urban earthquake hazards and risk in Utah: U.S. Geological Survey Open-File Report 84-763, p. 73–112.

Smith, R. B., and Sbar, M. L., 1970, Seismicity and tectonics of the Intermountain

seismic belt, western United States, Part II, Focal mechanism of major earthquakes: Geological Society of America Abstracts with Programs, v. 2, p. 657.

Smith, R. B., and Sbar, M. L., 1974, Contemporary tectonics and seismicity of the western United States with emphasis on the Intermountain seismic belt: Geological Society of America Bulletin, v. 85, p. 1205–1218.

Smith, R. B., Winkler, P. L., Anderson, J. G., and Scholz, C. H., 1974, Source mechanisms of microearthquakes associated with underground mines in eastern Utah: Bulletin of the Seismological Society of America, v. 64, p. 1295–1317.

Smith, R. B., Shuey, R. T., Pelton, J. R., and Bailey, J. P., 1977, Yellowstone hot spot: Contemporary tectonics and crustal properties from earthquake and aeromagnetic data: Journal of Geophysical Research, v. 82, p. 3665–3676.

Smith, R. B., and 8 others, 1982, The Yellowstone–eastern Snake River Plain seismic profiling experiment: Crustal structure of Yellowstone: Journal of Geophysical Research, v. 84, p. 2583–2596.

Smith, R. B., Richins, W. D., and Doser, D. I., 1985, The 1983 Borah Peak, Idaho earthquake: Regional seismicity, kinematics of, and tectonic mechanism, *in* Stein, R. S., Bucknam, R. C., eds., Proceedings, Workshop XXVIII, The Borah Peak, Idaho earthquake, Vol. A.: U.S. Geological Survey Open-File Report 85-290, p. 236–263.

Smith, R. B., Nagy, W. C., Julander, D. R., Viveiros, J. J., Barker, C. A., and Gants, D. G., 1989, Geophysical and tectonic framework of the eastern Basin and Range–Colorado Plateau–Rocky Mountain transition, *in* Pakiser, L. C., and Mooney, W. D., eds., Geophysical framework of the continental United States: Geological Society of America Memoir 172, p. 205–233.

Smith, R. B., Byrd, J. O., and Susong, D. D., 1990a, Neotectonics and structural evolution of the Teton fault, *in* Roberts, S., ed., Geologic field tours of western Wyoming and parts of adjacent Idaho, Montana, and Utah, field trip no. 6: The Geological Survey of Wyoming, Public Information Circular No. 29, p. 126–138.

Smith, R. B., Byrd, J. O., Susong, D. D., Sylvester, A. G., Bruhn, R. L., and Geissman, J. W., 1990b, Three Year Progress Report, An evaluation of earthquake hazards of the Grand Teton National Park emphasizing the Teton fault (unpublished report to the University of Wyoming–National Park Service Research Center): Salt Lake City, University of Utah, 149 p.

Sparlin, M. A., Braile, L. W., and Smith, R. B., 1982, Crustal structure of the Eastern Snake River Plain determined from ray trace modeling of seismic refraction data: Journal of Geophysical Research, v. 87, p. 2619–2633.

Stein, R. S., and Barrientos, S. E., 1985, Planar high-angle faulting in the Basin and Range: Geodetic analysis of the 1983 Borah Peak, Idaho, earthquake: Journal of Geophysical Research, v. 90, p. 11,355–11,366.

Stevenson, P. R., 1976, Microearthquakes at Flathead Lake, Montana: A study using automatic earthquake processing: Bulletin of the Seismological Society of America, v. 66, p. 61–80.

Stickney, M. C., 1988, Montana seismicity, 1986: Butte, Montana Bureau of Mines and Geology Open-File Report 204, 39 p.

Stickney, M. C., and Bartholomew, M. J., 1987, Seismicity and late Quaternary faulting of the northern Basin and Range province, Montana and Idaho: Bulletin of the Seismological Society of America, v. 77, p. 1602–1625.

Stover, C. W., 1985, Isoseismal map and intensity distribution for the Borah Peak, Idaho, earthquake of October 28, 1983, *in* Stein, R. S., and Bucknam, R. C., eds., Proceedings, Workshop XXVIII, The Borah Peak, Idaho, earthquake, Vol. A: U.S. Geological Survey Open-File Report 85-290, p. 401–408.

Stover, C. W., Reagor, B. G., and Algermissen, S. T., 1986, Seismicity map of the State of Utah: U.S. Geological Survey Miscellaneous Field Studies Map MF-1856, scale 1:1,000,000.

Sullivan, J. T., Nelson, A. R., LaForge, R. C., Wood, C. K., and Hansen, R. A., 1988, Central Utah regional seismotectonic study for USBR dams in the Wasatch Mountains: U.S. Bureau of Reclamation Seismotectonic Report 88-5, 269 p.

Thenhaus, P. C., and Wentworth, C. M., 1982, Map showing zones of similar ages of surface faulting and estimated maximum earthquake size in the Basin and Range province and selected adjacent areas, U.S. Geological Survey Open-File Report 82-742.

Tocher, D., 1962, The Hebgen Lake, Montana, earthquake of August 17, 1959, MST,: Bulletin of the Seismological Society of America, v. 52, p. 153–162.

Townley, S. D., and Allen, M. W., 1939, Descriptive catalog of earthquakes of the Pacific Coast of the United States, 1769 to 1928: Bulletin of the Seismological Society of America, v. 29, p. 1–297.

Veneziano, D., Shimizu, Y., and Arabasz, W. J., 1987, Suppressed earthquake clustering in the Wasatch Front region, Utah [abs.]: EOS American Geophysical Union Transactions, v. 68, p. 1368.

Wahlquist, W. L., 1981, Atlas of Utah: Provo, Utah, Brigham Young University Press, Weber State College, 300 p.

Westaway, R., and Smith, R. B., 1989a, Strong ground motion in normal-faulting earthquakes: Geophysical Journal of the Royal Astronomical Society, v. 96, p. 529–559.

Westaway, R., and Smith, R. B., 1989b, Source parameters of the Cache Valley (Logan), Utah, earthquake of 30 August 1962: Bulletin of the Seismological Society of America, v. 79, p. 1410–1425.

Williams, D. J., and Arabasz, W. J., 1989, Mining-related and tectonic seismicity in the East Mountain area, Wasatch Plateau, Utah, U.S.A.: PAGEOPH, v. 129, p. 345–368.

Williams, J. S., and Tapper, M. L., 1953, Earthquake history of Utah, 1850–1949: Bulletin of the Seismological Society of America, v. 43, p. 191–218.

Witkind, I. J., 1964, Reactivated faults north of Hebgen Lake, in the Hebgen Lake, Montana, earthquake of August 17, 1959: U.S. Geological Survey Professional Paper 435, p. 37–50.

Witkind, I. J., 1975a, Preliminary map showing known and suspected active faults in Idaho: U.S. Geological Survey Open-File Report 75-278, scale 1:500,000.

Witkind, I. J., 1975b, Preliminary map showing known and suspected active faults in Wyoming: U.S. Geological Survey Open-File Report 75-279, scale 1:500,000.

Witkind, I. J., 1975c, Preliminary map showing known and suspected active faults in Montana: U.S. Geological Survey Open-File Report 75-285, scale 1:500,000.

Witkind, I. J., Myers, W. B., Hadley, J. B., Hamilton, W., and Fraser, G. D., 1962, Geologic features of the earthquake at Hebgen Lake, Montana, August 17, 1959: Bulletin of the Seismological Society of America, v. 52, p. 163–180.

Wong, I. G., and Chapman, D. S., 1990, Deep intraplate earthquakes in the western United States and their relationship to lithospheric temperatures: Bulletin of the Seismological Society of America, v. 80, p. 589–599.

Wong, I. G., and Humphrey, J. R., 1989, Contemporary seismicity, faulting, and the state of stress in the Colorado Plateau: Geological Society of America Bulletin, v. 101, p. 1127–1146.

Wong, I. G., Humphrey, J. R., Adams, J. A., and Silva, W. J., 1989, Observations of mine seismicity in the eastern Wasatch Plateau, Utah, U.S.A.: A possible case of implosional failure: PAGEOPH, v. 129, p. 369–405.

Wood, C., 1988, Earthquake Data—1986, Jackson Lake Seismograph Network, Jackson Lake Dam, Minidoka project, Wyoming: U.S. Bureau of Reclamation Seismotectonic Report 88-1, 41 p.

Woodward-Clyde Consultants, 1979, A seismic hazard study for the Treat Reactor Facility, at the INEL, Idaho (unpublished report prepared for Idaho National Engineering Laboratory, Idaho Falls, Idaho): San Francisco, California, Woodward-Clyde Consultants, 109 p.

Woolard, G. P., 1958, Areas of tectonic activity in the United States as indicated by earthquake epicenters: EOS (American Geophysical Union Transactions), v. 39, p. 1135–1150.

Youngs, R. R., Swan, F. H., Power, M. S., Schwartz, D. P., and Green, R. K., 1987, Probabilistic analysis of earthquake ground shaking hazard along the Wasatch Front, Utah, *in* Gori, P. L., and Hays, W. W., eds., Assessment of regional earthquake hazards and risk along the Wasatch Front, Utah, Vol. 2: U.S. Geological Survey Professional Paper 87-585, p. M1–110.

Zandt, G., and Owens, T. J., 1980, Crustal flexure associated with normal faulting

and implications for seimicity along the Wasatch Front, Utah: Bulletin of the Seismological Society of America, v. 70, p. 1501–1520.

Zandt, G., McPherson, L., Schaff, S., and Olsen, S., 1982, Seismic baseline and inducation studies, Roosevelt Hot Springs, Utah and Raft River Idaho: Salt Lake City, University of Utah Research Institute, Earth Science Laboratory Technical Report, Department of Energy Contract No. DE-AS07-78ID01821, 58 p.

Zoback, M. L., 1983, Structure and Cenozoic tectonism along the Wasatch fault zone, Utah, *in* Miller, D. M., Todd, V. R., and Howard, K. A., eds., Tectonics and stratigraphy of the eastern Great Basin: Geological Society of America Memoir 157, p. 3–27.

Zoback, M. L., 1989, State of stress and modern deformation of the northern Basin and Range province: Journal of Geophysical Research, v. 94, p. 7105–7128.

Zoback, M. L., and Zoback, M. D., 1989, Tectonic stress field of the continental United States, *in* Pakiser, L. C., and Mooney, W. D., eds., Geophysical framework of the continental United States: Geological Society of America Memoir 172, p. 523–539.

Zollweg, J. E., and Richins, W. D., 1985, Late aftershocks of the 1983 Borah Peak, Idaho, earthquake and related activity in central Idaho, *in* Gori, P. L., and Hays, W. W., eds., Proceedings, Workshop XXVI, Evaluation of regional and urban earthquake hazards and risk in Utah: U.S. Geological Survey Open-File Report 84-763, p. 345–356.

MANUSCRIPT ACCEPTED BY THE SOCIETY FEBRUARY 25, 1991

Printed in U.S.A.